

Article

Taxonomic Status and Composition of the Genera *Caulaster*, *Porcellanaster* and *Eremicaster* (Asteroidea) Based on Juvenile Morphology and Molecular Phylogenetic Data

Alexandr N. Mironov¹, Anna B. Dilman^{1,*}, Nikolay B. Petrov² and Irina P. Vladychenskaya²

¹ Shirshov Institute of Oceanology, Russian Academy of Sciences, Nakhimovsky pr., 36, Moscow 117997, Russia; miron@ocean.ru

² Belozerskii Institute of Physicochemical Biology, Moscow State University, Leninskie Gory 1, bld. 40, Moscow 119992, Russia; petr@belozersky.msu.ru (N.B.P.)

* Correspondence: annadilman@gmail.com

Abstract: The genus *Porcellanaster* Thomson 1878 has hitherto included two species, the type species *P. ceruleus* Thomson, 1878 and *P. ivanovi* Belyaev, 1969. According to WoRMS, the full list of junior synonyms of *P. ceruleus* consists of 15 specific names, including porcellanasterids of the genera *Caulaster* Perrier 1882 and *Albatrossia* Ludwig 1905. In this paper, the morphology of juvenile and adult *Porcellanaster* and synonymized species from the Atlantic, Pacific, Indian and Southern Oceans are studied. As a result, the composition of the genus *Porcellanaster* has been revised. The genus *Caulaster* is re-established and now includes two species, and two new morphological forms of *Caulaster* are described. The genera *Albatrossia* and *Damnaster* H.E.S Clark & McKnight, 1994 are considered junior synonyms of *Caulaster*. The number of species of the genus *Porcellanaster* has increased to five, including the recovered *P. caulifer*, *P. fragilis* and *P. sladeni*. The study of representatives of the closely related genus *Eremicaster* Fisher, 1905 has not led to a change in its species composition. The main diagnostic feature of *Caulaster* is the presence of adambulacral and dorsal pedicellariae both in adults and juveniles with a major radius (R) greater than 3.5 mm. Pedicellariae have never been found in *Porcellanaster* or *Eremicaster* at any stage of postlarval development. The species of *Caulaster* and some species of *Porcellanaster* are the smallest porcellanasterids, with the most simplified morphology and reduced papulae and paxillae responsible for respiration. These genera are located on the phylogenetic tree in different clades, which demonstrates the parallel evolution of these taxa and confirms the validity of the genus *Caulaster*. One of the reasons for miniaturization is likely the burrowing mode of life with feeding on subsurface sediment of low nutritional value. The simplification of morphology can be traced by many morphological characters in many ways, including the reduction in papulae and paxillae.



Citation: Mironov, A.N.; Dilman, A.B.; Petrov, N.B.; Vladychenskaya, I.P. Taxonomic Status and Composition of the Genera *Caulaster*, *Porcellanaster* and *Eremicaster* (Asteroidea) Based on Juvenile Morphology and Molecular Phylogenetic Data. *Diversity* **2023**, *15*, 1032. <https://doi.org/10.3390/d15101032>

Academic Editors: Quentin Jossart, Camille Moreau and Bert W. Hoeksema

Received: 3 August 2023

Revised: 16 September 2023

Accepted: 18 September 2023

Published: 24 September 2023



Copyright: © 2023 by the authors. Licensee MDPI, Basel, Switzerland. This article is an open access article distributed under the terms and conditions of the Creative Commons Attribution (CC BY) license (<https://creativecommons.org/licenses/by/4.0/>).

Keywords: deep-sea asteroids; taxonomy; age-related variability; evolution; adaptations; lifestyle

1. Introduction

The family Porcellanasteridae is widely distributed throughout the world's oceans, with the exception of the Arctic at depths from 497 to 8720 m [1–4]. Porcellanasterid genera and species differ markedly from each other in body size and the complexity of external morphology. In the descriptions of asteroids, the size is usually given as R/r, where R is the distance from the center of the disk to the arm tips and r is the distance from the center of the disk to the interbrachial angle. The major radius of porcellanasterid species ranges from 9 to 146 mm [5]. The species of *Albatrossia* Ludwig, 1905 (*Albatrossaster* Ludwig, 1907 as an invalid replacement name), *Caulaster* Perrier, 1882 and *Damnaster* H.E.S Clark et McKnight, 1994, as well as some species of *Porcellanaster* Thomson 1878, are characterized by small R, usually 9–12 mm. Porcellanasterid species of small sizes differ from large ones in their simplified morphology, which has juvenile features. For this reason, smaller

species are often mistaken for juveniles of larger species. According to Madsen (1961) [3], all species of *Albatrossia* and *Caulaster* are junior synonyms of the larger species *P. ceruleus*. Belyaev and Mironov [6] re-established the genus *Caulaster*. They showed that the type species *Caulaster pedunculatus* Perrier, 1882 is distinguished from *Porcellanaster ceruleus* Thomson 1978 in having pedicellariae and in lacking plates on the ventrolateral areas. The size structure of *C. pedunculatus* populations also supports the validity of this genus and species. During the fourth cruise of RV *Akademik Mstislav Keldysh*, 443 specimens of *C. pedunculatus* were collected at 13 stations in the Reykjanes Ridge area [6]. For the period of this expedition from 30.07.1982 to 09.09.1982 (42 days), the maximum sizes of the specimens ($R + r$ 7.3 mm, $R + r \sim 11$ mm) did not change, while the size structure of the populations changed significantly: the population size peak ($R + r$) shifted from 3.5–4.5 mm to 8.5–9.5 mm (Figure 1). Belyaev and Mironov [6] suggested that a rapid increase in the proportion of large individuals in *C. pedunculatus* populations without increasing the maximum size of individuals indicates a very short period of growth from juvenile to adult forms.

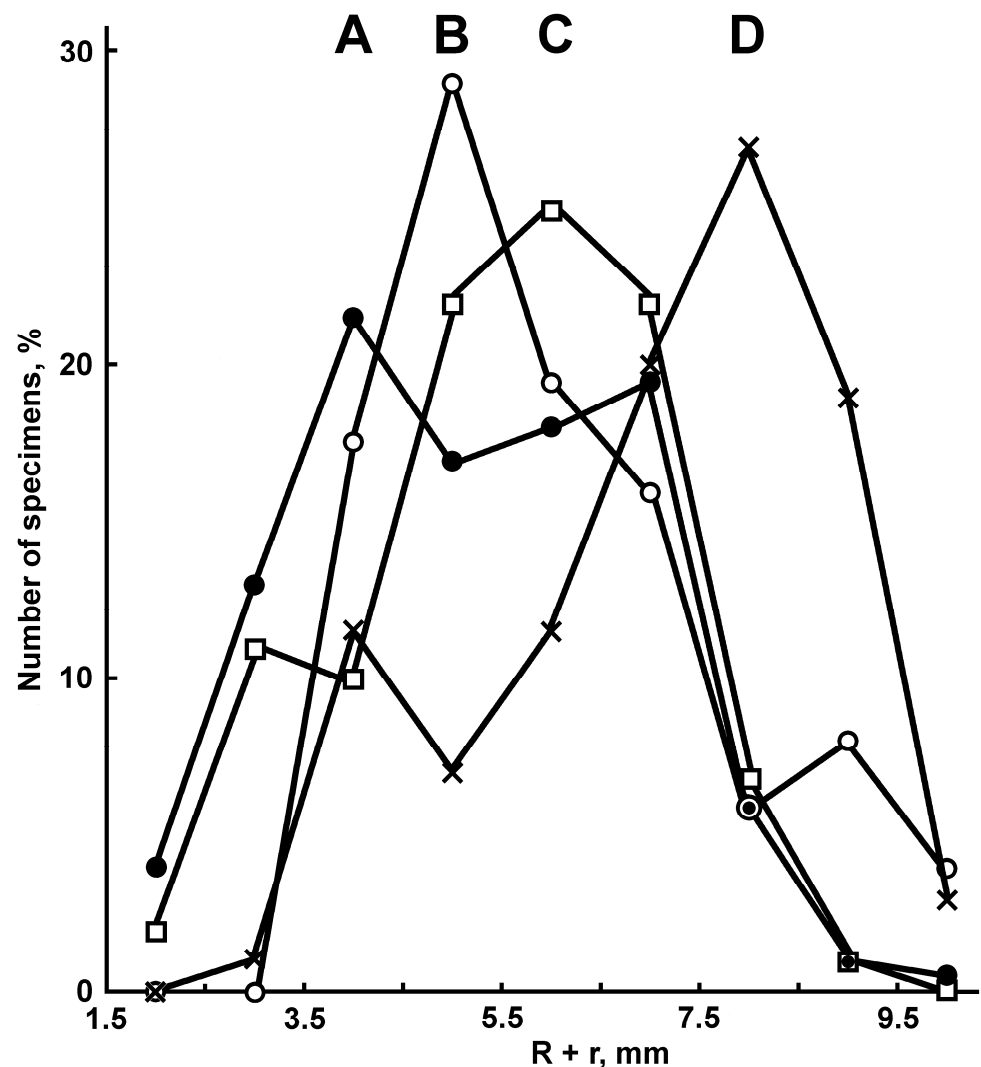


Figure 1. Changes in the size structure of populations of *Caulaster pedunculatus* from the Reykjanes Ridge over 42 days, from 30 July 1982 to 8 September 1982. A, black circles—RV *Akademik Mstislav Keldysh*, St. 268, 30.07.1982, 204 specimens; B, light circles—St. 316 and 317, 07–18.08.1982, 51 specimens; C, squares—St. 390 and 415, 21–25.08.1982, 91 specimens; D, crosses—St. 492 and 499, 08–09.09.1982, 70 specimens. Modified from Belyaev, Mironov ([6], Figure 4).

Despite the conclusions made by Belyaev and Mironov [6], many researchers consider *Caulaster* and *Albatrossia* juveniles of *Porcellanaster* [2,7–11]. The published data on the morphology, ontogeny and evolution of porcellanasterids are insufficient to judge with certainty the independence of *Caulaster* and *Albatrossia*. The aim of this study is to obtain additional data on morphology and genetics, confirming the validity of *Caulaster* and allowing a more accurate assessment of the species composition of the genera *Porcellanaster*, *Caulaster* and *Eremicaster*. The main focus is given to diagnostic features that are formed at the early stages of postlarval development. The study is based on materials collected throughout the world's oceans.

2. Material and Methods

2.1. Morphological Examination

Specimens of *Albatrossia*, *Caulaster*, *Damnaster*, *Eremicaster* and *Porcellanaster* were collected in the Atlantic, Indian, Pacific and Southern Oceans during twenty-seven cruises on thirteen research vessels: RV *Vityaz*, cruises 22 (1955), 29 (1958), 33 (1961), 34 (1961), 35 (1962), 43 (1968), 45 (1969), 48 (1970) and 57 (1975); RV *Ob*, The Second Antarctic Expedition (1957); RV *Akademik Kurchatov*, cruises 1 (1967), 4 (1968) and 43 (1986); RV *Jean Charcot*, expeditions NORTATLANTE (1969), WALDA (1971) and WALVIS (1978–1979); RV *Thalassa*, THALASSA Expedition (1971); RV *Meteor*, cruise 36 (1975); RV *Akademik Mstislav Keldysh*, cruise 4 (1982); RV *Dmitry Mendeleev*, cruises 41 (1988) and 43 (1989); RV *Le Noroît*, ECOFER 1 Expedition (1989); R/V *G.O. Sars*, MAR-ECO Expedition (2004); RV *Akademik Ioffe*, cruises 16 (2004) and 29 (2009); RV *L'Atalante*, cruise 12, BIONOD (2012); and RV *Sonne*, cruise 223 (2012). These porcellanasterids were sampled at 99 stations at depths ranging from 1261 to 8720 m using the Agassiz trawl, beamtrawl, epibenthic sledge, Galathea trawl, ocean grab, Sanders drag, Sigsbee trawl and USNEL Corers. The studied material includes 2361 specimens with R values from 0.38 to 34.0 mm, preserved in ethanol or dried.

Five qualitative and seven quantitative characters were used for descriptions of studied juveniles: presence/absence of dorsal pedicellariae; adapical appendage; adambulacral pedicellariae; cribriform organs; ventrolateral plates; number of superomarginal, inferomarginal, adambulacral and ventrolateral plates; number of vertical series of scales in cribriform organ; transversal series of ventrolateral plates; and dorsal spines on superomarginal plates. Most of these features are visible in the interradius sector from the oral side. In several cases, other characters were also used: the shape of terminal plate and number of spines on it, the presence/absence of segmental papillae and spines on ventrolateral plates, the distribution pattern of the plates on the dorsal side of the disc and others. The number of superomarginal, inferomarginal and adambulacral plates as well as dorsal spines in a row of superomarginal plates was counted in the space from the middle of the interradius to the end of the arm. The number of cribriform organs indicated in the species descriptions means number of organs in one interradius.

The genera of the family Porcellanasteridae differ significantly from each other, having complex or simplified external morphology. Simplification of morphology reaches its maximum in *Caulaster* and *Porcellanaster sladeni*. It concerns all morphological structures and is expressed in the disappearance of some structures (paxillae, papulae and spines on the surface of the oral, upper marginal, adambulacral and ventrolateral plates) and a decrease in the number of other structures (cribriform organs, furrow, oral and marginal spines and adambulacral, ventrolateral and superomarginal plates) [5]. The simplification of morphology in *Caulaster* is also clearly expressed in the partial or complete reduction in rows of the inferomarginal plates. Some complication in the morphology is observed only in the following: the spearhead-shaped furrow spines and spines of the dorsal disc are transformed into pedicellariae in *Caulaster* or segmental papillae in *Eremicaster crassus*.

The number of cribriform organs in one interradius was chosen here as the main measure of this simplification, since the smaller the number of cribriform organs, the smaller the size of adult porcellanasterids, and the simpler the external morphology of the genus (see Discussion). All genera were divided into three groups according to this

character: (i) number of cribriform organs, more than 3, (ii) 3 cribriform organs and (iii) one cribriform organ in one interradius. In addition to *Caulaster* and *Porcellanaster*, the monotypic genera *Lethmaster* Belyaev, 1969 and *Sidonaster* Koehler, 1909 belong to the group with one cribriform organ. The species of these genera (*L. rhipidophorus* Belyaev 1969 and *S. vaneyi* Koehler, 1909) are not considered in the present work, as they are easily distinguished from the species of *Porcellanaster*, *Caulaster* and *Eremicaster*.

The terminology of morphological characters of porcellanasterids follows that of Madsen [3].

2.2. Choice of Genetic Markers

Two mitochondrial (COI and 16S rRNA) genetic markers were used to assess the phylogenetic relationships within the family Porcellanasteridae. Various combinations of these markers proved useful for phylogenetic reconstructions within the class Asteroidea at ordinal or familial levels [12–17].

2.3. DNA Extraction, Amplification and Sequencing

DNA extraction, amplification and sequencing were performed as described earlier [16,17]. Primers for the amplification and sequencing are given in Table 1.

Table 1. Primers used for the PCR and sequencing.

Primer	Sequence 5'-3'	Reference
AsCOIF1	TTTCTACTAAACATAAGGACATTGG'	Petrov et al., 2016 [18]
HyCOIF1	TTTCTACTAAACACAAGGATATTGG'	Petrov et al., 2016 [18]
HyCOIR1	CTTCAGGGTGACCAAAAAATCA	Petrov et al., 2016 [18]
COIurF1	ACTGCCACGCCCCTAGTAATGATATTTTTTATGGT RATGCC	Hoareau and Boissin, 2010 [19]
COIurR2	TCGTGTGTCTACGTCCATTCCTACTGTRAACATRTG	Minin et al., 2014 [20]
Ech16SF	GTTTCGCCTGTTTACCAAAAA'	Petrov et al., 2016 [18]
Ech16SR	CGTAGATAGAAACTGACCTGGC	Petrov et al., 2016 [18]
LCOech1aF1	TTTTTCTACTAAACACAAGGATATTGG	Folmer et al., 1994 [21]
R-HCO2198	TAAACTTCAGGGTGACCAAAAAATCA	Folmer et al., 1994 [21]
16sbrH	CCGGTCTGAACTCAGATCACGT	Palumbi, 1996 [22]

In addition to published sequences, fragments of the two targeted genes were newly sequenced for five species (COI and 16S for *Eremicaster crassus*, *Styracaster* sp., *S. caroli* and *S. horridus* and 16S for *S. chuni*). GenBank accession numbers of sequences used are given in the Supplementary section, Table S1. The remaining sequences were taken from GenBank. In total, we were able to assemble alignments for 32 species, including concatenated fragments of both COI and 16S gene sequences (with the exception of *Sidonaster vaneyi*, for which only a fragment of COI is taken).

Some species names used for phylogenetic analyses do not coincide with those listed in GenBank. These discrepancies are marked with superscripts in Supplemental Table S1, where the full list of sequences is given. *Styracaster paucispinus* (voucher NHMUK: MCF 185546345) has been assigned to *Abyssaster paucispinus* based on an article by Mironov et al. (2015) [23], where it was shown that the species *S. paucispinus* most likely belongs to the genus *Abyssaster*. The specimen of *Porcellanaster nudus* (voucher BIO1216, GenBank KY908349 and KY908357) has been assigned to *Caulaster* sp. A (1) based on examination of the voucher specimen (present study). Specimens of *Porcellanaster* cf. *ceruleus* (vouchers NHM 168, GenBank KU519568 and NHM 253, GenBank KU519525) have been assigned to *Caulaster* sp. A (2) based on photos from an article by Glover et al. (2016) [24] and also based on a comparison with the specimens *Caulaster* sp. A from the same area, collected by RV *L'Atalante*, cruise 12, BIONOD Expedition, and RV *Dmitry Mendeleev*, cruise 41 (see *Material examined* section for *Caulaster* sp. A). Specimens of *Porcellanaster* cf. *pedunculatus* (vouchers AI2169-1 and AI2169-2, GenBank KY908350, KY908358) have been assigned to *Caulaster pedunculatus* based on the synonymy accepted in the present

study. The specimen of *Styracaster armatus* (voucher JC037-1, GenBank KY908353) has been assigned to *Styracaster chuni* based on examination of the voucher specimen.

2.4. Sequence Alignment and Phylogenetic Analyses

Sequences of COI genes were aligned manually and those of 16S were aligned in MUSCLE 3.8.31 [25] with the subsequent correction in a text redactor. The phylogenetic trees of the concatenated COI and 16S rRNA gene sequences were inferred using two methods: Bayesian inference (BI) using the MrBayes v. 3.2.7 software [26] and maximum likelihood (ML) implemented in IQ-TREE [27]. The best model of the nucleotide sequences evolution was determined using ModelFinder [28]. For our set of the gene COI and 16S rRNA sequences, the best model proved to be the model of reversible evolution of nucleotide sequences (GTR), taking into account the nucleotide frequencies (F), proportion of invariant (I) positions and gamma (G)-correction for the heterogeneity of positions in the rates of evolution (GTR + F + I + G). This model was used to construct the phylogenetic trees using both methods. For our set of twenty COI sequences, the best model of substitutions was estimated as TIM2 + F + G4. Statistical support of the BI consensus tree nodes was estimated as the posterior probability (PP), and that of the ML tree nodes was evaluated as bootstrap percentages (BS) by means of 60,000 replications in UFBoot2 ultrafast bootstrapping [29].

2.5. Testing of Topological Hypotheses

Constraint analyses were performed with the Bayes' factor testing [30] approach, which followed that of Bergsten et al. (2013) [31]. Three alternative hypotheses (H1–H3) were specified as equally informative sets of topologies (Table 2) and the consensus tree topology obtained from the BI/ML analysis (hypothesis H0). For each hypothesis, average marginal likelihood was calculated using the stepping-stone sampling method [32] implemented in MrBayes 3.2.7 [26]. The 2lnBF statistic was calculated as two times the difference between log marginal likelihoods of H0 and one of the alternative hypotheses. It was considered as strong evidence for H0 if its value was greater than 10 [30].

Table 2. Comparison of the tree topology obtained in present study (H0) and alternative hypotheses H1–H3 considering the places of *Porcellanaster* with or within other porcellanasterid groups.

Hypotheses	Bayes' Factor (BF) Testing with Stepping-Stone Sampling	
	Mean lnL	2lnBF
H0. Unconstrained BI/ML consensus tree topology	−11,319	(best)
H1. <i>Porcellanaster</i> with/within <i>Styracaster</i> group	−11,373	108
H2. <i>Porcellanaster</i> with/within <i>Caulaster</i> group	−11,384	130
H3. <i>Porcellanaster</i> with/within <i>Hyphalaster</i> group	−11,397	156

The average evolutionary distances within and between group sequences on the tree were conducted in MEGA X [33] using the Kimura 2-parameter model [34].

The abbreviations used for specimen repositories are as follows: IORAS, Shirshov Institute of Oceanology, Moscow, Russia; MNHM, National Museum of Natural History, Paris, France; ZMBN, University Museum of Bergen, University of Bergen, Norway; NHM, Natural History Museum, London, UK; SMF, Naturmuseum Senckenberg, Frankfurt am Main, Germany; NZOI, New Zealand Oceanographic Institute, Wellington, New Zealand; NNMNZ, Museum of New Zealand Te Papa Tongarewa, Wellington, New Zealand.

3. Results

3.1. Genetics

Figure 2A shows the phylogenetic tree of the concatenated COI and 16S gene sequences inferred by the MrBayes program. The values of statistical support of the tree nodes are specified as the proportions of the posterior probability (PP) for the Bayesian tree and bootstrap percentage (BS) for the ML tree. The sequences of the species from one family

form well-supported monophyletic groups (clades). Exceptions are the sequences of the family Astropectinidae, three of which form a weakly supported group with the sequences of species of the family Luidiidae. The sequences of the families Porcellanasteridae and Ctenodiscidae combine into a clade of a higher rank supported by PP (1.00) and BS (82%) values on the BI and ML trees. The sequences of the families Pseudarchasteridae and Benthopectinidae form a more weakly supported clade (0.9 and 80% on the BI and ML trees, respectively). The sequences of the families Astropectinidae and Luidiidae form a clade with moderate statistical support (0.6 and 62%). In this clade, the sequences of the family Astropectinidae form a paraphyletic group, as they divide into two subgroups, one of which forms a moderately supported clade with the sequences of the species of Luidiidae (0.6 and 62%).

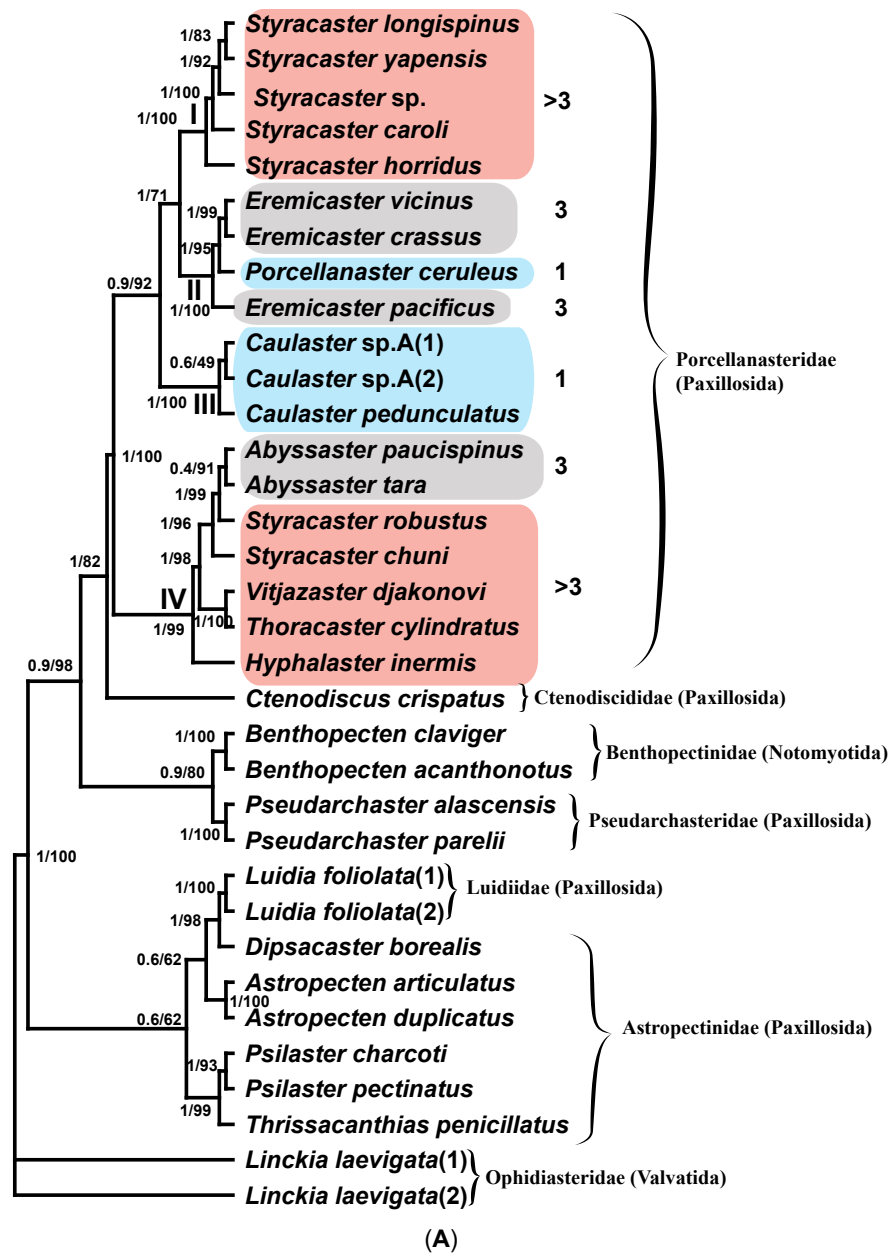
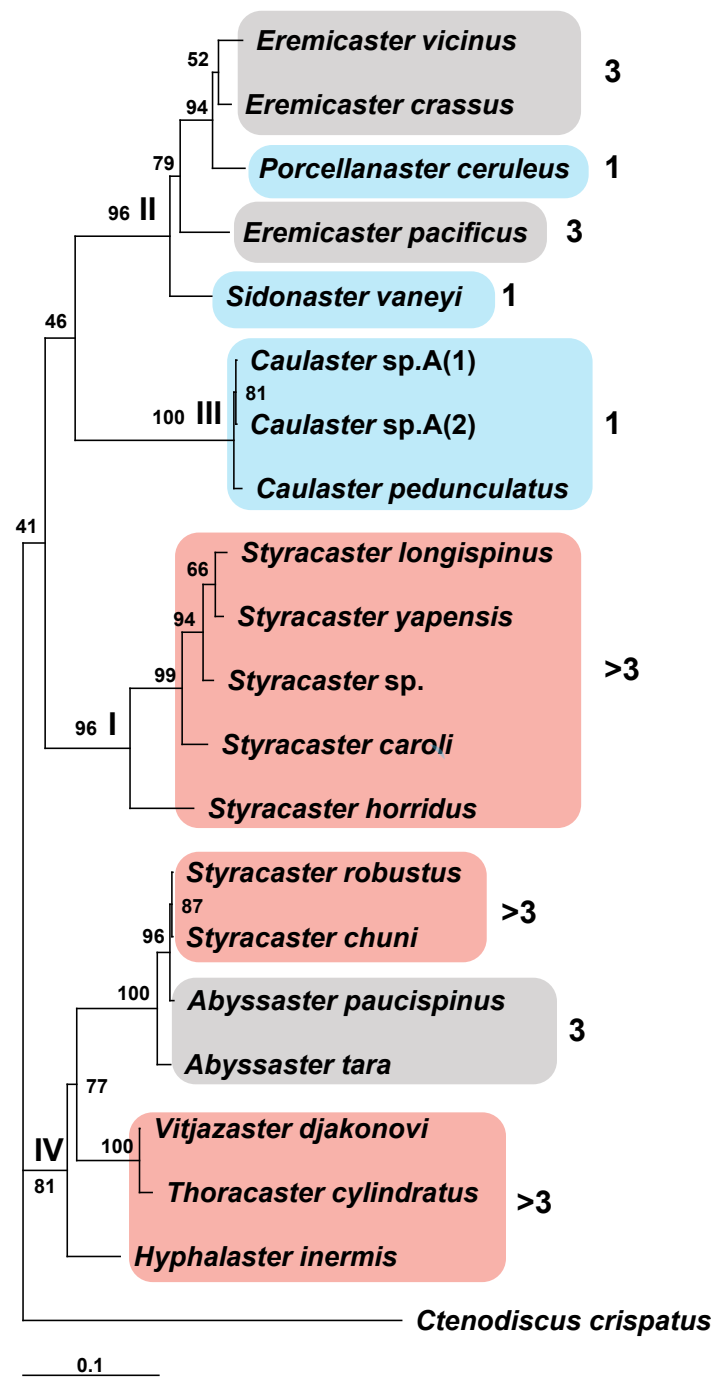


Figure 2. Cont.



(B)

Figure 2. (A) The non-scaled phylogenetic tree of the combined COI and 16S gene sequences produced by MrBayes and IQTree programs. The values of statistical support as the proportions of the posterior probability (PP) for the Bayesian tree and bootstrap percentage (BS) for the ML tree are shown to the left of the tree nodes. The clades of Porcellanasteridae are indicated by Roman numerals to the left of the corresponding nodes of the tree. The number of cribriform organs in species of different clades is shown in Arabic numerals on the right and marked with color: 1—blue, 3—gray and >3—pale red. (B) The scaled phylogenetic ML tree of the COI gene sequences inferred in IQTree program. The values of statistical support as bootstrap percentage (BS) are shown to the left of the tree nodes. The clades on the tree are indicated by Roman numerals to the left of the corresponding tree nodes. Number of cribriform organs is shown in Arabic numerals on the right and marked with color: 1—blue, 3—gray and >3—pale red.

The family Porcellanasteridae, represented in our analysis by sequences of COI and 16S rRNA gene fragments from 19 species (Figure 2A), as well as by sequences of COI from 20 species (Figure 2B), forms four well-supported clades (PP = 1, BS = 100% for Figure 2A and BS = 81–100% for Figure 2B). The clades I and III are homogeneous in composition: (I) “Styracaster” and (III) “Caulaster” groups. Clades II and IV are heterogenous: (II) “*Porcellanaster* + *Eremicaster*” (Figure 2A) or “*Porcellanaster* + *Eremicaster* + *Sidonaster*” (Figure 2B) and (IV) “*Abyssaster* + *Styracaster* + *Vitjazaster* + *Thoracaster* + *Hyphalaster*”.

The topology shows that the samples of the genera *Caulaster* and *Porcellanaster* fall into different clades. Within our four clades of the Porcellanasteridae family, the levels of the COI sequence divergence vary within the 0.55–11.04% range (clade I 8.56%, clade II 6.88%, clade III 0.55% and clade IV 11.04%) (Table S2). In Asteroidea, the levels of the COI gene intraspecific divergence vary within the 0.0–1.85% range (average of 0.53% in Ward et al., 2008 [35], and 1.6% in Hoareau and Boissin, 2010 [19]). The levels of congeneric divergence vary within the 0.0–27.06% range (average of 15.33%) [18,20,35,36]. The level of the COI gene divergence in the *Caulaster* clade (III) does not exceed the average intraspecific value for echinoderms. Two sequences named on the tree as *C. sp. A* are identical and differ from the COI sequence of *C. pedunculatus* only by five silent substitutions. Therefore, three COI sequences in this clade most likely belong to the same species, *Caulaster pedunculatus*.

Clade II, in addition to *Porcellanaster ceruleus*, includes the COI and 16S rRNA sequences of *Eremicaster* species. The level of sequence divergence in this clade is slightly lower than in homogenous clade *Styracaster* (I) but significantly lower than in heterogenous clade IV, including *Styracaster robustus*, *S. chuni*, *Thoracaster cylindricus*, *Vitjazaster djakonovi* and *Hyphalaster inermis*. The results of testing by stepping-stone sampling in MrBayes showing the affinities of *P. ceruleus* with other porcellanasterid clades suggests its best affinity with clade II (Table 2).

The stability of four Porcellanasteridae clades is confirmed by the equally high values of the statistical support of the four tree nodes. The results of testing in MrBayes affinities of *P. ceruleus* sequences by means of the stepping-stone sampling confirm their place within the *Eremicaster* clade. The places of the sequences *Porcellanaster* and *Caulaster* in the different clades are also confirmed, thus testing in favor of the genus *Caulaster* validity.

The fact that *P. ceruleus* is within the *Eremicaster* clade calls into question the validity of the genus *Eremicaster*.

The other result is that the genus *Styracaster* represents a polyphyletic taxon, divided into two groups: (i) *S. longispinus*, *S. yapensis*, *S. caroli*, *S. horridus* and *S. sp.* and (ii) *S. robustus* and *S. chuni*. The second group is clustered together with the species *A. paucispinus* and *A. tara*. However, the studying of relationships within the genus *Styracaster* is outside the scope of this article and requires additional data.

As we noted above, porcellanasterid genera and species differ markedly from each other in body size and the complexity of external morphology. One of the features, according to which morphology simplification is observed, is the number of cribriform organs, which varies from 19 to 1 in one interradius. In the phylogenetic tree, the number of cribriform organs is chosen as the main measure of miniaturization and simplification, since the body size and morphological features are correlated with this number. The small porcellanasterids *Caulaster* and *Porcellanaster* with one cribriform organ are located in two different clades (Figure 2A). This likely indicates a parallel evolution of these taxa, leading to the miniaturization and simplification of morphology (see Discussion for more details). The topology of the tree in Figure 2B also supports this conclusion. The tree contains one more genus with one cribriform organ—*Sidonaster*. It was shown that the genera *Sidonaster* and *Caulaster* are located in two different clades, like *Porcellanaster* and *Caulaster*.

3.2. Systematics

Family Porcellanasteridae Sladen, 1883

Included genera. *Abyssaster* Madsen, 1961, *Benthogenia* Fisher, 1911, *Caulaster* Perrier, 1882, *Eremicaster* Fisher, 1905, *Hyphalaster* Sladen, 1883, *Lethmaster* Belyaev, 1969, *Lysaster*

Bell, 1909, *Porcellanaster* Wyville Thomson, 1878, *Sidonaster* Koehler, 1909, *Styracaster* Sladen, 1883, *Thoracaster* Sladen, 1883 and *Vitjazaster* Belyaev, 1969.

Genus *Porcellanaster* Thomson, 1878

Included species. *P. caulifer* Sladen, 1883, *P. ceruleus* Thomson, 1878 (type species), *P. fragilis* Döderlein, 1921, *P. ivanovi* Belyaev, 1969 and *P. sladeni* (Perrier, 1885a).

Diagnosis. Porcellanasteridae with an R up to 36 mm. Pedicellariae on the dorsal disk and adambulacral plates are absent at all stages of postlarval development. Two furrow spines on the adambulacral plates are spearhead-shaped (not flat scale). The superomarginal plates are not contiguous midradially; dorsal spines are present at an R > 11–15 mm. The row of inferomarginal plates is usually continuous (not interrupted) and reaches the terminal plate. There is only a single lamelliform cribriform organ in each interradius. A single mouth spine is common for the two oral plates. The ventrolateral areas have pavement of plates at an R > 3.0 mm, except for *P. sladeni*. There is an odd interradiial marginal plate; the paxillae, suboral and subambulacral armament is always absent.

***Porcellanaster ceruleus* Thomson, 1878**

Figures 3A,F, 4A–C and 5A–C.

Porcellanaster ceruleus—Thomson, 1878: 351, 352, 353 (Figures 97 and 98) [37]; A.M. Clark, 1989 (part): 300–301 [2]; Clark, Downey, 1992 (part): 100–101 (Figure 18a,c) [7]; 27 A–C; Belyaev, Mironov, 1996: 887–892 (Figures 1 and 2) [6]; Dilman, 2008: 137 [38]; Dilman, 2013: 568 [39] and Dilman, 2014: 29 [40].

Porcellanaster inermis—Perrier, 1885a: 886 (nom. nud.) [41]; Perrier, 1885b: 50–53 [42] and Perrier, 1894: 212–215 [43].

Porcellanaster sladeni—Perrier, 1894: pl. 15.2, 2a, 2c [43] (by a lapse, non *P. sladeni* Perrier, 1885).

Porcellanaster granulatus—Perrier, 1885a: 886 [41] (nom. nud.); Perrier, 1885b: 53–55 [42] and Perrier, 1894: 216–218, pl. 171.1a–c [43].

Porcellanaster caeruleus—Verrill, 1885: 520, 543, pl. 14. 40–41 [44]; Sladen, 1889 (part): 134–138, pls. 201–7, 20A1–10 [10]; Madsen, 1961a (part): 127, 128, 129, 130, 136–138, (Figure 22) [3].

Porcellanaster irregularis—Lieberkind, 1932: 272–276, pls. 1.1–2; 3.1–3, 7.5–6; (textfigs. 1–4) [45].

Porcellanaster coeruleus—Lieberkind, 1935 (part): 5–19, pls. II 2–6, III 12; V 17; (textfigs. 1: B–D; 3:1,2, 4) [46].

Holotype. NHMUK 90.5.7.118, Challenger, St. 45, 03.05 1873, R/r = 22/10.5 mm.

Type locality. Challenger, St. 45, 03.05 1873, NW Atlantic, S. E. of New York, 38°34' N, 72°10' W, 2270 m.

Material examined. RV *Akademik Kurchatov*, cruise 1, St. 2, 08.01.1967, off Mauritania, Cape Timiris, 19°45' N, 18°21' W, 2850 m, 17 spms., R/r 3.5/2.0–28.0/8.0 mm, IORAS ECH02063.

RV *Akademik Kurchatov*, cruise 1, St. 14, 26.01.1967, Gulf of Guinea, 04°01.5' N, 05°05.5' W, 3500–3600 m, 10 spms., R/r 3.6/2.3 0–28.0/11.0 mm, IORAS ECH02045.

RV *Akademik Kurchatov*, cruise 43, St. 4934, 22.01.1986, off Namibia, 21°11.5'–21°09.2' S, 11°11.2'–11°09.5' E, 2580–2600 m, eight spms., R/r 4.5/2.2–25.0/8.5 mm, IORAS ECH02034.

RV *Meteor*, cruise 36, St. 99-AT, 26.02 1975, off Mauritania, Cape Blank, 21°36.2' N, 18°40.6' W, 2843–2786 m, 43 spms., R/r 8.9/3.5–24.8/8.7 mm, IORAS ECH02060 (these specimens constitute a small part of the sample stored at Zoologische Staatssammlung, München, stored as Eing. Kat. Nr. 595/M36/6 and Sach. Kat. Nr. 743/2, R from 8 to 26 mm).

RV *Meteor*, cruise 36 Sta. 100-AT, 26.02 1975, off Cape Blank, 20°27.1' N, 18°16.1' W, 2110–2049 m, seven spms., R/r from 14/4 to 30/9.5 mm, Zoologische Staatssammlung, München, Eing. Kat. Nr. 595/M36/9; Sach. Kat. Nr. 743/1.

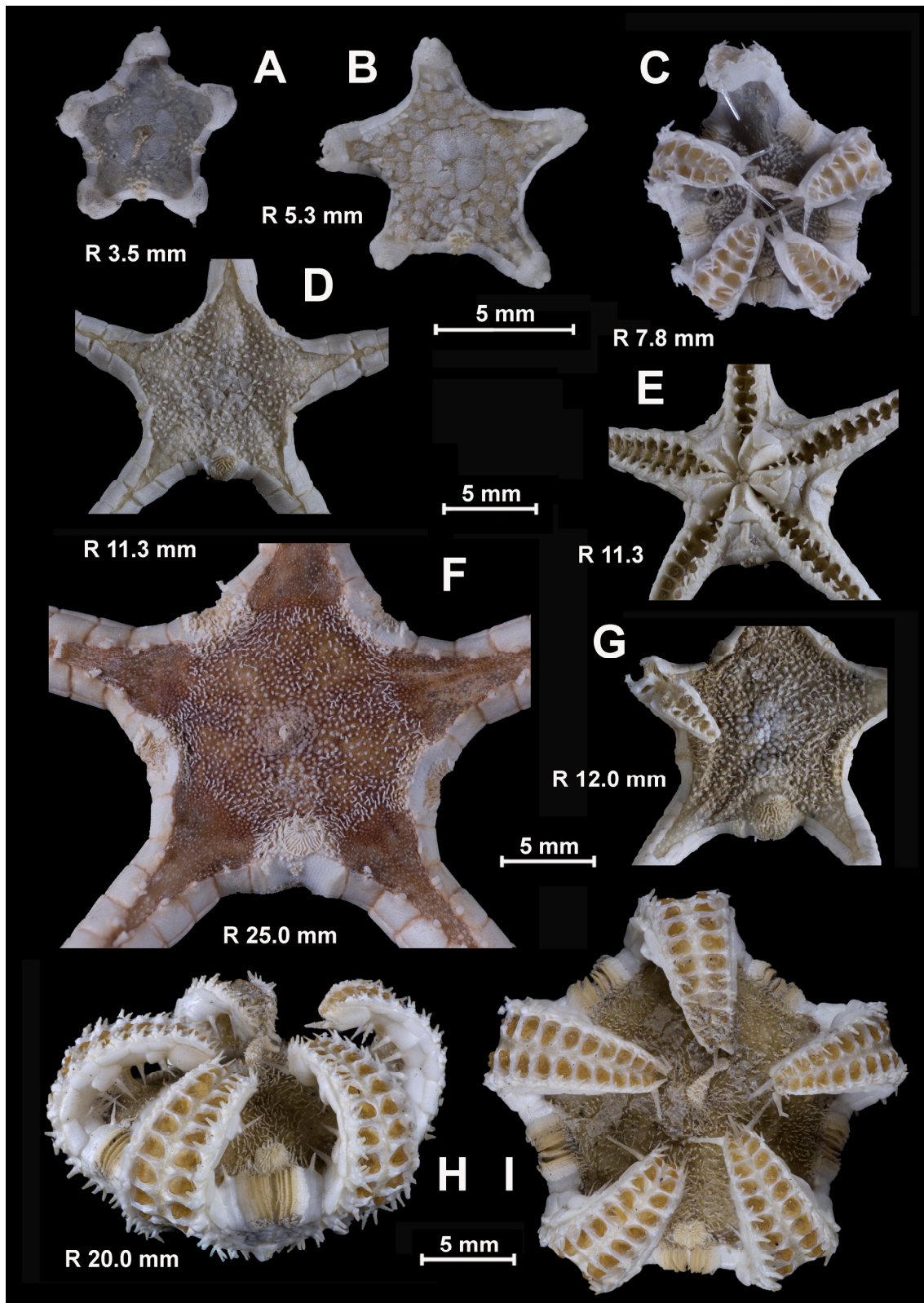


Figure 3. The species of the genus *Porcellanaster*, views from above (A–F,H), below (G) and side (I). (A,F) *P. ceruleus*, St. 14, RV Akademik Kurchatov (A) and St. 99, RV Meteor (F); (B,D,E,G) *P. ivanovi*, St. 7289, RV Vityaz; (C) *P. sladeni*, St. DS 28, RV Jean Charcot; (H,I) *P. caulifer*, St. CP 2, RV Jean Charcot. Scales: 5 mm. (A) R 3.5; (B) R 5.3 mm; (C) R 7.8 mm; (D) R 25 mm; (E) R 12.0 mm; (F,G) R 11.3 mm; (H,I) 20 mm.

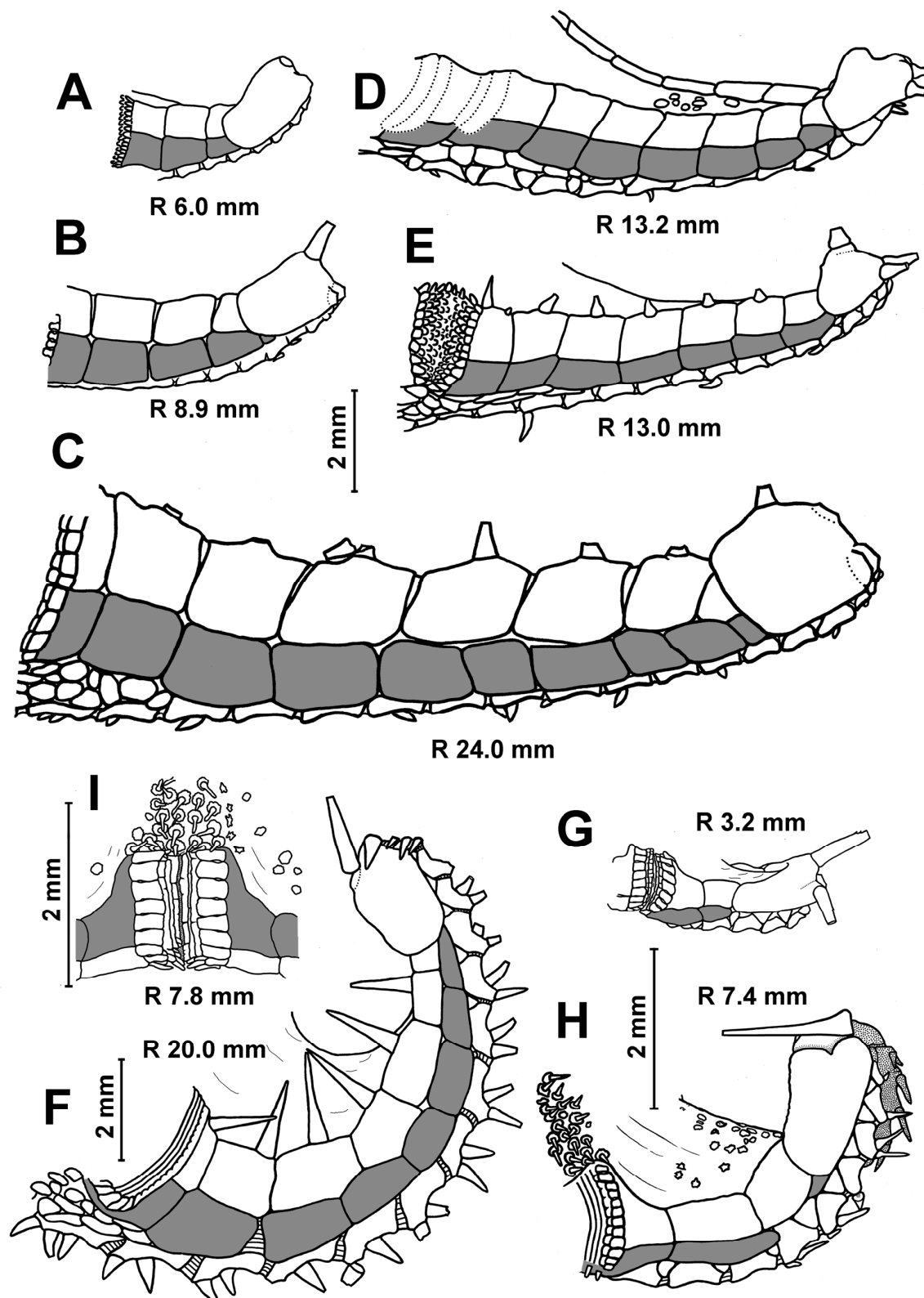


Figure 4. Age variability of the inferomarginal series and dorsal spines in *Porcellanaster*. Short dorsal spines in adult *P. ceruleus* (C), absence of spines or short spines in some adult *P. ivanovi* (D,E), long spines in *P. caulifer* (F) and absence of spines in *P. sladeni* (G–I). (A) St. 14, RV Akademik Kurchatov; (B,C) St. 99-AG, RV Meteor; (D) St. 7289, Vityaz; (E) St. 7291, RV Vityaz; (F) St. CP2, RV Jean Charcot; (G–I) St. DS28, RV Jean Charcot. Scales: 2 mm.

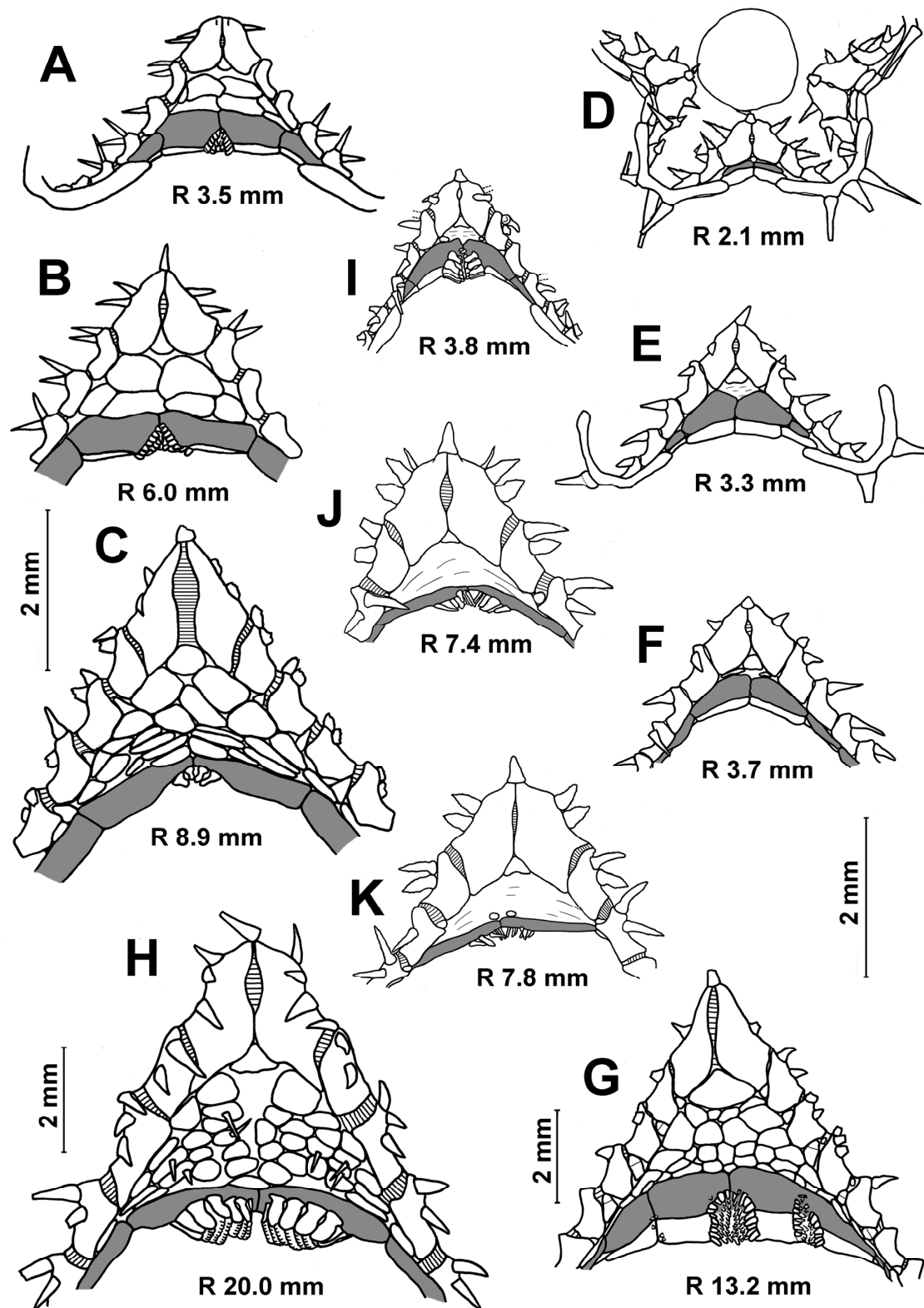


Figure 5. Age variability of the ventrolateral areas in *Porcellanaster*. Complete pavement of ventrolateral plates at all growth stages in *P. ceruleus* (A–C), late appearance of complete pavement in *P. ivanovi* (D–G), great skin spaces between plates in *P. caulifer* (H) and few tiny plates or their absence in *P. sladeni* (I–K). (A,B) St. 14, RV Aklademik Kurchatov; (C) – St. 99, RV Meteor; (D–G) St. 7289, RV Vityaz; (H) St. CP2, RV Jean Charcot; (I–K) St. DS28, RV Jean Charcot. Scales: 2 mm.

RV *Jean Charcot*, Campagne Noratlante, 13.08 1969, St. P 11, Maury Channel, 54°12'09" N, 27°51'05" W, 3085 m, two spms., R/r 13/6 and 15/7 mm, MNHM collection EcAs 2208.

RV *Thalassa*, THALASSA, St. X339, 15.10 1971, Bay of Biscay, 44°10' N, 04°30' W, 1520–1600 m, one spm., R/r ~3.8/1.5 mm, MNHM collection.

RV *Jean Charcot*, WALDA, St. CY 07, 17.06 1971, off Namibia, 22°53' S, 11°56' E, 2840 m, one spm., R/r ~13/6 mm, MNHM collection.

RV *Jean Charcot*, WALDA, St. CY 10, 28.06 1971, Angola Basin, 18°28' N, 10°31' E, 3530 m, five spms., R/r 24/10–32/11 mm, MNHM collection.

RV *Jean Charcot*, WALVIS, St. CP 15, 13.01 1979, Cape Basin, 32°29' S, 13°22' E, 3677 m, one spm., R/r 18/7.5 mm, MNHM collection.

R/V *G.O. Sars*, MAR-ECO Exp., St. 72/386, 27 July 2004, Mid-Atlantic Ridge, north-west of Charlie-Gibbs Fracture Zone, 53°16' N, 33°31' W, 2567–2522 m, five spms., R/r 7/4–21/10 mm, ZMBN 87154.

Total: There are 112 specimens from 11 stations, with R values from 3.5 to 32.0 mm. The specimens from the *Jean Charcot* and *Thalassa* collections were examined by A.N. Mironov during the visit to the Muséum National d'Histoire Naturelle, Paris, in 2002.

Description. In the smallest specimens (R 3.2–3.5 mm), the central part of the dorsal disc is covered with five large, perforated plates arranged in a ring. Five small, perforated plates adjoin this ring (Figure 3A). On the peripheral part of the disc, small widely separated perforate plates are evenly spaced; they are without spines. In each interradius near the border of the disc, there are 1–2 unperforated plates with a spine. As the size of body increases, the large plates of the central ring become separated from each other by skin spaces; the area occupied by small plates with spines increases. At an R of 5 mm, unperforated plates with a spine first appear in radial fields. The disc of the larger specimens has small, widely spaced plates with spines (Figure 3F). The spineless plates are preserved only at the base of arms and on arms. An apical appendage is present in both juvenile and adult specimens. Its length is variable, usually less than half the length of the interradius. In the young specimen from St. 14 of RV *Akademik Kurchatov* (R/r 4.8/2.2 mm), the length of the apical appendage (4.6 mm) is twice the length of the interradius. Dorsal pedicellariae are absent at all stages of postlarval development.

In the specimens with an R of 3.5–5.0 mm, the number of inferomarginals is equal to the number of superomarginals; these plates are located exactly opposite to each other. As the R increases, the inferomarginals gradually become shorter than the superomarginals (Figure 4B,C). In the largest specimens, the number of inferomarginal plates is greater than the number of superomarginal plates (by two or three plates). The shift of inferomarginals relative to superomarginals is the least pronounced in specimens from St. 4934 of RV *Akademik Kurchatov*. The height of inferomarginals and superomarginals is equal or inferomarginals are somewhat lower in young specimens. In the largest specimens, the ratio of the height of the distal inferomarginals and superomarginals is 0.5–0.75. The row of inferomarginals is continuous and always reaches the terminal plate. There are superomarginals without dorsal spines at an R < 11 mm (Figure 4A,B). The number of superomarginals with spines increases from one at an R of 11 mm to six in the largest specimens. The length of the dorsal spines also gradually increases, but never exceeds the height of superomarginals (Figure 4C). Some adult specimens (for example, the specimens with an R/r 21/10 mm from St. 72/386 of *G.O. Sars* and an R/r 25.0/8.5 mm from St. 4934 of RV *Akademik Kurchatov*) are without dorsal spines.

One cribriform organ is present in all interradii even in the smallest specimens with R values of 3.2–3.5 mm. Four adult specimens from St. 99AT of RV *Meteor* have two cribriform organs in one of the five interradii. One of two cribriform organs is slightly offset from the center of the interradius; the second is smaller and significantly offset from the center. Vertical rows of scales usually are bordered on the sides and bottom by a fringe of larger, broader scales. These scales are slightly smaller in the lower part of fringe than in its side parts. The number of vertical rows of scales in the cribriform organ (including side fringes) increases during growth from 2 to 24 (Table 3). The two furrow spines on each

adambulacral plate are spearhead-shaped (not flat scale) and never form pedicellariae. The ventrolateral area always has a pavement of plates in contact with each other. The skin spaces between the plates are usually small, but sometimes moderately large. The ventrolateral plates are without spines (Figure 4A–C). The L/W (length/width) ratio of the terminal plates increases unevenly from 0.5 to 1.25. There are usually three terminal spines, but sometimes (in the largest specimens) four or five.

Table 3. Age variability of the numerical characters of *Porcellanaster* species: sm—superomarginal plates, im—inferomarginal plates, ad—adambulacral plates, c.r.o.—cribriform organ, vl.pls—ventrolateral plates. If the interradii differ from each other in the number of spines, plates, rows of plates or scales, then the minimum and maximum numbers are indicated.

R/r, mm	Number of Plates			Number of Rows		Number of Dorsal Spines in sm Row
	sm	im	ad	Vertical Series of Scales in c.r.o.	Transversal Series of vl. pls	
<i>P. ceruleus</i> , RV <i>Akademik Kurchatov</i> , cruise 1, St. 2						
3.5/2.0 = 1.7	2	2	5	2–3	1	0
4.2/2.6 = 1.6	3	3	6	6–8	2–3	0
5.5/2.9 = 1.9	3	3	8	7–8	2	0
7.2/3.8 = 1.9	3	3–4		9 (10)	4	0
9.0/4.5 = 2.0	4	5	11	12–14	4–5	0
11.0/4.5 = 2.4	4	5	13	8–12	5	0
20.0/8.0 = 2.5	6	8	16 (17)	14–16	5–6	1–2
23.0/8.5 = 2.7	7	8–9	19	20–22	5	4
28.0/8.0 = 3.5	9	10–11	21	22	5	8
<i>P. ceruleus</i> , RV <i>Akademik Kurchatov</i> , cruise 1, St. 14						
3.6/2.3 = 1.6 fig	2	2	6	4	2	0
<i>P. ceruleus</i> , RV <i>Akademik Kurchatov</i> , cruise 43, St. 4934						
4.5/2.2	3	3	8	6–8	2	0
8.0/3.3	5	5	10	8	4	0
13.5/6.0	7	7–8	14	11–12	6	0
17.0/6.0	6	7	15	16	7	4
21.0/8.0	8	9	16	15–16	6–7	2–4
23.0/7.0	8	9	19	22	6–7	1–3
25.0/8.5	8	9–10	19	22	5–6	0
<i>P. ceruleus</i> , RV <i>Meteor</i> , cruise 36, St. 99-AT						
8.9/3.5 = 2.5	4	4 (5)	12	12	4	0
10.4/4.5 = 2.3	4	4 (5)	13	12–14	4	0
11.2/4.6 = 2.4	5	5	13	12–14	4	1–2
13.4/5.0 = 2.7	6	6–7	14–15	14–16	4–5	3–4
18.5/6.7 = 2.8	6	7	17	22	6	0
24.0/8.7 = 2.8	8	9–10	19	20	6–7	5–6
24.8/8.7 = 2.8	8	10 (11)	21	24	6	3–4
<i>P. ivanovi</i> , RV <i>Vityaz</i> , cruise 57, St. 7289						
2.1/1.5 = 1.4	1	1	2	0	0	0
3.3/2.2 = 1.5	2	2	4	0	0	0
3.7/2.2 = 1.7	2	2	5	0	0–1	0
4.4/2.2 = 2.0	3	3	6	0	1–2	0
5.1/2.8 = 1.8	4	4	7	0–4	2	0
8.5/4.3 = 2.0	5	5	10	2–6	2	0
11.3/4.7 = 2.4	5	5	13	6–11	2	0
13.2/6.0 = 2.2	8	8	14	8	4	0

Table 3. Cont.

R/r, mm	Number of Plates			Number of Rows		Number of Dorsal Spines in sm Row
	sm	im	ad	Vertical Series of Scales in cr.o.	Transversal Series of vl. pls	
<i>P. ivanovi</i> , RV Vityaz, cruise 57, St. 7298						
15.0/7.0 = 2.1	7	7	12	6–8	3	0
18.0/9.0 = 2.0	8	8	14	12–14	4–5	0–2
<i>P. caulifer</i> , RV Xiangyanghong 10, St. C19 [11], RV Jean Charcot, Estase II expedition, St. CP2 (present paper) and RV Galathea, St. 281 [3]						
11.0/6.0 = 1.8	4–5	4–5	?	14–16	2	2 (?3)
20.0/8.5 = 2.3	7	8	15	16–20	5	7
24.0/11.0 = 2.3	6	6–8	?	20	5	6
<i>P. sladeni</i> , RV Jean Charcot, WALDA Exp., St. DS 28						
3.4/1.5	3	3	8	6–8	0*	0
3.8/1.7	2	2 (3)	7	4–6	0*	0
4.1/1.8	3 (4)	3 (4)	8	7–8	0*	0
5.1/2.1	3	3	9	8–10	0*	0
6.5/2.8	3	2–3	11	8–10	0	0
7.4/2.9	3	3	10	10	0*	0
7.8/3.5	3	3	9	12–12	0*	0
8.0/3.0	4	4–5	11	10–12	0	0

* An amount of 1–2 tiny ventrolateral plates are present.

Remarks. According to Madsen [3], the species *P. ceruleus* includes 13 junior synonyms: *P. caulifer* Sladen 1883, *P. eremicus* Sladen 1889, *P. fragilis* Döderlein 1921, *P. granulatus* Perrier 1885, *P. inermis* Perrier 1885, *P. irregularis* Lieberkind 1932, *P. tuberosus* Sladen 1883, *Albatrossaster nudus* Ludwig 1907, *A. richardi* Koehler 1909, *Albatrossia semimarginalis* Ludwig, 1905, *Caulaster dubius* Koehler 1909, *C. pedunculatus* Perrier 1882 and *C. sladeni* Perrier 1885. Only three of them (*P. inermis*, *P. granulatus* and *P. irregularis*, all from the Atlantic Ocean) are considered here as junior synonyms of *P. ceruleus*. The remaining species are either re-established or treated as synonyms for other species of *Porcellanaster* and *Caulaster*, or their validity requires confirmation. Comparisons of the juvenile morphology of *P. ceruleus* with that of other species of *Porcellanaster*, as well as *Eremicaster* and *Caulaster*, are given below in the remarks to these species.

The specimens of *P. ceruleus* were most frequently misidentified with *Caulaster pedunculatus*, which is one of the most abundant species among deep-sea asteroids and has a wider distribution. Two diagnostic features make it possible to reliably distinguish *P. ceruleus* from *C. pedunculatus* in the early stages of postlarval development. The first is the absence of dorsal and adambulacral pedicellariae at all stages. In *C. pedunculatus*, pedicellariae first appear at an R of 2.5 mm. The second diagnostic feature of *P. ceruleus* is a cover of plates on the ventrolateral fields ($R > 3.5$ mm), which are completely naked or bear a few tiny plates in *C. pedunculatus*. Sladen [10] (p. 130) indicated that some *P. ceruleus* from the *Challenger* collection had pedicellariae. It follows that *Challenger's* material of *P. ceruleus* also contains *C. pedunculatus*. The smallest specimen in this collection has an R of 8 mm. Lieberkind [46] described the age series of *P. ceruleus* from the *Ingolf* expedition, St.36. The sample contained seven specimens with R values from 2.5 to 13.0 mm. The high-quality drawings of these specimens (Figure 1, pl. II.1–8; pl. III. 12) [21] allow us to establish that five out of seven specimens belong to *Caulaster pedunculatus*, since they have dorsal pedicellariae (pl. II. 5, 6; pl. III.12), adambulacral pedicellariae (plate II.2) or a ventrolateral area without plates (pl. II. 3). Specimen A with an R of 3.0 mm (plate II.1) belongs to *P. ceruleus* because its ventrolateral fields are covered with plates. The largest specimen with

an R of 13 mm probably also belongs to *P. ceruleus*, since pedicellariae are absent on the dorsal disc (plate II.8).

Madsen [3] reported on juvenile and adult *P. ceruleus* specimens collected at six stations during the *Galathea* expedition. In our opinion, only specimens from St. 52 (Gulf of Guinea) belong to this species. *P. ceruleus* from St. 52 with an R of 36 mm is the largest specimen known from *Porcellanaster*. It shows a peculiar abnormality in that the ambulacral furrow, as well as the ambulacral and adambulacral skeleton, extends beyond the terminal plates, according to Madsen [3] (Figure 22j–m). Madsen suggested that *P. ceruleus* with an R of about 30–32 mm reached the full size obtainable by normal growth. Any further growth after such a size becomes apparently abnormal. The specimens from *Galathea* St. 63 probably belong to *P. sladeni*, the specimens from St. 574 and St. 664 are representatives of *C. pedunculatus* and the morphology of the specimens from St. 281 and 282 corresponds to that of *P. caulifer*.

A large collection of porcellanasterids, including more than 3000 specimens, identified as *P. ceruleus*, was collected in the Rockall Trough area (NE Atlantic) during the cruises of the RV *Challenger* in 1973–1985 [47,48]. The morphology of these porcellanasterids has not been described, except for specimens from St. 56, RV *Challenger*, 01.03.1976, 54°40' N, 12°16' W, 2886 m. The study of the latter showed that their morphology fully corresponds to that of *C. pedunculatus* [6]. The abundance of small porcellanasterids in the Rockall Trough collection supports the assumption that most of the other specimens most likely belong to *C. pedunculatus*.

The early development of *P. ceruleus* with an R from 0.47 to 6.0 mm was described by Sumida et al. [49]. However, this description lacks information about the characters (the presence of pedicellariae and ventrolateral plates) that are necessary to distinguish *C. pedunculatus* from *P. ceruleus*. Qualitative photos from the oral side are given only for specimens with R values of 0.47–1.67 mm (Figure 6A–H [49]), when differences between *P. ceruleus* and *C. pedunculatus* have not yet formed.

Distribution. Atlantic Ocean from Davis Strait to Maryland in the west and from southern Iceland to Cape Basin in the east, including the northern Mid-Atlantic Ridge and Azores. Depth range 1520–3677 m. Reports from the depths of more than 3700 m require confirmation. *P. ceruleus* not known with certainty from the Pacific and Indian Oceans.

Porcellanaster fragilis Döderlein, 1921

Porcellanaster fragilis—Döderlein, 1921: 15–16, pl. 3.1–1g [50].

Porcellanaster caeruleus—Madsen, 1961a (part): 131–132 [3].

Syntypes. RV *Siboga*, 1899, St. 175 and St. 211, R/r 12.0/4.5 and 18.0/6.0 mm.

Type locality. RV *Siboga*, 1899: St. 175, Ceram Sea, 02°38' S, 130°33' E, 1914 m, and St. 211, south of Sulawesi, 5°41' S, 120°46' E, 1158 m.

Remarks. *P. fragilis* is not represented in our collection. It is known from three specimens collected by RV *Siboga*. Sizes were given for only two specimens: R/r values of 12/4.5 and 18/6 mm with six and eight superomarginal plates, respectively. According to Döderlein [50], *P. fragilis* differs from *P. ceruleus* in having longer arms and more complete spine-armature dorsally. We agree with Madsen [3] that neither of these characters have taxonomic value. In our opinion, a valuable character of *P. fragilis* is that most adambulacral plates bear only one spine. Among the species of the family Porcellanasteridae, only *P. ivanovi* Belyaev, 1969 is characterized by a single furrow adambulacral spine. Differences between these species are indicated in the description of *P. ivanovi*.

Distribution. Malay Archipelago. Depth range 1158–1914 m.

Porcellanaster ivanovi Belyaev, 1969

Figures 3B,D,E,G, 4D,E and 5D–G

Porcellanaster ivanovi—Belyaev, 1969: 11–14 (Figures 6 and 7) [51]; Belyaev, Mironov, 1977: 13 [52]; Belyaev, 1985a: 542–545 (Figures 1B and 3) [1]; A.M. Clark, 1989: 301 [2].

Holotype. Shirshov Institute of Oceanology, IORAS ECH02066, RV *Vityaz*, cruise 22, St. 3503, 14.10.1955, R/r 16/8 mm.

Type locality. RV *Vityaz*, cruise 22, St. 3503, 27.10.1955, Volcano Trench, 23°03' N, 144°59' E, 7584–7614 m.

Material examined. RV *Vityaz*, cruise 22, St. 3503, 27.10.1955, Volcano Trench, 23°03' N, 144°59' E, 7584–7614 m, holotype.

RV *Vityaz*, cruise 57, St. 7289, 27.03.1975, Palau Trench, 07°43,5' N, 134°56,6' E, 7970–8035 m, 109 spms., R/r 2.1/1.5–13.2/6.0 mm, IORAS ECH02035-ECH02037, ECH02044, ECH02059 and ECH02069.

RV *Vityaz*, cruise 57, St. 7291, 27-28.03.1975, Palau Trench, 07°50' N, 135°03' E, 7000–7170 m, 40 spms., R/r 2.8/2.0–13.5/6.0 mm, IORAS ECH02043 and ECH02058.

RV *Vityaz*, cruise 57, St. 7298, 29-30.03.1975, Yap Trench, 08°23.4' N, 137°52' E, 8560–8720 m, two spms., R/r 15.0/7.0 and 18.0/9.0 mm, IORAS ECH02042 and ECH02070.

Total: There are 152 specimens from four stations, with R values of 2.1–18.0 mm.

Description. The superomarginal and inferomarginal plates first appear at an R of about 1.9 mm; the scales of the cribriform organ at an R of 5 mm; the apical appendage at an R of 18; the ventrolateral plates at an R of 3.7 mm and the dorsal spines on superomarginal plates at an R of 13 mm. The change in numerical characters depending on body size is shown in Table 3. In juveniles, the central part of the dorsal disc is covered with 5–7 large, perforated plates arranged in complete ring. At an R of 8–11 mm, the large, perforated plates are gradually replaced by smaller plates. At an R > 11 mm, the dorsal disc is completely covered with small plates, each with a spine. Plates without spines occur only at the bases of arms and on arms; they do not form interradiial bands (Figure 3D,G). An exception is the specimens from the Yap Trench (St. 7298), in which the radial bands of plates without spines extend from the bases of arms to the center of the disc. Dorsal pedicellariae and an apical appendage are absent (Figure 3B,D,G), except for two specimens from St. 7298: the largest specimen (R 18 mm) has a short apical process, and the second specimen (R 15 mm) has an apical cone in the center of the disk.

In juveniles and most adults, the number of inferomarginals is equal to the number of superomarginals; the inferomarginal series is continuous and reaches the terminal plate (Figure 4D,E). Inferomarginals lie usually opposite the adjacent superomarginals in the specimens with R values of 3.5–5.0 mm; the height of the inferomarginals and superomarginals is equal or inferomarginals are somewhat lower. In the largest specimens, the ratio of the height of distal inferomarginals and superomarginals is 0.3–0.2. An exception is the holotype, in which the inferomarginal series is broken and does not reach the terminal plate; the distal inferomarginals are tiny. The superomarginals are without dorsal spines (Figure 4D), except for two specimens: the specimen with an R of 13 mm from St. 7289 carries dorsal spines (0.7 mm in length) on the first six superomarginal plates (Figure 4E), and the largest specimen with an R of 18 mm from St. 7298 bears short dorsal spines on the second and third plates.

Cribriform organs are usually absent at an R of 2–5 mm, but presented in the madreporite interradius at an R of 5–8 mm, and were present in all interradii at an R > 8 mm. The most noticeable deviation was found in a juvenile specimen from St. 7291 (R 2.8 mm), which has a rudimentary cribriform organ in the madreporite interradius. Many specimens (20%) have two or three cribriform organs per interradius; cribriform organs located on the sides are rudimental (Figures 3G, 4D and 5G). The arrangement of scales in a vertical series is sometimes indistinct; the central series are composed of rather papilliform scales widely separated from each other.

There are one or two furrow spines on each adambulacral plate; they are spearhead-shaped (not flat scale) and never form pedicellariae (Figure 5E–G). The share of adambulacral plates with two furrow spines is very different in specimens of the same size, from 0% to about 40%. However, this proportion tends to decrease with body size. Usually, adambulacral plates with paired furrow spines are located proximally. The ventrolateral area is provided with a complete pavement of plates at an R > 3.7 mm; the skin spaces between plates are usually small (Figure 5G). The ventrolateral plates are without spines. There are usually 3 terminal spines, but sometimes 4–6 (in the largest specimens).

The specimens from the three hadal trenches differ from each other. The single specimen from the Volcano Trench (the holotype) is characterized by the irregularity and distal disappearance of inferomarginal series. Two specimens from the Yap Trench differ in having a short apical appendage or apical cone on the dorsal disc and radial bands of plates without spines; the adambulacral plates are always with a single furrow spine. There are numerous anomalies in the form, number and position of superomarginals, inferomarginals, cribriform organs and terminal plates.

Remarks. According to Belyaev [1] (Figure 1B), the population size peaks occur at an R of 6–10 mm. The share of specimens with 2–3 cribriform organs in the interradius increases with body size: 7% at an R of 2–6 mm, 17% at an R of 6.1–10 mm and 52% at an R > 10 mm. The juveniles of *P. ivanovi* with an R < 5 mm differ from *P. ceruleus* of the same size in having single furrow spines on most adambulacral plates and in lacking an apical appendage, dorsal spines and ventrolateral plates. A short apical appendage was found only in the largest specimen (R 18 mm), and dorsal spines were present only in two specimens of *P. ivanovi* with an R 13.0 and 18.0 mm (Figure 3E).

The dorsal surface of the specimens *P. ivanovi* and *P. ceruleus* with an R > 9 mm is provided with a complete pavement of close-set plates in the former and an incomplete pavement of plates (separated from each other by skin spaces) in the latter.

The arrangement of scales in the vertical series of cribriform organs is less distinct in *P. ivanovi* than in *P. ceruleus*. The hadal species *P. ivanovi* is similar to the bathyal *P. fragilis* in having single furrow spines on most adambulacral plates and differs from *P. fragilis* in lacking an apical appendage, papulae and dorsal spines on superomarginals. However, the largest specimen of *P. ivanovi* has an apical appendage, and two specimens bear dorsal spines. The taxonomic value of papulae is unknown. Generally, papulae are very difficult to observe, showing themselves only when the disk is well expanded [3]. In addition, papulae are more common for bathyal porcellanasterids than for lower abyssal and hadal species. That is, diagnostic characters of *P. ivanovi* are not reliable, and additional material is required to confirm the validation of this species. It is possible that the differences between these two species are the result of intraspecific variability associated with living at different depths.

Distribution. West Pacific: Volcano, Palau and Yap Trenches. Depth range 7000–8720 m.

***Porcellanaster caulifer* Sladen, 1883**

Figures 3H,I, 4F,I and 5H.

Porcellanaster caulifer—Sladen, 1883: 222–223 [53]; Sladen, 1889: 138–140, pls. 21.5–10 [10]; 27.9–12.

Koehler, 1909a: 33–34, pls. 11.5, 13.1 [54].

Porcellanaster caeruleus—Madsen, 1961a (part): 130–131, 138–139 (Figure 23d–i) [3].

Porcellanaster ceruleus—Zhang et al., 2018 (part): 185–187 (Figures 2 and 3) [11].

Holotype. RV *Challenger*, St. 191, R/r 21.0/6.5 mm.

Type locality. RV *Challenger*, St. 191, 23.09.1874, the Arafura Sea in the Indo-Malay Archipelago, 05°41' S, 134°05' E, 1463 m.

Material examined. RV *Jean Charcot*, *Estase II* expedition, St. CP2, 14.11.1984, South China Sea, off Luzon Island, 14°05' N, 120°02' E, 1980 m, one spm., R/r 20.0/8.5 mm, MNHM collection.

Description. The arms are rather long and curved over the disk. The R/r ratio is 2.3. The dorsal surface of the disc has a complete pavement of close-set plates bearing spines. An exception is the peripheral part of the disk at the base of the arms, where the plates are without spines. The dorsal pedicellariae and papulae are absent. There is a long apical appendage. There are seven superomarginal plates and eight inferomarginal plates. All superomarginals are armed with a long dorsal spine, up to 1.8 mm in length; the length of the dorsal spines is greater than the height of the plate (Figures 3H,I and 4F). The inferomarginals are shorter and lower than the superomarginals (about two-thirds of height); they are slightly shifted relative to each other in the distal part of the arm. The cribriform organs are broad and located both on superomarginals and inferomarginals,

with 16–20 vertical scale series (Figures 3I and 4I). The scales are broad and very thin in the cross section and strongly arranged in vertical series, so that the boundaries between adjacent scales of the same vertical series are hardly visible. Vertical rows of scales, as usual, are bordered on the sides and from below by a fringe of larger, broader scales. These scales are slightly larger in the lower part of the fringe than in its side parts. There are 15 adambulacral plates and two or three furrow spines. They are spearhead-shaped (not flat scale) and never form pedicellariae. The ventrolateral area has a pavement of plates, separated by large skin spaces; the ventrolateral plates are naked or have one spine (Figure 5H). The terminal plates have three spines.

Remarks. *P. caulifer* differs from *P. ceruleus* in having an incomplete pavement of plates on the ventrolateral areas (Figure 5H); (pl. XXI.6; 3; Figure 23d,f [10]); there are spines on some of the ventrolateral plates, longer dorsal spines on the superomarginals (Figure 4F); [10] (pl. XXI.7, 9; 3, Figure 23e,g,h) and larger scales of the fringe bordering the cribriform organs from below. The scales of this lower fringe are arranged in a straight line rather than an arc, as shown by Sladen [10] (pl. XXVII.12; 11, Figure 3a,c). In *P. ceruleus*, ventrolateral plates are usually naked, sometimes with very minute spines or tubercles [3,10,55].

P. caulifer was established on the basis of a single specimen with an R/r of 21.0/6.5 mm [10]. Koehler [54] reported about a dozen specimens with an R of 12–16 mm and one with an R of about 22 mm. He did not give any description, apart from mentioning that some specimens, especially among the large ones, carry spines on ventrolateral plates. Madsen [3] described in detail three specimens with R/r values of 21/19, 23/11 and 24/11 mm (RV *Galathea*, St. 281), and Zhang [11] examined a specimen with an R/r of 11/6 mm. In both cases, the specimens were identified as *P. ceruleus*. However, their morphology fully corresponds to that of *P. caulifer*. The age variability in the numerical characters is shown in Table 3 based on both published and new data.

P. tuberosus Sladen 1883 was established for a single specimen collected by the HMS *Challenger* off southern Japan: St. 237, 34°37' N, 140°32' E, 3429 m, with an R/r of 18.5/6.0 mm [10]. The only differences from *P. ceruleus* that were noted [3,10] are fewer superomarginals (4 instead of 6–7 plates in *P. ceruleus* of the same size) and its rectangular shape. *P. caulifer* also has rather rectangular superomarginals. However, *P. tuberosus* differs from *P. caulifer* of the same size in having less numerous superomarginals (four), short dorsal spines, small scales of the fringe bordering cribriform organ (compare Figures 12 and 16 in Sladen, 1889, pl. XXVII [10]) and complete pavement of plates in ventrolateral areas. In our opinion, additional material is required to confirm the validity of *P. tuberosus*.

Numerous specimens of *P. ceruleus* were reported from the New Zealand area by Clark H.E.S. and McKnight D. [56–58]. In 1973, McKnight [58] (Figure 1) gave short descriptions for two early juveniles (R/r 1.0/0.5 mm and 1.5/0.7 mm), the generic features of which, in fact, have not yet been formed, and, therefore, there is no certainty that the specimens belong to this species. Clark [56] examined six specimens collected at three stations of RV *Eltanin*, cruise 26: St. 1837, 1844 and 1846. From the description, it is clear that a large specimen from St. 1846 (R 18 mm) indeed belongs to the genus *Porcellanaster*, since the superomarginal plates have a dorsal spine. The small specimen (R 7 mm) from St. 1837 should be assigned to the genus *Caulaster*, as it has dorsal pedicellariae. Clark and McKnight [59] later assigned some specimens from St. 1837, St. 1844 and St. 1846 to the new genus and species *Damnaster tasmani*, which is treated here as a junior synonym of *Caulaster pedunculatus*. In 2000, Clark and McKnight [58] published results on all porcellanasterid material from the NZOI and NMNZ asteroid collections. They examined 126 specimens of *Porcellanaster ceruleus* (R from 4 to 27 mm), but only one specimen with an R/r of 15/5 mm was described. This specimen is stored at NZOI St. S151, 45°45.80' S, 174°30.40' E, 1586 m. It is similar to *P. caulifer* in having incomplete pavement of plates on ventrolateral areas [57] (Figure 34c). It has ventrolateral plates without spines, as in *P. caulifer* of the same size. The cribriform organ is large, with 16–20 vertical rows of lamelliform scales, bordered by a fringe of larger, very regular, broad scales. The cribriform organs are more similar to those

in *P. caulifer* than in *P. ceruleus*. The form of the scales of the fringe bordering the cribriform organ from below and the length of the dorsal spines on superomarginals are unknown. More detailed descriptions of *Porcellanaster* from the New Zealand area are required for more reliable species identification.

Distribution. Indo-Malay Archipelago, South China Sea, Bay of Bengal, Gulf of Oman and south of Ceylon. Depth range 1400–3310 m.

***Porcellanaster sladeni* (Perrier, 1885)**

Figures 3C, 4G–I and 5I–K.

Caulaster sladeni—Perrier, 1885a: 886 [41] (nom. nud.); Perrier, 1885b: 47–50 [42]; Perrier, 1894: 208–210 [43] and Mironov et al., 2016: 505, (Figure 3e [5]).

Porcellanaster inermis—Perrier, 1894: pl. 15.2b and 3a-c [43] (by a lapse, non *P. inermis* Perrier, 1885).

Porcellanaster caeruleus—Madsen, 1961 (part): 132, 140 (Figure 24a,b [3]) (non *Porcellanaster caeruleus* Thomson, 1877)

Syntypes. MNHN-IE-2014-336, RV *Talisman*, St. DR30, 16.06.1883, two specimens (EcAh 3147 and EcAh 3148), R/r ~10/5 mm.

Type locality. RV *Talisman*, TALISMAN Exp. 1983, St. DR30, 16.06.1883, off Morocco, 32°37'59.9916" N, 09°49'0.012" W, 1435 m.

Material examined. RV *Jean Charcot*, WALDA Exp., St. DS 28, 11.08 1971, Gulf of Guinea, 04°21' N, 04°35' E, 1261 m, 10 sp., with an R/r of 3.4/1.5–8.0/3.0 mm. In addition, A.N. Mironov examined the syntype EcAh 3148 (RV *Talisman*, St. DR30) during the visit to the Muséum National d'Histoire Naturelle, Paris, in 2002.

Description. The arms are always curved over the disc (Figure 3C). In the specimens with an R of 3.4–3.8 mm, the pavement of plates on the dorsal disc is like that of juveniles of other species of the genus *Porcellanaster*. The central part of the dorsal disc is covered with a few large, perforated plates arranged in a complete ring. Most of the remaining dorsal disc is covered by smaller plates, slightly separated from each other by skin spaces. Some plates located along the interradii are equipped with a spine. At an R of 4–7.0 mm, interradial bands with close-set plates bearing spines become gradually more distinguishable from radial bands with small spineless plates widely separated from each other. Dorsal pedicellariae absent. The apical appendage always long, 1.6–2.5 in length. The madreporite plate round, 0.7–1.1 mm in diameter.

The first superomarginal plate is unequal in height: the proximal half is much higher than the distal and extends significantly into the disk (Figure 4H,I). The number of inferomarginals is equal to the number of superomarginals or more. Inferomarginals are displaced opposite the adjacent superomarginals. The inferomarginal series reaches the terminal plate or not; this feature is not correlated with the size of specimens. This series is continuous, except for the specimen with an R of 7.4 mm (Figure 4H).

The ratio between the height of the inferomarginals and superomarginals is about 0.25 in the first plate, 0.7 in the second plate and 0.25 in the most distal plates in adults. The superomarginals are without dorsal spines.

One developed cribriform organ presents in every interradius, even in the smallest specimens, both on the superomarginals and inferomarginals. The scales are broad and very thin in the cross section and strongly arranged in vertical series, so that the boundaries between adjacent scales of the same vertical series are hardly visible. There are two or three (rarely) furrow spines on each adambulacral plate; they are spearhead-shaped and never form pedicellariae. The ventrolateral areas are naked or have 1–2 tiny, rounded plates (Figure 5I–K). The L/W ratio of the terminal plate is 1.0–1.1. There are always three terminal spines. The gonads are clearly visible through the skin on the base of the arm at an R > 5 mm.

Remarks. *P. sladeni* is the smallest species of *Porcellanaster*. The specimens with an R of 5 mm already have developed gonads and an adult appearance: there are developed cribriform organs and interradial bands with close-set plates bearing spines. The morphology of *P. sladeni* is transitional between *Porcellanaster* and *Caulaster*. The spearhead-shaped

furrow spines and the absence of dorsal and adambulacral pedicellariae for all body sizes are features of other species of *Porcellanaster*, while the small body size and absence of ventrolateral plates (or a few tiny plates) are features of *Caulaster*. This combination of features is also characteristic for the specimen *P. ceruleus*, described by Madsen [3] from the *Galathea* expedition, St. 63.

It differs from other *P. sladeni* specimens only in having spines on two tiny ventrolateral plates [3] (Figure 24a). This Galathean specimen with an R of 11 mm seems to be the largest representative of *P. sladeni*.

Distribution. Western Atlantic Ocean, off Morocco and Gulf of Guinea. Depth range 1261–1520 m.

Genus *Eremicaster* Fisher, 1905

Included species. *E. crassus* (Sladen, 1883) (type species), *E. pacificus* (Ludwig, 1905) and *E. vicinus* Ludwig, 1907.

Diagnosis. Porcellanasteridae with an R up to 60 mm. The pedicellariae on the dorsal disk are absent at all stages of postlarval development. The superomarginals have dorsal spines and are not contiguous midradially. The inferomarginal rows are continuous and reach the terminal plate. There are three lamelliform cribriform organs in each interradius at an R > 3.5mm. Each jaw with a single apical spine is common to two oral plates. The ventrolateral areas have a pavement of large plates at an R > 2.6 mm. There are odd interradiial marginal plates, and the paxillae, suboral and subambulacral armament is absent.

Remarks. The differential diagnoses of *Porcellanaster* and *Eremicaster* differ only in the number of cribriform organs: one cribriform organ in the first genus and three in the second. However, some of the adult *E. crassus* at our disposal have only one cribriform organ (see below). The juveniles of both genera have one cribriform organ. Hence, the validity of the genus *Eremicaster* is not supported by the results of both genetic and morphological analyses. To conclude on the validity of *Eremicaster*, additional molecular data on species of the genus *Porcellanaster* are needed, which are currently very scarce.

Eremicaster crassus (Sladen, 1883)

Figure 6A–C.

Porcellanaster crassus—Sladen, 1883: 225–227 [53]; 1889: 141–143, pls. 22.4–7; 27.1–4 [10].

Porcellanaster gracilis—Sladen, 1883: 227–229 [53]; 1889: 143–145, pls. 221–3, 275 [10]; Madsen, 1961a: 155–161, pl. XIII, 1–2 (Figures 29 and 39) [3]; Bernasconi, 1967: 445–447 [60]; Bernasconi, 1977: 81–82 [61] and Luke, 1982: 11 [62].

Porcellanaster (*Eremicaster*) *tenebrarius*—Fisher, 1905: 293–294 [63].

Porcellanaster walthavii—Ludwig, 1905: 92–97, pl. 526–527 [64].

Eremicaster tenebrarius—Fisher, 1911: 24–29, pls. 1.1–4, 2.4, 53.4–4a [65]; H.L. Clark, 1913: 187 [66]; H. L. Clark, 1920: 76–77 [67]; Macan, 1938: 327–329 [68] and Djakonov, 1950: 21 (Figure 31) [69].

Eremicaster gracilis—Madsen, 1961a: 155–160, Figure 29. pl. XIII, 1–2 [3].

Eremicaster crassus—Madsen, 1961a: 145–155, Figures 25–27, 39, pl. XI.1–12, pl. XII.1–7 (non—Figure 28, pl. XII. 8: = *E. vicinus*) [3]; Luke, 1982: 10–11 [62]; Belyaev, 1985b: 866–870, (Figure 1A) [70]; A.M. Clark, 1989: 299 [2]; Clark and Downey, 1992: 96–97, pl. 27D–F (Figures 18d and 19h) [7]; Lambert and Boutillier, 2011: 84, Figure 64 [55] and Mironov et al., 2019: 366 (Figure 6B) [71].

Holotype. NHMUK 90.5.7.123, H.M.S. *Challenger*, St. 286, R/r 25/10.5 mm.

Type locality. H.M.S. *Challenger*, St. 286, mid-South Pacific, 33°29' S, 133°22' W, 4270 m.

Material examined. RV *Vityaz*, cruise 29, St. 4131, 09.11.58, north-east of the Aleutian Trench, 55°47' N, 145°19' W, 3949 m, one sp., R/r 9/3 mm, IORAS ECH02057.

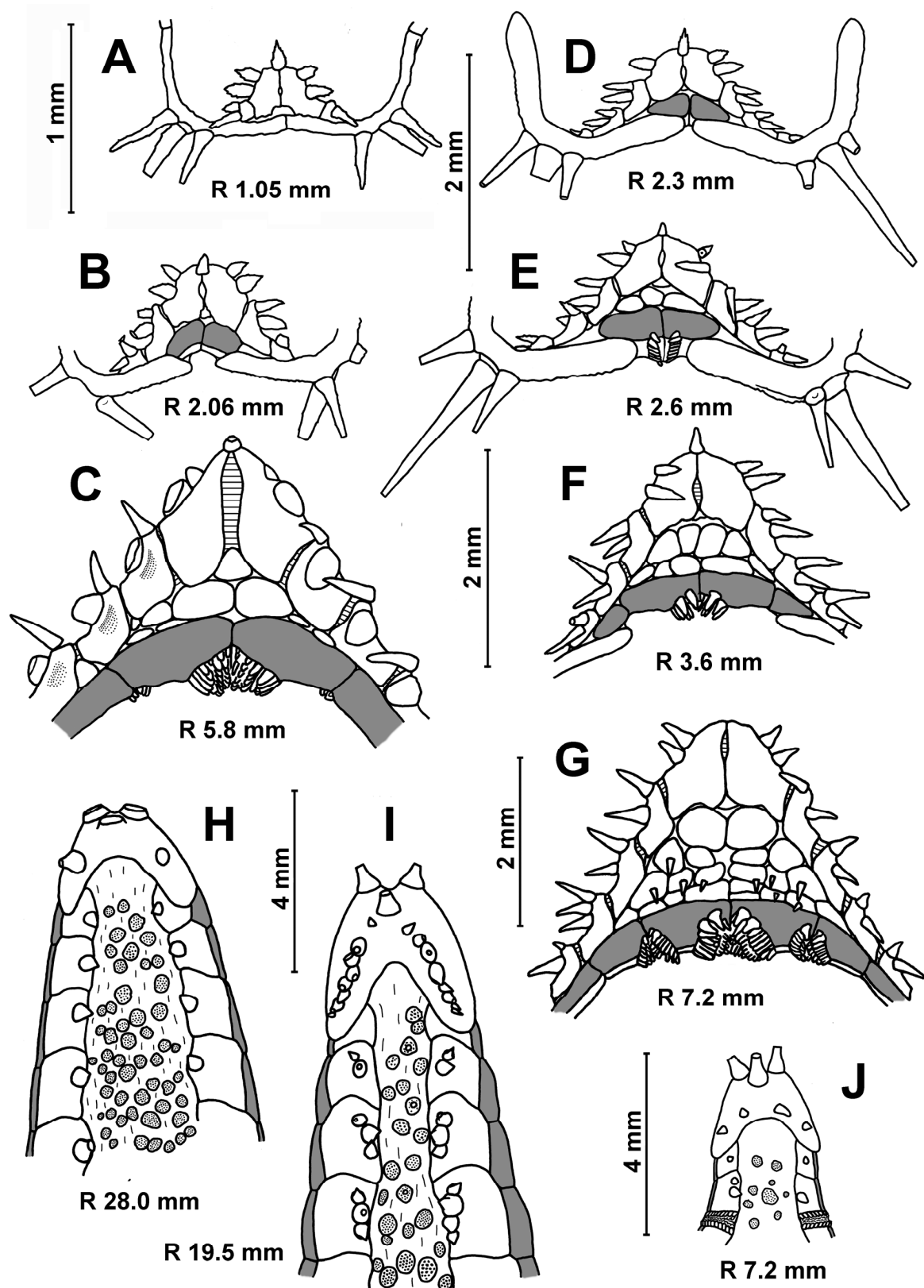


Figure 6. Age variability of the ventrolateral areas (A–G) and dorsal spines (H–J) in *Eremicaster crassus* (A–C) and *E. pacificus* (D–J). (A,B) St. 2–10, RV Sonne; (C) St. 11–11, RV Sonne; (D–G) St. 220, RV Akademik Kurchatov; (H) St. 308, RV Akademik Kurchatov; (I,J) St. 3537, RV Vityaz. Scales: 1 mm (A), 2 mm (B–G) and 4 mm (H–J).

RV *Vityaz*, cruise 39, St. 5620, 15.08.1966, east of the Kuril-Kamchatka Trench, 44°48' N, 156°33' E, 5005–5045 m, nine sp., R/r 13.0/6.2–26.5./11.2 mm, IORAS ECH01136.

RV *Vityaz*, cruise 39, St. 5622, 18.08.1966, east of the Kuril-Kamchatka Trench, 45°14' N, 155°15' E, 5090–5100 m, three sp., R/r 10.5/4.4–26.1./10.2 mm, IORAS ECH01154.

RV *Vityaz*, cruise 39, St. 5623, 19.08.1966, east of the Kuril-Kamchatka Trench, 45°26' N, 154°59' E, 4995–5045 m, eight sp., R/r 9.7/4.2–26.1./10.2 mm, IORAS ECH01091.

RV *Vityaz*, cruise 39, St. 5624, 20.08.1966, east of the Kuril-Kamchatka Trench, 45°26' N, 154°12' E, 5200 m, five sp., R/r 14.3/5.7–34.0./10.8 mm, IORAS ECH01185.

RV *Vityaz*, cruise 43, St. 5939, 28.01.1968, Central Pacific Basin, 02°17' S, 179°30' E, 5460 m, one sp., R/r 11.5/5.8 mm, IORAS ECH01088.

RV *Vityaz*, cruise 45, St. 6088, 04.05.1969, south-east of Aleutian Trench, 53°58' N, 157°36' W, 5740 m, 15 sp., R/r 5.1/2.4–22.5/8.7 mm, IORAS ECH01028 and ECH01157.

RV *Vityaz*, cruise 45, St. 6107-2, 13.05.1969, Gulf of Alaska, 57°35.5' N, 143°01' W, 3800 m, two sp., R/r 4.0/2.3 and 17.0/7.0 mm, IORAS ECH01178.

RV *Vityaz*, cruise 45, St. 6117, 18.05.69, Gulf of Alaska, 56°12' N, 139°12'1" W, 3350–3370 m, 13 sp., R/r 4.5/2.2–23/8 mm, IORAS ECH01005.

RV *Vityaz*, cruise 45, St. 6135, 09.06.69, north-east of the Aleutian Trench, 53°32' N, 163°22' W, 2880–2930 m, four sp., R/r 4.6/2.4–21.0/8.0 mm, IORAS ECH01177.

RV *Dmitry Mendeleev*, cruise 16, 21.02.1976, St. 1349, south-west of Tasmania, 43°36' S, 144°03' E, 4464 m, two sp., 22.0/7.0 and 22.5/8.0 mm, IORAS ECH01158.

RV *Akademik Mstislav Keldysh*, cruise 79, St. 6691, 24.02.2020, West Scotia Basin, 59°45.0531' S, 59°30.7549' W—59°44.2155' S, 50°31.87592792' W, 3756–3771 m, five sp., R/r 6.0/3.5–26.0/11.0 mm, ID 6691si-102B and 6691si-102F.

RV *Sonne 223*, KuramBio, St. 02-10, 03.08.2012, east of the Kuril-Kamchatka Trench, 46°14.77' N–46°14.99' N, 155°32.79' E–155°32.62' E, 4859–4865 m, EBS, 15 sp., R/r 0.5/0.4–2.1/1.5 mm, SMF 6922.

RV *Sonne 223*, KuramBio, St. 11-11, 30.08.2012, south-east of the Kuril-Kamchatka Trench, 40°13.55' N–40°12.90' N, 148°06.77' E–148°06.20' E, 5349–5352 m, nine sp., R/r 5.8/2.8–34.0/14.5 mm, SMF 6923.

RV *Sonne 223*, KuramBio, St. 11-12, 31.08.2012, south-east of the Kuril-Kamchatka Trench, 40°12.328'–40°12.106' N, 148°5.738'–148°5.538' E, 5350–5348 m, two sp., R/r 0.56/0.42 and 3.2/2.0 mm. Total: There are 94 specimens from 15 stations, with R values from 0.5 to 34.0 mm.

Description. The adambulacral plates first appear at an R of 0.8 mm and bear single furrow spines. The superomarginals and inferomarginals first appear at an R of 2.0 mm; dorsal spines at an R of 11 mm; ventrolateral plates, segmental papilla and scales of central cribriform organ at an R of 2.8 mm; apical appendage at an R of 3 mm and the scales of lateral cribriform organs at an R of 3.5 mm. The change in numerical characters depending on body size is shown in Table 4. The number of inferomarginals is usually equal to the number of superomarginals; they are arranged exactly opposite to each other. The superomarginals are slightly taller or the same height as the inferomarginals at the center of the interradius and 1 and 1.5 times higher than the inferomarginals in the distal part of the arm. The inferomarginal row is continuous and always reaches the terminal plate. The length of the dorsal spines gradually increases with age, but never exceeds the height of the superomarginal plates. Two marginal spines on each side of the oral plates are spearhead-shaped at an R of 0.4–1.0 mm, wide and flattened at an R of 1.0–2.0 mm (Figure 6A) and they are like flat scales in larger specimens (Figure 6B,C). Both furrow spines are spearhead-shaped at an R of 1.0–2.0 mm (Figure 6A). As the size of the asteroids increases, the more distal furrow spine gradually flattens and modifies into so-called 'segmental papilla'—a rounded ossicle covering an excavated pit on the surface of the adambulacral plate like a lid (Figure 6C). The furrow spines never form pedicellariae. The ventrolateral areas are provided with a pavement of spineless plates, and the skin spaces are usually small (Figure 6A–C). There are usually three terminal spines.

Table 4. Age variability in the numerical characters of *Eremicaster* species: sm—superomarginal plates, im—inferomarginal plates, ad. pls.—adambulacral plates; cr.o.—cribriform organ; vl. pls.—ventrolateral plates.

R/r, mm	Number of Plates			Number of Rows		Number of Dorsal Spines in sm Row
	sm	im	ad	Vertical Series of Scales in Central cr.o.	Transversal Series of vl. pls.	
<i>E. crassus</i> , RV Sonne 223, St. 2–10						
0.5/0.4	0	0	0	0	0	0
1.1/0.9	0	0	1	0	0	0
2.1/1.5	1	1	2	0	0	0
<i>E. crassus</i> , RV Sonne 223, St. 11–11 and St. 11–12						
3.2/2.0	2	2	4	2–4	1	0
5.8/2.8	4	4	8	4–8	1–2	0
11.0/4.5	6	6	11	12	4–5	0
15.5/7.0	7–8	7–8	16	16	7	4
26.0/11.5	10	10	20	16–20	9	6–7
34.0/14.5	10–11	10–11	22	22	10–11	5–7
<i>E. pacificus</i> , RV Akademik Kurchatov, cruise 4, St. 220						
2.3/1.7	1	1	3	0	0	0
2.6/1.9	1	1	3–4	2	1	0
3.6/2.4	2	2	5	4–5	2	0
4.0/2.5	2	2	5	4	3	0
4.6/2.7	3	3	6	6–7	4	1
7.2/4.5	4	4	8	8	4	3
15.0/7.8	6	6	11	14	6–7	6
<i>E. pacificus</i> , RV Ob, St. 648						
8.7/4.6	4	4	9	8	4	3–4
14.6/5.7	7	7	14	12–14	4–5	6
21.6/9.4	9	9–11	16	16	6	8–9
25.8/11.0	13–14	14–17	19	16	7	11–12

In the specimens from stations RV *Vityaz* 5620, 5622, 5623 and 5624, the stereome is coarser than usual. For this reason, the surface of the superomarginal, inferomarginal, adambulacral and terminal plates is strongly porous and sometimes (St. 5620) has a dense cover of tiny thorns. In some specimens, some morphological structures are formed in the process of ontogeny later or earlier than usual. In the specimen from RV *Vityaz* St. 4666 (R/r 13.0/6.0 mm), the cribriform organs are less developed than usual in specimens of the same size: 8 vertical series in the central cribriform organ and 2–4 series in the lateral cribriform organs. The specimens from RV *Vityaz* St. 6135 are also with slow development: the lateral cribriform organs are absent at an R of 4.6 mm; the dorsal spines on the superomarginals are absent at an R of 20 mm and first appear at an R of 21 mm.

Remarks. *E. crassus* differs from *E. pacificus*, *E. vicinus* and all *Porcellanaster* species already starting from an R of 1.0–2.0 mm: its marginal spines of oral plates are wide and flattened (Figure 6B,C), while they are spearhead-shaped in other species. However, the juveniles of *E. crassus* and *Caulaster* at this stage are difficult to distinguish, as *Caulaster*'s marginal spines are also wide and flattened. Starting from an R of 2.8 mm, *E. crassus* is easily distinguished from *E. pacificus*, *E. vicinus* and all *Porcellanaster* and *Caulaster* species due to the presence of segmental papillae (Figure 6C).

E. crassus, like other porcellanasterids, is characterized by the presence of a few specimens with a morphology that is transitional from one species to another, or even from one genus to another. For example, the specimens from RV *Vityaz* St. 4131 and 6107, with

an R of 3.5–17.0 mm, differ from typical *E. crassus* in having only one cribriform organ per interradius. In this respect, they are similar to representatives of the genera *Porcellanaster* and *Caulaster*. The morphology of a specimen from RV *Vityaz* St. 5939 with an R/r of 11.5/5.8 mm is transitional to that of *Caulaster* (see remarks on *Caulaster* sp. B). Madsen [3] reported that some *E. crassus* from *Galathea* St. 474 lack segmental papillae (feature of *E. pacificus* and *E. vicinus*), and specimens from *Galathea* St. 716 had spines on ventrolateral plates (feature of *E. pacificus*). Representatives of *Porcellanaster*, *Eremicaster* and *Caulaster* are regularly found together, and specimens with transitional morphology may be the result of interspecific hybridization.

Distribution. Pacific Ocean, Indian Ocean, Antarctic and off Uruguay in the Atlantic. Depth range 2418–6328 m.

***Eremicaster pacificus* (Ludwig, 1905)**

Figure 6D–J.

Porcellanaster pacificus—Ludwig, 1905: 89–92, pl. 6.28–29 [64].

Eremicaster pacificus—Fisher, 1911: 29–31, pl. 2.1–3 [65]; H. L. Clark 1913: 187 [66]; H. L. Clark 1920: 76 [67]; Baranova, 1957: 154–155 [72]; Djakonov, 1958: 282–284 [73]; Madsen, 1961a: 160–161 [3]; Luke, 1982: 11 [63]; Belyaev, 1985b: 870–871 (Figure 1B) [70]; A.M. Clark, 1989: 299 [2]; Lambert and Boutillier, 2011: 83 (Figure 63) [55] and Mironov et al., 2018: 344 [74].

Syntypes. USNM 34401 (two alcohol), Albatross, St. 3360; USNM 34402 (two alcohol), Albatross, St. 3362; USNM 34399 (one alcohol), Albatross, St. 3376; USNM 34400 (six alcohol), Albatross, St. 3392; USNM 34398 (two alcohol), Albatross, St. 3400; USNM 34403 (one alcohol), Albatross, St. 3411; USNM 34404 (one alcohol), Albatross, St. 3415 (2).

Type locality. Exact locality not stated. Description based on specimens from seven stations between latitudes 14°46' N and 0°36' S and longitude 98°40' W in the region of the Gulf of Panama; 2070–3446 m.

Material examined. RV *Ob*, First Antarctic expedition, St. 115, 16.05 1956, Kergelen Ridge, 58°43' S, 80°52' E, 1580–1601 m, nine sp., R/r 18.5/6.5–29/17 mm, IORAS ECHO1343 and ECHO1355.

RV *Ob*, St. 698, 09.04 1963, off Endeby Land, 66°48' S, 45°42' E, 1820–2020 m, eight sp., R/r 8.7/4.6–25.8/11.0 mm, IORAS ECHO1341 and ECHO1350.

RV *Vityaz*, cruise 10, St. 1599, 27–28.06 1952, Bering Sea, 58°57' N, 167°55' E, 2995–3130 m, four sp., R/r 23.0/10.0–25.0/13.0 mm, IORAS ECHO1342 and ECHO1352.

RV *Vityaz*, cruise 24, St. 3577, 10.05.1957, east of the Japan Trench, 38°40' N, 143°29' E, 3042 m, eight sp., R/r 7.2/3.6–20.5/9.5 mm, IORAS ECHO1702.

RV *Vityaz*, cruise 39, St. 5637, 09.09.1966, west of the Japan Sea, 44°29' N, 149°06' E, 3605–3015 m, one sp., R/r 14.8/6.5 mm, IORAS ECHO1347.

RV *Vityaz*, cruise 45, St. 6105, 12.05.1969, 58°55'0" N, 142°03'0" W, 2970–2980 m, five sp., R/r 8.0/3.2–20.6/10.2 mm, IORAS ECHJ01701.

RV *Vityaz*, cruise 45, St. 6111, 56°16' N, 137°58' W, 2880–2890 m, two sp., R/r 9.4/4.3 and R/r 13.0/6.0 mm, IORAS ECHO1335.

RV *Vityaz*, cruise 45, St. 6135, 09.06.1969, 53°32'0" N, 163°22'0" W, 2880–2930 m, four sp., R/r 3.1/2.1–19.5/9.0 mm, IORAS ECHO1334 and ECHO1345.

RV *Akademik Kurchatov*, cruise 4, St. 220, 30.08 1968, 00°25'0" S, 85°00'0.1" W, 2265 m, eight sp., R/r 2.3/1.7–15.0/7.8 mm, IORAS ECHO1344.

RV *Akademik Kurchatov*, cruise 4, St. 308, 08.11.1968, off Ecuador, 01°46'7" S, 82°58'0" W, 2150 m, 19 sp., R/r 5.4/2.9–28.0/13.0 mm, IORAS ECHO1361.

RV *Akademik Kurchatov*, cruise 17, St. 1471, 03.03.1974, 2400–2600 m, seven sp., R/r 5.5/3.1–20.0/8.0 mm, IORAS ECHO1362.

RV *Dmitry Mendeleev*, cruise 20, St. 1648, 15.03.1978, 10°46' N, 79°00' W, 2330 m, one sp., R/r 20.0/9.5 mm, IORAS ECHO1346.

RV *Dmitry Mendeleev*, cruise 38, St. 3491, 11.02.1987, off Ecuador, 2850 m, three sp., R/r 8.5/4.8–24.5/11.0 mm, IORAS ECHO1366.

Total: There are 79 specimens from 13 stations, with R values from 2.3 to 29.0 mm.

Description. The superomarginal plates first appear at an R of 2.3 mm; the scales of the central cribriform organ, ventrolateral plates and apical appendage at an R of 2.6 mm (Figure 6E); the scales of the lateral cribriform organs at an R of 3.2 mm, the dorsal spines at an R of 4.6 mm and the spines on ventrolateral plates at an R of 5.4 mm. The change in numerical characters depending on body size is shown in Table 4. The two furrow spines are uniform (slender and pointed) at all stages of postlarval development.

The specimens from the East Pacific and Antarctic (the stations of RV *Akademik Kurchatov*, RV *Dmitry Mendeleev* and RV *Ob*) differ from the those from the North Pacific (the stations of RV *Vityaz*) by the number of terminal and dorsal spines. In the first group of specimens, the number of terminal spines increases from 3 at an R < 7 mm to 5–7 in adults. The superomarginal plates usually bear no more than one dorsal spine. In the North Pacific, the number of terminal spines increases from 3 at an R < 5 mm to 5–7 at an R of 5–7 mm and further up to 7–11 in adults. The maximum number of terminal spines in the specimen from RV *Vityaz* station 3577 (R 19.5 mm) is 19 (Figure 6I). The maximum number of dorsal spines per superomarginal plate increases from 0 to 3–4 as the sea star grows.

Remarks. The differences in the number of dorsal and terminal spines between *E. pacificus* from the North and East Pacific (Figure 6H–J) likely do not have taxonomic significance but show great intraspecific variability. Similar variability has been previously described for *E. crassus* [3]. Dorsal spines first appear much earlier in *E. pacificus* than in *E. crassus* and *E. vicinus*, at an R of 4.3 mm and an R of 11–13 mm, respectively. *E. pacificus* is easy to distinguish from *E. crassus* at an R of approximately 2.8 mm due to the absence of segmental papillae. The main diagnostic character of *E. pacificus* is the presence of spines on the ventrolateral plates (Figure 6G), which first appear at an R of 5.4 mm. However, Madsen [3] (Figure 29) reported two specimens of *E. crassus* that combine features such as segmental papillae on adambulacral plates and spines on ventrolateral plates. These two specimens with R values of 46 mm were found in a sample of 86 typical *E. crassus* specimens with an R from 8 to 52 mm.

Distribution. From the Bering Sea to Japan and Chile, also Antarctic. Distribution range in the East Pacific is limited to the narrow zone extending meridionally along the base of the American continental slope. Some other deep-sea echinoderms have similar range [23]. Depth range 1570–4088 m.

***Eremicaster vicinus* (Ludwig, 1907)**

Figure 7E–H.

Porcellanaster vicinus—Ludwig, 1907: 318 [75].

Porcellanaster vicinus inermis—Ludwig, 1907: 318 [75].

Eremicaster vicinus—H. L. Clark, 1920: 77–78, pl. 27–29 [67]; Madsen, 1961a: 161–165, Figure 30 [3]; Belyaev and Mironov, 1977: 16, 17 [52]; Belyaev, 1985b: 871–873 (Figure 1G) [70]; A.M. Clark, 1989: 299 [2]; Clark A.M. and Downey, 1992: 97–98 (Figure 18e [7]); Clark H.E.S. and McKnight, 2000: 119–120; pl. 33 (Figure 32) [57]; Dilman, 2013: 567–568 [39]; Mironov et al., 2015: 366 [23]; Petrov et al., 2016: 566 (Figure 1b) [16] and Mironov et al., 2019: 3–4 [71].

Eremicaster pacificus—Madsen, 1951: 76–78 (Figure 1) [76] and Madsen, 1956: 26–27 [77] (non *E. pacificus* Ludwig).

Syntypes. USNM E941, 2 dry and 25 alcohol, USFC Albatross, St. 4670; USNM E704, one dry, USFC Albatross, St. 4670.

Type locality. USFC Albatross, St. 4670, off Peru, 12°08' S, 79°02' W, 5869 m.

Material examined RV *Vityaz*, cruise 29, St. 4120, 05.11.1958, Aleutian Trench, 47°19' N, 175°49' E, 6296–6328 m, four sp., R/r 16.0/7.05–21.0/9.5 mm, IORAS ECHO1429.

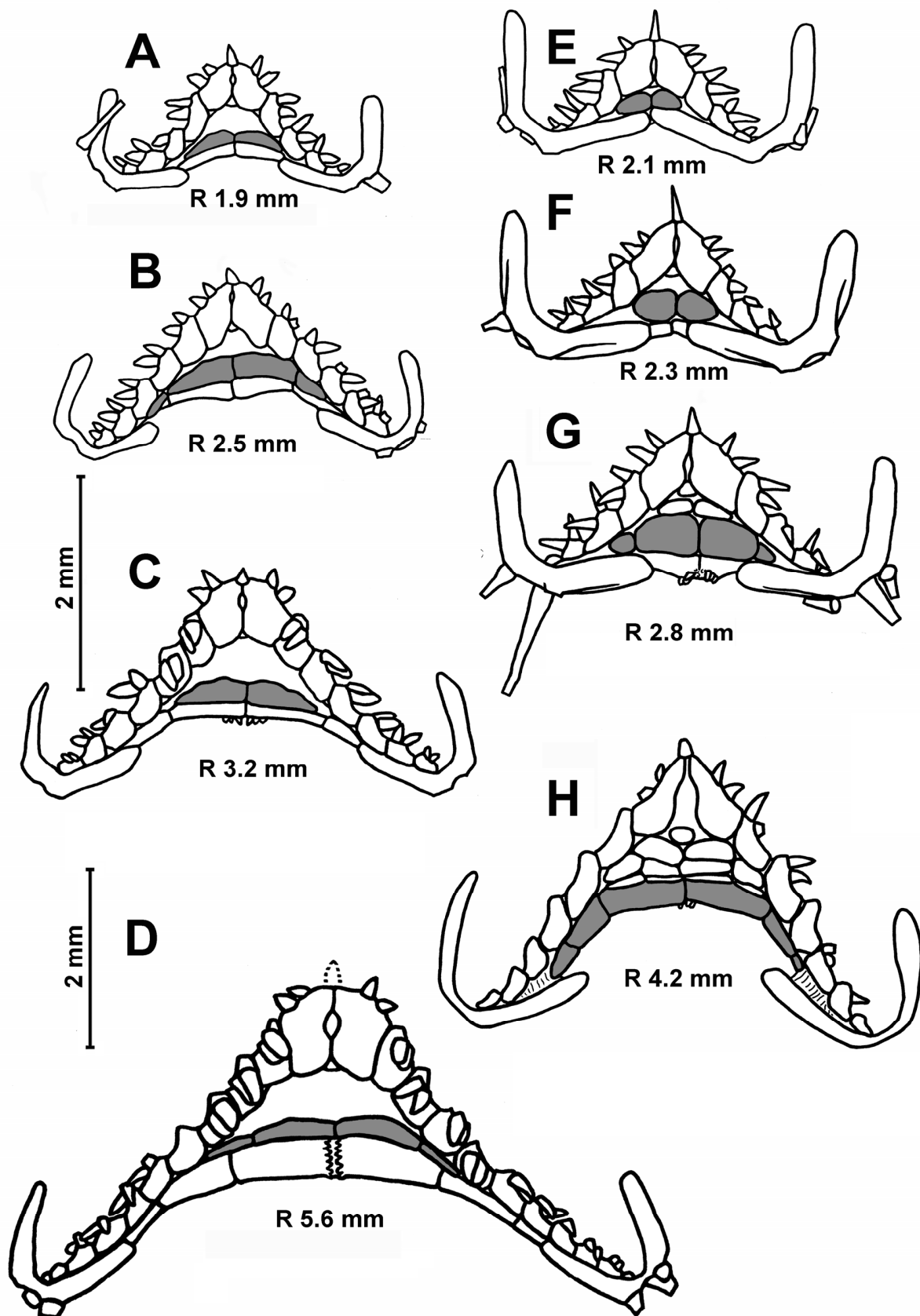


Figure 7. Age variability of the ventrolateral area pavement in *Caulaster pedunculatus* (A–D) and *Eremicaster vicinus* (E–H) from the Cape Verde Basin, RV *Akademik Ioffe*, St. 1608. Ims are marked in gray. Scales: 2 mm.

RV *Akademik Ioffe*, cruise 16, Sta. 1605, 21.10.2004, 11°31,5' N, 27°56.9 W; 11°30.4' N 27°57.7' W; 5956–5958 m, 60 sp., R 2.4/1.7–19.0/? mm, IORAS ECH02176 and ECH02189.

RV *Akademik Ioffe*, cruise 16, St. 1608, 22.10.2004, Cape Verde Basin, 11°26.4'–11°25.5' N, 28°02,3'–28°03,4' W, 5837–5840 m, 74 sp., R/r 1.4/1.2–24.0/10.0 mm, IORAS ECH02180.

RV *Akademik Ioffe*, cruise 29, St. 2169, 05.11 2009, Romanche Fracture Zone, 00°23'07" N–00°23'47" N, 16°23'34"–16°24'34" W, 5560 m, 13 sp., R/r 4.8/2.9–26/13 mm, IORAS ECH02174.

RV *Jean Charcot*, BIOVEMA, Sta. DS 09. 11°36' N, 32°52' W, 5875 m, 25.11.1977, one juv., R/r = ~2.6/1.6 mm.

Total: There are 152 specimens from five stations, with R values from 1.4 to 26 mm.

Remarks. The main differences between the juveniles of *E. vicinus*, *E. crassus* and *E. pacificus* were mentioned above (see remarks for *E. pacificus*), and the study of age variability in *E. vicinus* does not provide anything new in this respect. Samples obtained by RV *Akademik Ioffe* in the Atlantic basins contain hundreds of specimens of two species, *E. vicinus* and *Caulaster pedunculatus*, with an R from 1.4 to 26.0 mm. Specimens of *E. vicinus* were easily determined and started from an R of about 2.8 mm due to the presence of ventrolateral plates (Figure 7G,H). The identification at smaller sizes is less reliable and based on the following two differences: (i) the superomarginals first appear at an R of 2.3 mm in *E. vicinus* and at an R of 1.4 mm in *C. pedunculatus* (Figure 7A,F); (ii) juvenile inferomarginals are rounded in the former and oblong in the latter (Figure 7A,B,E,F).

Distribution. The Pacific, Indian, Atlantic and Southern Oceans. Depth range 2605–7250 m. Among asteroids, *E. vicinus* is the most widely distributed species at depths greater than 6000 m. It is known from the Aleutian, Izu-Bonin, Japan, Kermadec, Kuril-Kamchatka, Peru–Chile (Atakama) and South Sandwich trenches [3,16,71,78–80].

Genus *Caulaster* Perrier, 1882

Albatrossia Ludwig, 1905 [64]; type species *A. semimarginalis* Ludwig, 1905.

Albatrossaster Ludwig, 1907 [75]; a name to replace *Albatrossia* considered invalid.

Damnaster H.E.S Clark et McKnight, 1994 [59]; type species *D. tasmani* H.E.S Clark et McKnight, 1994.

Included species. *C. pedunculatus* Perrier 1882 (type species) and *C. semimarginalis* (Ludwig, 1905). *Caulaster* sp. A and *Caulaster* sp. B are treated here as possibly two new species.

Diagnosis. Small porcellanasteridae with an R up to 20 mm. The dorsal pedicellariae are usually present at an R > 5 mm. The furrow spines on the adambulacral plates are scale-shaped or pedicellaria-like. The superomarginal plates of the arm are spineless and not contiguous midradially. The inferomarginal rows in adult specimens are usually interrupted and do not reach the terminal plate. There is only a single lamelliform cribriform organ in each interradius. Each jaw with a single apical spine is common to the two oral plates. The ventrolateral areas are naked or with a few tiny plates, except for *C. semimarginalis*. There are odd interradial marginal plates; the paxillae, suboral and subambulacral armament are absent.

Remarks. Some specimens of *Porcellanaster* have been described or imaged as having pedicellariae [3,7,10,28,46,56,60,76,80]. They are considered by us below as belonging to the genus *Caulaster*. The differences between *A. semimarginalis* and *C. pedunculatus* are probably significant enough to re-establish the genus *Albatrossia* (see Discussion).

Caulaster pedunculatus Perrier, 1882

Figures 7A–D, 8A,B and 9A–I.

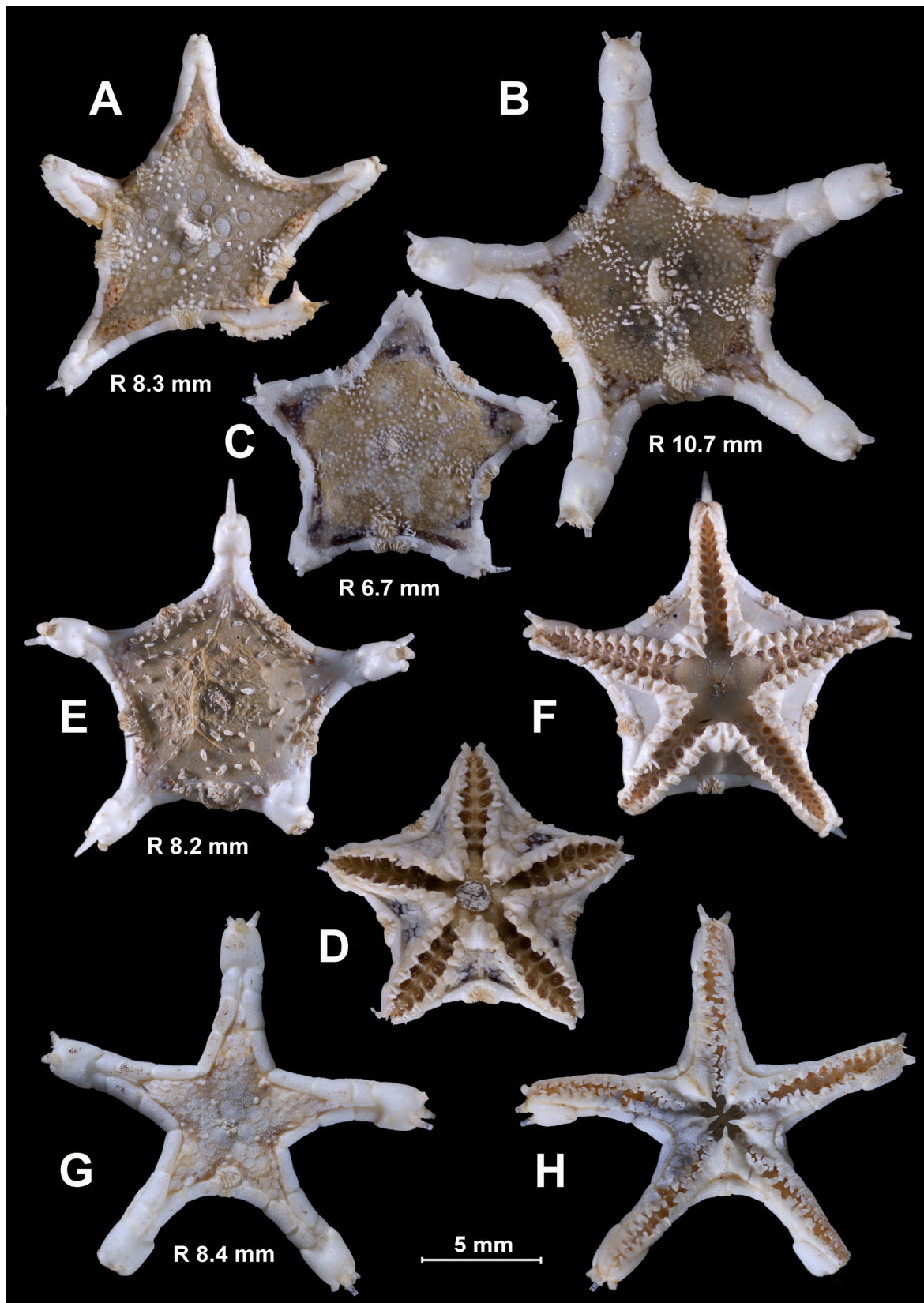


Figure 8. The species of the genus *Caulaster*, views from above and below. (A) *C. pedunculatus*, St. 4158, RV Vityaz; (B) *C. pedunculatus*, St. 5082, RV Vityaz; (C,D) *C. semimarginalis*, St. 308, RV Akademik Kurchatov; (E,F) *C. sp. A*, St. 3904, RV Dmitry Mendeleev; (G,H) *C. sp. B*, St. 5159, RV Vityaz. Scale: 5 mm.

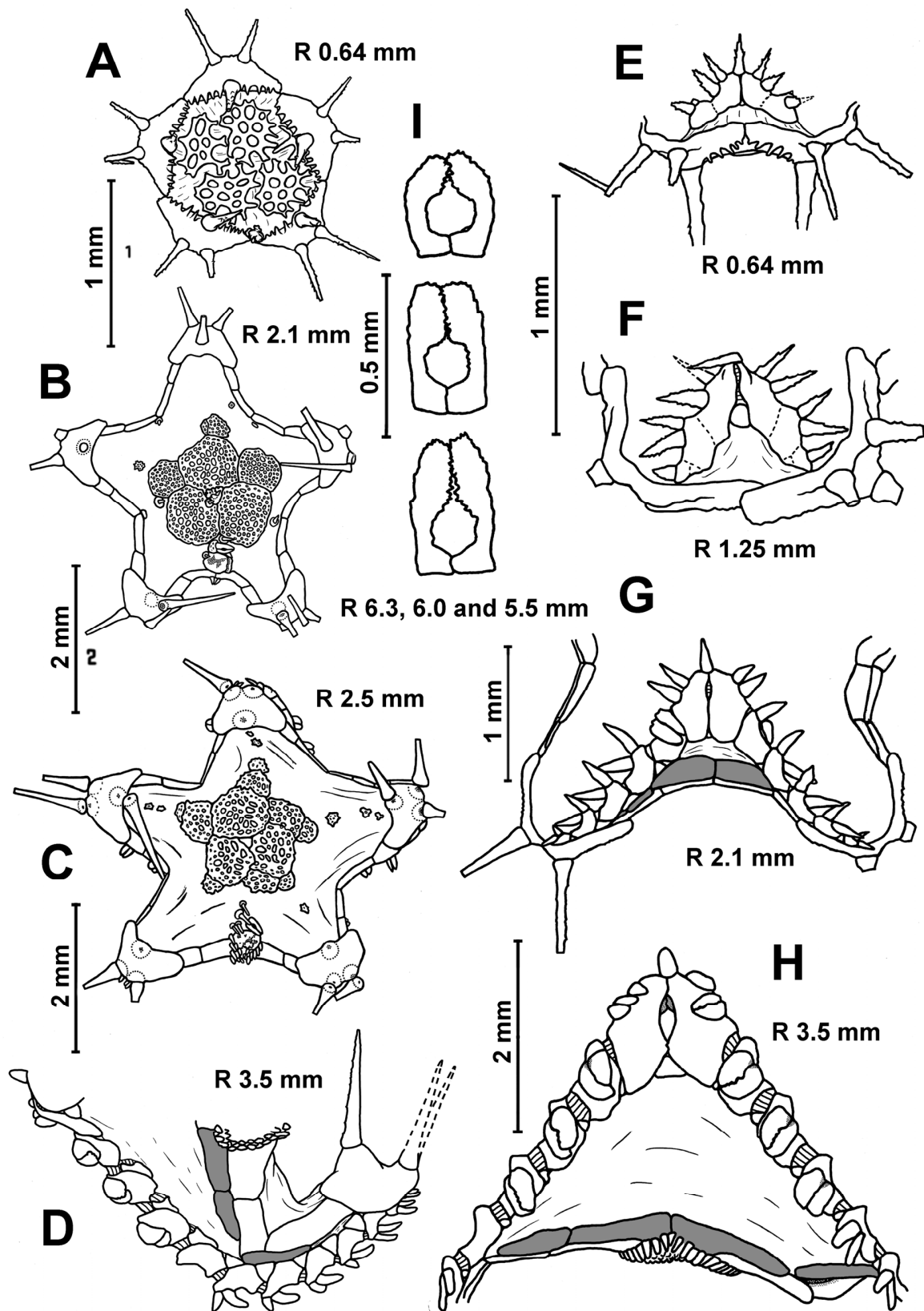


Figure 9. Age variability in the dorsal disk pavement (A–C), furrow spines (D–H) and dorsal pedicellariae (I) in *Caulaster pedunculatus* from the Gulf of Bicay (near type locality). (A,E) St. KG 30; (B,C,F,G) St. CP 01; (D,H,I) St. KG 36, RV *Le Noroit*. Scales: 1 mm (A), (E–G); 2 mm (B–D,H); 0.5 mm (I).

Caulaster pedunculatus—Perrier, 1882: 1379–1381 (Figures 1–5) [81]; Perrier, 1885b: 45–47 [42]; Perrier, 1894: 202–208, pl. XV. 1. A–e [43]; Belyaev, Mironov, 1986: 896–898 (Figures 1–5) [6]; Clark A.M., Mah, 2001: 332 [82]; Dilman, 2006: 179 [83]; Dilman, 2008: 135–136 [38]; Dilman, 2014 [40]: 28 and Mironov et al., 2016: 505 (Figure 1e) [5].

Porcellanaster eremicus—Sladen, 1889: 145–149, textfig. [10].

Albatrossaster richardi—Koehler, 1909b: 25–28, pl. 19.7–9 [84].

Porcellanaster coeruleus—Lieberkind, 1935 (part): pls. II.2-6, III.12, V.17; (Figure 1B–D. 3. 1–2,4,+ [46]).

Porcellanaster caeruleus—Madsen, 1951: 74–76 [76]; Madsen, 1961a (part): 127, 128, 129, 132, 133, 134, 142, (Figure 24 i–k (RV *Galathea*, St. 574)) [3]; Bernasconi, 1967: 443–445 (Figures 3–6) [60] and Clark H.E.S., 1970 (part): 14 (St. 1837), pl. 1 E–F [56].

Porcellanaster ceruleus—Gage et al., 1983 (part): 275–276 [47]; Clark A.M., 1989 (part): 300 [2] and Clark A.M., Downey, 1992 (part): 100–101 [7] (non *Porcellanaster ceruleus* Thomson, 1877).

Caulaster eremicus—Belyaev, Mironov, 1996: 896–898 (Figure 5) [6] and Clark A.M., Mah, 2001: 332 [81].

Damnaster tasmani—Clark H.E.S, McKnight, 1994: 1368–1371 (Figures 1–4) [58]; Clark H.E.S, McKnight, 2000: 116–117, (Figure 31, pl. 32) [56]; Clark A.M., Mah, 2001: 332–333 [82] and Mah, 2023: WoRMS on 2023-07-30 [8].

Syntypes. Muséum National d’Histoire Naturelle, Paris, Syntype # EcAs 3145 (E 296a), RV *Travailleur* 1881, St. 4, R/r 5/3 mm; Syntype # EcAs 3146 (E1 296b), RV *Travailleur* 1880, St. 10, 07.26.1880, R/r 3.2/1.7 mm.

Type localities. RV *Travailleur* 1881, St. 4, Bay of Biscay, 43°00′ N, 9°37′ W, 2020 m; RV *Travailleur* 1880, St. DR10, 07.26.1880, Bay of Biscay, 43°39′ N, 3°28′ E, 1960 m.

Material examined. RV *Ob*, Second Antarctic Expedition, St. 115, 16.05.1956, Kergelen Ridge, 58°43′ S, 80°52′ E, 1580–1600 m, one spm., R/r 9.0/4.0 mm, IORAS ECHO2623.

RV *Ob*, The Second Antarctic Expedition, St. 285, 11.04.1957, Australian–Antarctic Basin, 59°25′ S, 97°23′ E, 4540 m, three spms., R 11.0–16.0 mm, IORAS ECHO1826.

RV *Vityaz*, cruise 29, St. 4066, 16.10.1958, SW of Aleutian Trench, 47°19′ N, 175°49′ E, 5681–5740 m, five spms., R/r 6.5/3.0–7.0/3.2 mm, IORAS ECHO1825 and ECHO1869.

RV *Vityaz*, cruise 29, St. 4074, 20.10.1958, North-East Pacific Basin, 40°19′ N, 175°45′ E, 6065 m, five spms., R/r 5.1/2.3–11/4.8 mm, IORAS ECHO1866.

RV *Vityaz*, cruise 29, St. 4120, 05.11.1958, Aleutian Trench, 47°19′ N, 175°49′ E, 6296–6328 m, two spms., R/r 2.6/1.4 and 9.5/4.5 mm, IORAS ECHO2134 and ECHO1823.

RV *Vityaz*, cruise 29, St. 4158, 26.11.1958, East Pacific Basin, 46°56′ N, 143°59′ W, 4661–4665 m, 39 spms., R 1.5–9.0 mm, IORAS ECHO1822, ECHO1900 and ECHO1917.

RV *Vityaz*, cruise 33, St. 4936, 03.02.1961, Bay of Bengal, 13°35′ N, 86°53′ E, 3103 m, one spm., R/r 4.4/2.0 mm, Cat. No. 1886.

RV *Vityaz*, cruise 34, St. 5082, 16.09.1961, north of Iles Marquises, 05°58′ N, 139°57′ W, 4842 m, seven spms., R/r 9.5/4.5–13.5/6.0 mm, IORAS ECHO1821, ECHO1865, ECHO1873 and ECHO1874. RV *Vityaz*, cruise 35, St. 5210, 01.09.1962, north-west of Cocos Island, 06°58′ S, 91°01′ E, 5175 m, one spm., R/r 11.0/3.8 mm, IORAS ECHO1916.

RV *Vityaz*, cruise 35, St. 5249, 30.09.1962, east of Chagos Archipelago, 05°07′ S, 77°09′ E, 2970–2931 m, one spm., R/r ?/2.1 mm, IORAS ECHO1824.

RV *Vityaz*, cruise 45, St. 6088, 04.05.1969, south-east of Aleutian Trench, 53°58′ N, 157°36′ W, 5740 m, one spm., R/r = 7.0/3.5 mm, IORAS ECHO1870.

RV *Jean Charcot*, BIOVEMA, St. CP 06, 20.11.1977, Cape Verde Basin, 11°34′ N, 32°54′ W, 5880 m, 90 spms., R/r 5/2.5–11/4 mm.

RV *Jean Charcot*, BIOVEMA, St. DS 09, 25.11.1977, Cape Verde Basin, 11°36′ N, 32°52′ W, 5875 m, 25 spms., R/r 0.46/0.38–11/4.5.

RV *Jean Charcot*, BIOVEMA, St. DS 11, 26.11.1977, Cape Verde Basin, 11°37′ N, 32°54′ W, 5867 m, 37 spms., R/r 0.50/0.41–10.2/4.8 mm.

RV *Jean Charcot*, WALVIS 1, St. CP 01, 24.12.1978, Cape Basin, 33°54′ S, 05°07′ E, 5040 m, two spms., R/r 4.0/2.0–5.6/2.3 mm.

RV *Jean Charcot*, WALVIS 1, St. DS 01, 24.12.1978, Cape Basin, 33°54' S, 05°06' E, 5205 m, one spm., R/r 9.0/4.0 mm.

RV *Jean Charcot*, WALVIS 1, St. CP 06, 30.12.1978, Cape Basin, 33°22' S, 02°36' E, 4550 m, one spm., R/r 6.5/3.5 mm.

RV *Akademik Kurchatov*, St. 22, 20.04.1967, 12°22' N, 61°16' E–12°22' N, 61°15' E, 2880–2920 m, one spm., R/r 5.5/2.8 mm, IORAS ECHO1918.

RV *Akademik Mstislav Keldysh*, cruise 4, St. 268, 30.07.1982, Reykjanes Ridge, 58°53' N, 24°06' W, 2665–2667 m, 204 spms., R/r 2.3/1.5–8.5/4.8 mm, IORAS ECH01820, ECH01857, ECH01859 and ECH01867.

RV *Akademik Mstislav Keldysh*, cruise 4, St. 415, 25.08.1982, Reykjanes Ridge, 58°24' N, 31°31' W, 1535–1830 m, six spms., R/r 2.2/1.4–7.3/3.7 mm, IORAS ECH01864 and ECH01868.

RV *Akademik Mstislav Keldysh*, cruise 4, St. 499, 09.09.1982, Reykjanes Ridge, 58°04' N, 30°21' W, 2429–2440 m, 54 spms., R/r 2.2/1.4–7.3/3.7 mm, IORAS ECH01887, ECH01904 and ECH01926.

RV *Dmitry Mendeleev*, cruise 43, St. 4104, 02.04.1989, Weddell Sea, 62°33.4'–62°36.4' S, 15°28.1'–15°32.7' W, 5110–5120 m, 67 spms., R/r 2.0/1.2–12.1/6.0 mm, IORAS ECH01850, ECH01852, ECH01853 and ECH01854.

RV *Le Noroît*, ECOFER 1, St. CP 01, 05.07.1989, Bay of Biscay, 44°46.20' N, 02°38.15' W, 3017 m, five spms., R/r 0.83/0.65–5.0/2.5 mm.

RV *Le Noroît*, St. CP 02, Bay of Biscay, 44°46.14' N, 02°38.92' W, 3000 m, 18 spms., R/r 2.2/1.2–7.6/3.2 mm.

RV *Le Noroît*, St. KG 30, Bay of Biscay, 3055 m, two spms., R/r 0.63/0.49 and 4.5/2.4 mm.

RV *Le Noroît*, St. KG 35, Bay of Biscay, 3024 m, one spm., R 2.9 mm.

RV *Le Noroît*, St. KG 36, Bay of Biscay, 3055 m, two spms., R/r ?/3.5–?/2.7 mm.

RV *Akademik Ioffe*, cruise 16, St. 1605, 21.10.2004, Cape Verde Basin, 11°31.5'–11°30.4' N, 27°56.9'–27°57.7' W, 5956–5958 m, 460 spms., R/r 1.5/1.1–12.5/6.0 mm, IORAS ECH01855, ECH02178, ECH02190, ECH02605, ECH02606 and ECH02607.

RV *Akademik Ioffe*, cruise 16, St. 1608, 22.10.2004, Cape Verde Basin, 11°26.4'–11°25.5' N, 28°02.3'–28°03.4' W, 5837–5840 m, 502 spms., R/r 1.4/1.0–10.9/4.7 mm, IORAS ECH01856, ECH02173 and ECH02177.

RV *Akademik Ioffe*, cruise 29, St. 2169, 05.11.2009, Romanche Fracture Zone, 00°23'07" N–00°23'47" N, 16°23'34"–16°24'34" W, 5560 m, 133 spms., R/r 2.2/1.5–20.0/9.0 mm, IORAS ECH02179, ECH02181 and ECH02187.

RV *Akademik Ioffe*, cruise 29, St. 2192, 25.11.2009, Cape Basin, 36°22'37.51"–36°21'55.51" S, 05°48'56.40"–05°50'36.05" E, 5066–5044 m, five spms., R 3–5 mm, ECH02622.

RV *Sonne*, cruise 237, Vema-TRANSIT, St. 4–9, 27.12.2014, Cape Verde Basin, 10°25.65'–10°25.66' N, 31°02.98'–31°02.98' W, 5733 m, 33 spms., R/r 0.38/0.31–9.5/3.8 mm, SMF 6924.

Total: 1715 specimens from 32 stations, R from 0.38 to 20.0 mm.

Description. The change in quantitative characters of the *C. pedunculatus* depending on body size is shown in Table 5. In the smallest specimens (R 0.46–1.40 mm), the terminal plates touch each other, since the supermarginals and infermarginals have not formed yet (Figures 8A and 9A,E,F). A continuous ring of 3–8 large, perforated plates occupy almost the entire dorsal surface of the disc at an R of 0.46–0.80 mm (Figure 9A–C). A few small plates with a spine appear in the interradius at an R of 2.0–2.5 mm. As the size of the body increases, five interradiial bands of small plates bearing spines are gradually formed. They alternate with five radial bands of spineless perforated plates (Figure 8A,B). The plates are usually separated from each other by skin spaces. An apical appendage is present or absent. The dorsal pedicellariae first appear near the madreporite at an R of 2.1 mm (Figure 9B,C), but are sometimes absent in larger specimens. The shape of the pedicellariae valves varies from narrow to wide (Figure 9I).

Table 5. Age variability in the quantitative characters of *Caulaster pedunculatus* from the Atlantic and Antarctic. Sm—superomarginal plates, im—inferomarginal plates, ad—adambulacral plates, vl—ventrolateral plates, cr.o.—cribriform organ.

R/r, mm	Number				Dorsal Pedicellariae	Rows of Lamellae in cr.o. **
	Plates					
	sm *	im *	ad	vl		
Bay of Biscay, 3055 m, RV <i>Le Noroît</i> , ECOFER, St. KG30						
0.6/0.5	0	0	1	0	0	0–0
Bay of Biscay, 3017 m, RV <i>Le Noroît</i> , ECOFER, St. CP1						
0.8/0.6	0	0	2	0	0	0–0
2.1/1.2	2	2	5	0	1	0–2
2.5/1.5	2	2	6	0	1	0–4
Bay of Biscay, 3033 m, RV <i>Le Noroît</i> , ECOFER, St. CP2						
3.2/1.6	2	2	6	0	?	0–4
5.1/2.5	3	2–3	9	0	2	4–8
5.5/2.2	3	3	10	0	16	4–8
5.5/2.6	4	4–5	10	3–9	0	8–10
6.8/3.2	4	4	11	0–2	2	10–12
7.6/3.2	4	3–5	12	0–1	16	10–14
Reykjanes Ridge, 2665–2667 m, RV <i>Akademik Mstislav Keldysh</i> , cruise 4, St. 268						
2.3/1.5	2	2	5	0	0	0–0
3.0/1.8	2	2–3	6	0	0	0–2
3.5/1.8	2	2	7	0	2	0–4
3.9/2.4	3	3–4	8	0	0	0–2
4.2/2.5	3	2	8	0	0	0–6
5.2/2.9	4	4	9	0–2	0	4–8
5.3/3.0	3	2–3	10	0–1	0	6–8
5.8/3.1	4	3	10	0	0	6–8
6.4/3.4	3	3	10	0	0	6–8
8.5/4.8	4	4	13	0–1	0	8–12
Cape Verde Basin, 5837–5840 m, RV <i>Akademik Ioffe</i> , cruise 16, St. 1608						
1.4/1.0	1	1	3	0	0	0–0
1.9/1.3	1	1	4	0	0	0–0
2.5/1.4	2	2	5	0	0	0–0
3.2/1.8	2	1–2	6	0	0	0–2
3.6/2.0	2	2	7	0	0	0–4
5.6/2.8	3	2	9 (10)	0	3	2–8
6.8/3.2	3	2–4	11	0–1	?	4–8
8.5/3.5	4	3–5	13	0	?	6–8
10.8/5.2	3	1–2	13	2–20	?	6–10
11.0/5.2	4	1–3	15	0–2	7	6–6
Cape Verde Basin, 5956–5958 m, RV <i>Akademik Ioffe</i> , cruise 16, St. 1605						
8.5/3.5	4	1–2	12	0	?	4–6
9.0/4.0	3	3–4	12	0–9	2	4–8
10.5/4.1	5	4–5	13	0	0	8–10
12.5/6.0	3	3–4	14	0	0	8–10

Table 5. Cont.

R/r, mm	Number				Dorsal Pedicellariae	Rows of Lamellae in c.r.o. **
	Plates					
	sm *	im *	ad	vl		
Romanche Fracture Zone, 5560 m, RV <i>Akademik Ioffe</i> , cruise 29, St. 2169						
2.8/1.8	1 (2?)	1 (2?)	5	0	0	0–4
5.0/3.1	3	2–3	9	0	0	2–6
5.4/3.0	3	3–4	9	0	0	0–6
7.1/4.1	3	3	10	0	3	0–6
11.5/6.0	4–5	5–7	15	0–2	23	4–8
18.5/8.0	3–4	2	20	0	34	12–18
19.0/9.5	4–5	3–6	18	0	54	10–12
Weddell Sea, 5110–5120 m, RV <i>Dmitry Mendeleev</i> , cruise 43, St. 4104						
2.1/1.5	2	2	3–4	0	0	0–0
4.7/2.5	3	3	8	8	0	?
5.0/2.6	3–4	3–4	8	0–4	0	0–4
5.5/2.7	4	4	9	0–1	1	0–5
6.0/3.0	4	4	9 (10)	2–13	0	2–7
6.5/3.2	4	4–5	10	1–4	0	2–8
7.5/3.2	4 (5)	4	10	0–2	3	4–?
8.5/3.5	5–6	2–3	12	0	14	4–10
9.5/4.0	5	5	12	30–41	0	?–?
10.5/4.2	5–6	2–4	12 (13)	5–9	70	6–14
10.5/4.5	6–7	3–5	13	0–3	5	8–15
Australian–Antarctic Basin, 4540 m, RV <i>Ob</i> , St. 285						
11.2/5.0	5	5	12	2–5	0	7–9
13.5/5.5	5	5–6	12	0	0	10–13
16.0/6.2	6	4–6	15	0–3	4	13–18

* Number of superomarginals or inferomarginals from midline of interradius to terminal plate. ** Number of vertical lamellae rows in a cribriform organ of non-madrepore interradius and madrepore interradius.

Tiny superomarginals and inferomarginals appear at an R of 1.4 mm, a rudimental cribriform organ in the madrepore interradius at an R of 2.1 mm and a rudimental cribriform organ in other interradii at an R of 3.6 mm. As it can be seen from Table 5, cribriform organs may be absent in significantly larger specimens. In juveniles, the number of inferomarginals is equal to the number of superomarginals. In adults, the number of inferomarginal plates may be greater or less than the superomarginal ones. The inferomarginal series usually do not reach the terminal plate. The distal inferomarginals are significantly smaller than superomarginals. In most cases, the position of these rows is shifted relative to each other, and the inferomarginal row is interrupted (Figure 9D,H). The dorsal spines on the superomarginal plates is always absent. The arrangement of scales of the cribriform organs into vertical rows is less distinct than in *Porcellanaster*. The scales of the same row are separated from each other.

There are two furrow spines on each adambulacral plate, and sometimes three on the proximal plates. The form of the proximal furrow spines gradually changes with age: the spearhead-shaped spines transform into flat scales, and then (at an R > 2.1–2.5 mm) the flat scales transform into pedicellariae. All stages of development of the adambulacral pedicellariae can be seen in the same adult specimen: spearhead-shaped spines on the distalmost adambulacral plates, flat scales in the middle of the arm and pedicellaria-like spines on the proximal adambulacral plates. Unlike the adambulacral pedicellaria, the dorsal pedicellaria are not represented by different stages of development. Only fully formed pedicellariae are known. The number of pedicellaria-like adambulacral spines in

adult specimens highly varies from complete absence to their presence on all adambulacral plates, with the exception of the two or three most distal ones. The ventrolateral areas are completely naked or almost naked (with a few tiny spineless plates). There are 3 terminal spines, and sometimes 4–6 (in the largest specimens). The terminal spines and upper margins of the terminal plates are denticulate in juveniles at an $R < 0.9$ mm (Figure 9A,E) and smooth in larger specimens.

Remarks. *Porcellanaster eremicus* and *Damnaster tasmani* are considered here as the junior synonyms of *C. pedunculatus* since there are numerous transitional variants between these species and typical *C. pedunculatus*. According to Belayev and Mironov [6], the low abyssal species *P. eremicus* differs from the typical *C. pedunculatus* in having denser plate pavement on the dorsal disc and more numerous dorsal and adambulacral pedicellariae. However, the density of plate pavements and the number of pedicellaria gradually increase with increasing depth of habitat. Adult specimens of *C. pedunculatus* with low density of plate coverage and few pedicellariae are more common in the bathyal zone, at depths of 1565–2667 m (stations of RV *Akademik Mstislav Keldysh* on the Reykjanes Ridge). Specimens from the upper abyssal depths, 3000–3100 m (stations of RV *Le Noroît*, Bay of Biscay), have denser plate pavement on the dorsal disc and more numerous pedicellariae than those from the bathyal zone. The most dense plate pavement and most numerous pedicellariae are found in the lower abyssal zone, at depths greater than 4000 m (stations of RV *Akademik Ioffe*, *Dmitry Mendeleev* and *Ob*). Therefore, the low abyssal *C. pedunculatus* here examined corresponds to morphology of the type specimens of *P. eremicus*. Clark and McKnight [56] did not note any differences between *D. tasmani* and *P. eremicus* and considered that the type specimen of *P. eremicus* (Challenger, St. 137) should be referred to as *D. tasmani*.

Belyaev [85] reported about *Porcellanaster* sp. and *Albatrossia* sp. collected in the Aleutian Trench at St. 4120 and 6328 m. The examination of these two specimens showed that they belonged to *C. pedunculatus*. It is the deepest record for the species.

Distribution. *C. pedunculatus* was found in the Atlantic, Pacific, Indian and Southern Oceans from the Davis Strait, Aleutian Trench and Bay of Bengal southward to the Antarctic (Figure 10). Depth range 1520–6328 m.

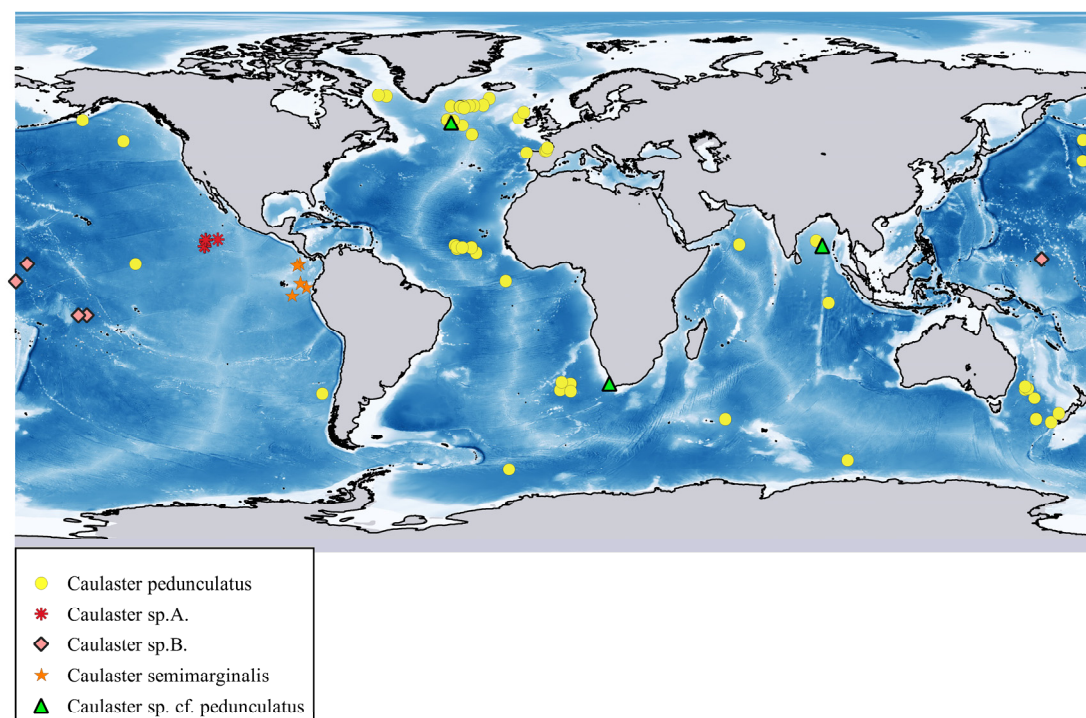


Figure 10. Distribution of the *Caulaster* species.

Caulaster cf. *pedunculatus* Perrier, 1882
Figure 11A.

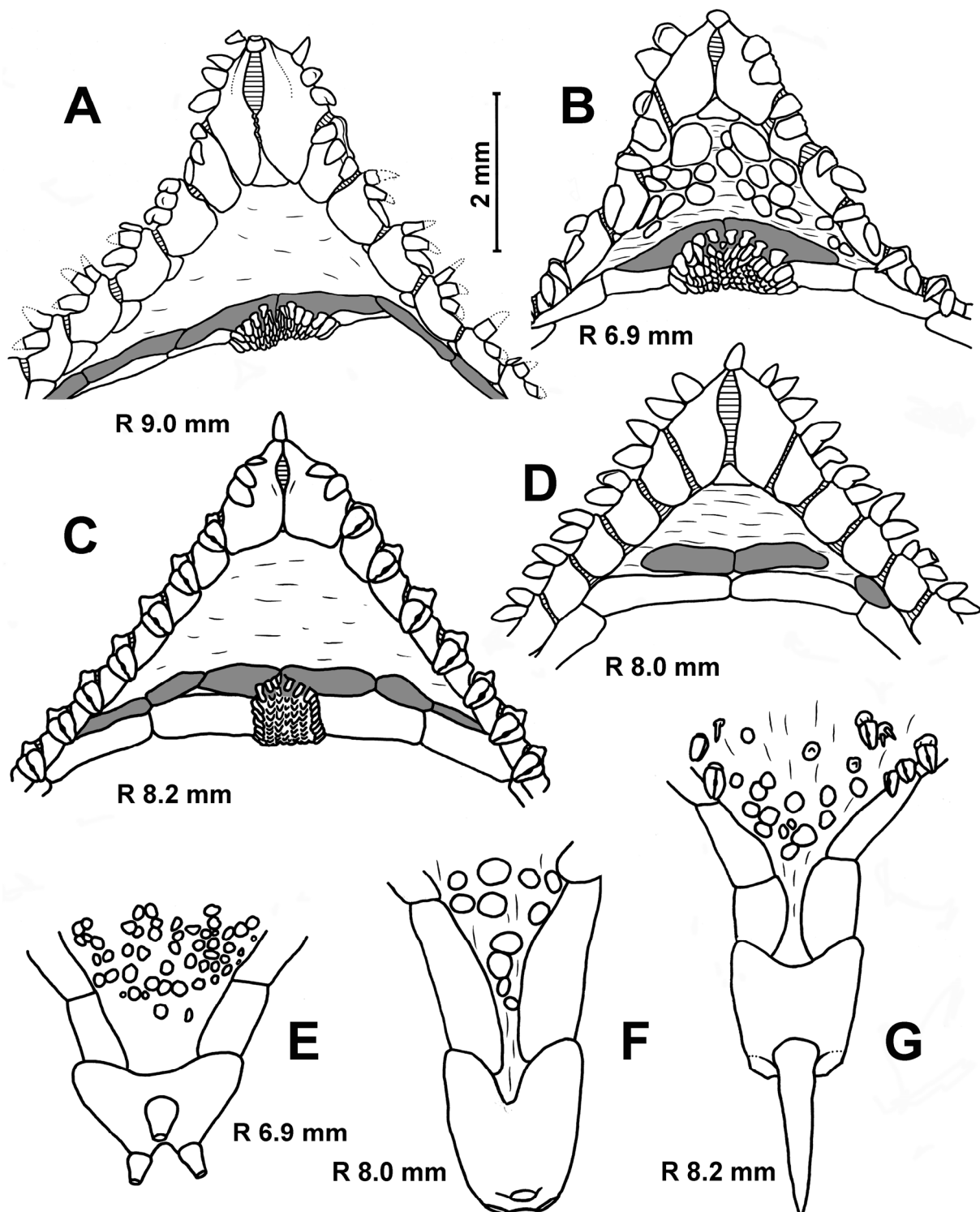


Figure 11. Interradii (A–D) and terminal plates (E–G) of the *Caulaster* species. (A) *Caulaster* cf. *pedunculatus*, St. 68/384, R/V G.O. Sars; (B,E) *C. semimarginalis* (Ludwig, 1905), St. 308, RV Akademik Kurchatov; (C,G) *C. sp. A*, St. 3904, RV Dmitry Mendeleev; (D,F) *C. sp. B*, St. 6334, RV Vityaz. Scale: 2 mm.

Caulaster cf. *dubius*—Dilman, 2008: 136 [38].

Material examined. R/V *G.O. Sars*, MAR-ECO Expedition, St. 68/384, 25.07 2004, northern Mid-Atlantic Ridge, 53°08' N, 34°46' W, 2306–2374 m, one spm., R/r 9/4.5 mm, ZMBN 87146.

Remarks. Most specimens of the genus *Caulaster* have two furrow spines on each adambulacral plate. Sometimes the first two adambulacral plates have three spines. Koehler [54] established *Caulaster dubius* for a specimen with three furrow spines on four–five proximal adambulacral plates in each row. Later, two more specimens with the same feature (three–four adambulacral plates with three spines) were described: one from the *Galathea* station 92, with an R/r of 7/3–4 mm [3] (Figure 24f–h), and another from the MAR-ECO station 68/384 [38]. No other differences from *C. pedunculatus* were found. We suggest that the presence of three furrow spines on the first three–five proximal plates is likely a result of intraspecific variation.

Distribution. The holotype of *C. dubius* was collected in the Bay of Bengal, 11°58' N, 88°55'17" E, 3197 m. The *Galathea* specimen is from the South Africa area, St. 92, 33°50' S, 17°59' E, 2176 m. Our specimen came from the northern Mid-Atlantic Ridge. The geographical distribution is shown in Figure 10. Depth range 2306–2374 m.

Caulaster sp. A

Figures 8E,F and 11C,G.

Porcellanaster cf. *ceruleus*—Glover et al., 2016: 19–21 (Figure 11) [28].

Caulaster nudus—Mironov et al., 2016 (Figure 2e) [5] (non *Albatrossaster nudus* Ludwig, 1907).

Porcellanaster ceruleus—Amon et al., 2017: 18 (Figure 9) [80] (non *Porcellanaster ceruleus* Thomson, 1877).

Material examined. RV *Dmitry Mendeleev*, cruise 41, St. 3904, 07.03 1988, the Clarion-Clipperton Fracture Zone, 13°59'9" N, 112°32'5" W, 4120 m, one spm., R/r 8.2/4.3 mm, IORAS ECH01927.

RV *L'Atalante*, cruise 12, BIONOD Expedition, St. Bio12-16, 04.04 2012, EBS, Clarion-Clipperton Fracture Zone, German license area, 11°45.69'–11°47.71' N 116°50.09'–116°53.17' W, 4135–4136 m, two spms., R/r ~8.3/3.0 mm and 11.0/5.0 mm.

RV *L'Atalante*, Cruise 12, BIONOD Expedition, St. Bio12-33, 07.04 2012, the Clarion-Clipperton Fracture Zone, German license area, 11°49.17'–11°51.91' N 117°03.73'–117°03.13' W, 4133–4127 m, one spm., R/r 11.0/4.8 mm. Total: four specimens from three stations, R from 8.2 to 11.0 mm.

Description. The R/r ranges from 8.2/4.3 mm to 11.0/5.0 mm. The numerical characters of these four specimens are shown in Table 6. The R/r ratio is from 1.9 to 2.8. The perforate plates on the dorsal disk are few in number and only at the base of the arm. Small plates with spines and pedicellariae are scattered almost evenly across the disk, separated from each other by wide skin spaces, and are not arranged in radial bands (Figure 8E). The dorsal pedicellariae are very numerous, from 46 to 110. There is an apical appendage present that is 1.0–2.5 in length. The madreporite plate is round and 0.93–1.22 mm in diameter. There are 3 supermarginals and 1–4 inferomarginals that are much shorter and lower than the supermarginals. Most specimens have an inferomarginal row extended to the middle of the supermarginals. The cribriform organs are broad and located both on supermarginals and inferomarginals, with 6–12 vertical scale rows. Two or three flat broad marginal oral spines are usually lying on the oral plate. There are 12–15 adambulacral plates. There are two or (rarely) three furrow spines on each adambulacral plate, and most of them form pedicellariae (Figure 11C). The ventrolateral plates are absent. The L/W ratio of the terminal plates is 0.93–1.10. There are always three terminal spines.

Table 6. Numerical characters of *Caulaster* species.

R/r, mm	Number				Dorsal Pedicellariae	Rows of Lamellae **
	Plates					
	sm *	im *	ad	vl		
<i>Caulaster</i> sp. A, East Pacific, 4120 m, RV <i>Dmitry Mendeleev</i> , cruise 41, St. 3904						
8.2/4.3	3	2–4	12	0	58	6–9
<i>Caulaster</i> sp. A, East Pacific, 4127–4136 m, RV <i>L'Atalante</i> , St. Bio12-16 (2 sp.) and St. Bio12-33						
8.3/3.0	3	2–3	12	0	46	6–8
11.0/5.0	3	1	15	0	64	8
11.0/4.8	3	1	14	0	110	10–12
<i>Caulaster</i> sp. B, Central Pacific, 4916 m, RV <i>Vityaz</i> , cruise 34, St. 5159						
6.7/2.7	3	3	12	0	0	2–6
7.2/2.5	3	1–2	12 (13)	0	0	0–2
7.5/3.0	3	1–3	12	0	0	0 (2)
7.8/3.3	3	1–3	13	0	1	0–4
8.2/2.8	3–4	2–3	13	0	13	0–6
8.2/3.0	3	1–2	13	0	1	0–6
8.3/2.9	3–4	2–3	13 (14)	0	2	0–4
8.7/3.2	3	2–4	14	0	9	0–4
<i>Caulaster</i> sp. B, Central Pacific, 5040 m, RV <i>Vityaz</i> , cruise 48, St. 6277-4						
7.0/2.6	3	1–2	10	0	0	0–4
<i>Caulaster</i> sp. B, Central Pacific, 5240–5300 m, RV <i>Vityaz</i> , cruise 48, St. 6334						
6.3/2.7	3	1–2	11	0	0	0–2
7.2/2.8	3	2–3	11 (12)	0	0	0–4
7.2/3.1	4	2–3	12	0	0	0–2
8.0/3.9	2	1–2	12	0–2	3	0–4
<i>C. semimarginalis</i> , off Ecuador, 2265 m, RV <i>Akademik Kurchatov</i> , cruise 4, St. 220						
2.7/1.9	1	1	4	3–4	0	2–5
6.1/3.2	2	2	8	14–16	0	10–12
6.5/3.7	2	2	7	14–24	0	12–13
<i>C. semimarginalis</i> , off Ecuador, 2149–2150 m, RV <i>Akademik Kurchatov</i> , cruise 4, St. 308						
5.6/3.5	2	1–2	7	7–9	0	10–10
6.0/4.1	2	1	8	8–11	0	10–10
??/4.3	2	1	9	16–22	0	12–12
6.9/4.5	2	1	7–8	16–22	0	12–14
7.0/4.0	2	1	8	22–26	0	12–14

sm—superomarginal plates, im—inferomarginal plates, ad—adambulacral plates, vl—ventrolateral plates, c.o.—cribriform organ. * Number of superomarginals or inferomarginals from midline of interradius to terminal plate. ** Number of vertical lamellae rows in a cribriform organ of non-madreporite interradius and madreporite interradius.

Remarks. In *Caulaster* sp. A, the number and arrangement of plates, spines and pedicellariae on the dorsal disk are different from those of *C. pedunculatus*. The number of dorsal pedicellariae is more than 40 in the former and usually much less 40 in the latter.

The spines and pedicellariae are evenly distributed over the dorsal disc in *Caulaster* sp. A, and they are arranged into interradian bands in *C. pedunculatus*. *Caulaster* sp. A differs also in lacking large spineless perforate plates. *C. pedunculatus* shows a tendency to increase the density of coverage with large, perforated plates with depth. Therefore, the differences between *Caulaster* sp. A and *C. pedunculatus* become even more significant if we compare the morphology of specimens collected in the lower abyssal only, at depths greater than 4000 m.

According to morphology, the specimens of *Caulaster* sp. A most likely belong to a new species. The genetic analysis does not yet support this assumption (Figure 2). A more advanced genetic analysis is required to confirm the species status of this morphological form.

Distribution. The tropical eastern Pacific Ocean, the polymetallic nodule areas of the eastern Clarion-Clipperton Zone. Depth range 4054–4500 m (Figure 10).

Caulaster sp. B

Figures 8G,H and 11D,F.

Caulaster sp.—Mironov et al., 2016: 505 (Figure 3d) [5].

Material examined. Central Pacific: RV *Vityaz*, cruise 34, St. 5133, 05.11.1961, N of Howland Island, 5°58' N, 176°4' W, 5360 m, one sp., R/r 8.0/3.0 mm, IORAS ECH01943.

RV *Vityaz*, cruise 34, St. 5159, 02.12.1961, SE of Caroline Islands, 07°36' N, 162°01' E, 4916 m, TS, 13 sp., R/r 6.7/2.7–9.5/4.0 mm, IORAS ECH02621, ECH01919 and ECH01920.

RV *Vityaz*, cruise 43, St. 5939, 17.03.1968; Central Pacific Basin, east of Gilbert Islands, 02°17' S, 179°30' E, 5460 m, TS, one sp., R/r 7.3/3.3 mm, IORAS ECH01922.

RV *Vityaz*, cruise 43, St. 5988-19, 17.03.1968, off southern Line Islands, 11°03.7' S, 156°12' W, 5270 m, TS, one sp., R/r 8.0/3.0 mm, IORAS ECH01924.

RV *Vityaz*, cruise 48, St. 6277-4, 05.06.1970, E of Gilbert Islands, 00°14' N, 179°50' W–00°18' N, 179°53' W, 5040 m, TS, one sp., R/r 7.0/2.6 mm, IORAS ECH01921.

RV *Vityaz*, cruise 48, St. 6334, 31.07.1970, E of Manihiki Island, 11°06.2' S, 159°00' W, 5240–5300 m, TS, four sp., R/r 6.3/2.7–8.0/3.9 mm, IORAS ECH01923.

Total: There are 21 specimens from six stations, with an R from 6.3 to 9.5 mm.

Description. The specimen from St. 5159 with an R/r of 8.7/3.2 mm is selected as the most typical for *Caulaster* sp. B. Its arms are rather long, with a ratio of R/r = 2.6. The perforate plates on the dorsal disk are large and arranged in five radial bands. The small plates that have a spine are few and are separated from each other by skin spaces arranged in faintly distinguishable interradian bands. There are nine dorsal pedicellariae. The apical appendage or apical cone is absent. The madreporite plate is round, small and about 1 mm in diameter. There are 2 supermarginal plates and 2–4 inferomarginal plates. When there are two inferomarginal plates, then the length of the first inferomarginal plate is half or one-third of the first supermarginal plate, and the second tiny inferomarginal plate is located at some distance from the first—at the base of the second supermarginal plate, at a distance from the first inferomarginal. When there are four inferomarginals (one case), then the fourth tiny plate is located at the base of the third supermarginal plate. There is only one cribriform organ, which is located in the madreporite interradius; it is rudimentary and does not continue to the inferomarginal plate, with four vertical scale rows. There are two flat, broad marginal spines. There are 14 adambulacral plates, with two or (rarely) three furrow spines. On the proximal adambulacral plates the furrow spines are flat and broad (flat-scale) or pedicellaria-like. The ventrolateral areas are very small, without plates. The terminal plate is long, with an L/W of 1.19. There are three terminal spines.

Regarding the other specimens, the R/r ranges from 6.3/2.7 to 8.5/3.0 mm. The numerical characters of the 13 specimens are shown at Table 6. The arms are rather long, with a ratio of R/r from 2.0 to 2.9. The dorsal disk always flat, not swollen. The apical appendage or apical cone is absent (Figure 8G). The cribriform organ is located in the madreporite interradius only, with 2–6 vertical scale rows. Only one specimen has rudimentary cribriform organs in other interradii, each consisting of two vertical rows of scales. The inferomarginals are rudimentary, spaced and do not reach the terminal plate. There are two adambulacral furrow spines, and sometimes three spines on the one proximal adambu-

lacr plate in the row. One specimen from St. 5159 has three proximal adambulacral plates with three spines in each of its nine rows and two proximal adambulacral plates with three spines in one row (Figure 11D). This feature corresponds to the morphology of *Caulaster dubius*, in which 3–5 proximal adambulacral plates have three furrow spines.

In specimens from St. 5159, the number of marginal spines varies as follows: four specimens have two spines on all oral plates, six specimens have three spines on all plates and three specimens have two or three spines. The ventrolateral plates are absent, with two exceptions: one specimen has one small plate in one interradius, and another specimen has two small round plates in one interradius. The length of the terminal plate is usually greater than its width; the ratio of L/W varies from 0.9 to 1.25.

Remarks. *Caulaster* sp. B differs from the adults of *C. pedunculatus* and *Caulaster* sp. A in lacking an apical appendage and having a cribriform organ in one interradius only. These characters are common with *Lethmaster rhipidiphorus* Belyaev, 1969. In addition, *Caulaster* sp. B is similar to *L. rhipidiphorus* in that it has a small body size and very small ventrolateral areas; the inferomarginals directly border the adambulacral and oral plates (Figure 8H). However, *L. rhipidiphorus* differs in some characters: the presence of dorsal spines on the supermarginals, having spear-shaped furrow spines and a peculiar structure on the inferomarginals consisting of large scales and columnar papillae [26] (Figure 4). The large scales are arranged in an arcuate row surrounding a group of columnar papillae.

It is possible that *Caulaster* sp. B would be assigned to a new species. To confirm this assumption, a genetic analysis and studying of the morphological age variability are necessary.

One specimen of *Eremicaster crassus* (R 11.5 mm) was caught together with *Caulaster* sp. B (R 7.3 mm) at St. 5939 (RV *Vityaz*). The specimen has a transitional morphology between *E. crassus* and *Caulaster* sp. B: the apical appendage and spines on the supermarginals are absent, and there is a single cribriform organ only in the madreporite interradius. Perhaps we are dealing here with hybrid specimens.

Distribution. Central Pacific from 07°36' N to 11°06.2' S and from 162°01' E to 156°12' W. Depth range 4916–5460 m (Figure 10).

***Caulaster semimarginalis* (Ludwig, 1905)**

Figures 8C,D and 11B,E.

Albatrossia semimarginalis—Ludwig, 1905: 97–100, pl. 6.30–31 [64] and Ahearn, 1995: 37 [86].

Albatrossaster nudus—Ludwig, 1907: 318–319 [75] and Ahearn, 1995: 31 [86].

Albatrossia nuda—Clark H.L., 1920: 81, pl. 2.5–6 [67].

Porcellanaster coeruleus—Liberkind, 1935 (part): 5–19 [46].

Porcellanaster caeruleus—Madsen, 1961a (part): 134–135 [3].

Non: *Caulaster nudus*—Mironov et al., 2016: 505 (Figure 2e) [5] (= *Caulaster* sp. A).

Syntypes. USNM 34340, RV *Albatross*, St. 3362, 26.02.1891, R/r 9/4 and 11/5.5 mm.

Type locality. RV *Albatross*, St. 3362, 26.02.1891, east of Cocos Island, 05°56' N, 85°10'30" W, 2149 m.

Material examined. RV *Akademik Kurchatov*, cruise 4, St. 220, 30.08.1968, off Ecuador, 00°25'0" S, 85°00'1" W, 2265 m, three spms., R/r 2.7/1.9, 6.1/3.3 and 6.5/3.7 mm, IORAS ECH02939 and ECH02619.

RV *Akademik Kurchatov*, cruise 4, St. 308, 08.11.1968, off Ecuador, 01°46'7" S, 82°58'0" W, 2150 m, five spms., R/r 5.6/3.5–7.0/4.0 mm, IORAS ECH01915 and ECH02620.

Total: There are eight specimens from two stations, with R values from 2.7 to 7.0 mm.

Description. The small specimen has an R/r of 2.7/1.9 mm. There arms are short, with a ratio of R/r of 1.4. The dorsal disk is almost completely naked, with a few small, perforated plates. The central ring of the perforate plates, spines, apical appendage and dorsal pedicellariae are absent. There is a single inferomarginal and superomarginal plate, and the former is shorter. There is one cribriform organ in all interradii, with 2–5 vertical scale rows. The furrow spines on the proximal and distal adambulacral plates

are moderately wide. There are three–four ventrolateral plates covering about 50% of the ventrolateral area. The terminal plate is short, with three terminal spines.

The other specimens have an R/r of 5.6/3.5–7.0/4.0 mm. The arms are short, with a ratio of R/r from 1.5 to 1.8. There are five interradian bands of small plates with spines on the dorsal disk. The perforate plates are small and separated from each other by skin spaces (Figure 8C). An apical appendage is present. The dorsal pedicellariae are absent. The madreporite plate is round, small and 0.75–0.89 mm in diameter. There are two superomarginals and one–two inferomarginals in each row. The inferomarginal plates are shorter and lower than the adjacent superomarginals and do not reach the terminal plate. The suture between the first superomarginal and inferomarginal plate is poorly visible, since it is covered with a cribriform organ (Figure 11B). The cribriform organ is broad, with 10–14 vertical scale rows in all interradii, located both on superomarginals and inferomarginals (Figure 11B). There are two or (rarely) three flat, broad marginal spines lying on the oral plate. There are 7–9 adambulacral plates with two or (rarely) three furrow spines. On the proximal plates, the spines are flat (Figure 11B) or pedicellaria-like, but never form true pedicellariae. The ventrolateral plates range from small to large and are usually separated from each other by broad skin spaces, covering 30–90% of the ventrolateral area (Figure 11B). The terminal plate is short, with an L/W of 0.58–0.65 (Figure 11E). There are always three terminal spines. The specimens with an R of 5.6–7.0 mm (except for one specimen with an R of 6.1 mm) have large gonads. They are visible clearly through the skin, located at the base of the arms and partially extend into the arms; they are yellow in alcohol specimens and dark brown in dry specimens.

Remarks. The genus *Albatrossia* and species *A. semimarginalis* have been established for two specimens with an R/r of 9.0/4.0 and 11.0/5.5 mm [65]. They have two and three unarmed superomarginals, eight and nine adambulacral plates and ventrolateral areas with spaced plates. The inferomarginals are absent or rudimentary. Afterwards, Ludwig [77] created the new name *Albatrossaster* “to replace his *Albatrossia* of 1905, in order to avoid confusion with *Albatrossa* (a bird), but as Clark H.L. in 1920 notes, such a confusion does not seem probable and in any case the name *Albatrossia* was not invalidated by the name *Albatrossa*” (from Madsen, 1961) [3] (p. 134).

Later, the genus *Albatrossia* was synonymized with *P. ceruleus* by Madsen [3], and since then, the taxonomic position of this genus has not been revised.

An examination of the specimens from RV *Akademik Kurchatov* cruise 4 (Table 6) showed good agreement with that of the type specimens of *A. semimarginalis*, except for the presence of inferomarginals in our specimens (Figure 11B).

The assignment of *A. semimarginalis* to the genus *Caulaster* is based on two features of adult specimens: the presence of wide and flat furrow spines and small inferomarginals not reaching the terminal plate. In addition, in our specimens, as in the type specimens of *A. semimarginalis*, large gonads are visible through the thin skin at the base of the arms and in the arms. According to Ludwig, the gonads of the smaller specimen of *A. semimarginalis* were found to be male; a larger specimen has a considerable number of eggs that are 0.4 mm in diameter [65].

The species *Albatrossaster nudus* was described from a single specimen with an R/r of 7.0/4.5 mm [77]. The holotype has two superomarginals, two inferomarginals, eight adambulacral plates and ventrolateral areas with spaced plates. It corresponds to *A. semimarginalis* in every regard. Ludwig [77] and Clark H.L. [68] noted the almost complete absence of spines on the dorsal disk. *C. semimarginalis*, with an R/r of 6.5/3.7 mm from St. 220, does not differ from *A. nudus* in this character.

Distribution. East of Cocos Island and off Ecuador. Depth range 1408–2265 m. The holotype of *A. nudus* was collected by *Albatross* south-east of the Galapagos Islands (04° 33' S, 87° 43' W) at a depth of 3667 m (Figure 10).

4. Discussion

As a result of studying the morphology of juvenile and adult specimens of *Porcellanaster*, the number of species in the genus increased from two to five (*P. caeruleus*, *P. ivanovi*, *P. caulifer*, *P. fragilis* and *P. sladeni*), and the genus *Caulaster* was re-established. According to the present study, *Caulaster* consists of *C. pedunculatus*, *C. semimarginalis* and two new forms, *Caulaster* A and *Caulaster* B (Table 7).

Table 7. Species of the genera *Caulaster*, *Eremicaster* and *Porcellanaster* according to Madsen, 1961a [3] and present work.

Original Name	Madsen, 1961a [3]	Present Work
<i>Albatrossia semimarginalis</i> Ludwig 1905	<i>P. caeruleus</i>	<i>C. semimarginalis</i>
<i>Albatrossaster nudus</i> Ludwig 1907	<i>P. caeruleus</i>	<i>C. semimarginalis</i>
<i>Albatrossaster richardi</i> Koehler 1909	<i>P. caeruleus</i>	<i>C. pedunculatus</i>
<i>Caulaster dubius</i> Koehler 1909	<i>P. caeruleus</i>	<i>C. cf. pedunculatus</i>
<i>Caulaster pedunculatus</i> Perrier 1882	<i>P. caeruleus</i>	<i>C. pedunculatus</i>
<i>Caulaster sladeni</i> Perrier 1885	<i>P. caeruleus</i>	<i>P. sladeni</i>
<i>Damnaster tasmani</i> H.E.S. Clark & McKnight 1994	-	<i>C. pedunculatus</i>
<i>Porcellanaster caulifer</i> Sladen 1883	<i>P. caeruleus</i>	<i>P. caulifer</i>
<i>Porcellanaster caeruleus</i> Thomson 1877	<i>P. caeruleus</i>	<i>P. caeruleus</i>
<i>Porcellanaster crassus</i> Sladen 1883	<i>E. crassus</i>	<i>E. crassus</i>
<i>Porcellanaster eremicus</i> Sladen 1889	<i>P. caeruleus</i>	<i>C. pedunculatus</i>
<i>Porcellanaster fragilis</i> Döderlein 1921	<i>P. caeruleus</i>	<i>P. fragilis</i>
<i>Porcellanaster gracilis</i> Sladen 1883	<i>E. gracilis</i>	<i>E. crassus</i>
<i>Porcellanaster granulatus</i> Perrier 1885	<i>P. caeruleus</i>	<i>P. caeruleus</i>
<i>Porcellanaster inermis</i> Perrier 1885	<i>P. caeruleus</i>	<i>P. caeruleus</i>
<i>Porcellanaster irregularis</i> Lieberkind 1932	<i>P. caeruleus</i>	<i>P. caeruleus</i>
<i>Porcellanaster ivanovi</i> Belyaev 1969	-	<i>P. ivanovi</i>
<i>Porcellanaster pacificus</i> Ludwig 1905	<i>E. pacificus</i>	<i>E. pacificus</i>
<i>Porcellanaster (Eremicaster) tenebrarius</i> Fisher 1905	<i>E. gracilis</i>	<i>E. crassus</i>
<i>Porcellanaster tuberosus</i> Sladen 1883	<i>P. caeruleus</i>	<i>P. tuberosus</i> or <i>P. caulifer</i>
<i>Porcellanaster vicinus</i> Ludwig 1907	<i>E. vicinus</i>	<i>E. vicinus</i>
<i>Porcellanaster waltharii</i> Ludwig 1905	<i>E. gracilis</i>	<i>E. crassus</i>
-	-	<i>Caulaster</i> sp. A
-	-	<i>Caulaster</i> sp. B

The genera *Albatrossia* and *Damnaster* are considered junior synonyms of *Caulaster*. The study of representatives of the closely related genus *Eremicaster* did not lead to a change in its species composition.

The main features of juveniles useful for species identification are shown in Table 8. The table is missing information about dorsal spines on superomarginals. Dorsal spines are always absent in *Caulaster* and *P. sladeni* and absent in *P. ivanovi* juveniles but are sometimes present in its adults. Adult *P. caulifer* have the longest dorsal spines, and their length exceeds the height of the superomarginal plates. The dorsal spines of *Eremicaster pacificus* are more numerous and first appear in smaller specimens than those of *E. crassus* and *E. vicinus*.

Table 8. Diagnostic characters of *Porcellanaster*, *Eremicaster* and *Caulaster* species for juvenile specimens with R 4–7 mm. Species are in brackets when there are no data for the juvenile morphology, and adult characters are indicated.

Species	Feature Present (+) or Absent (-)						Number	
	ped.	vl. pls.	vl. sps	iims ser.	ap. app.	seg. pap.	fur. sps	cr.o
<i>P. ceruleus</i>	-	+	+	+	+	-	2–3	1 (3)
(<i>P. fragilis</i>)	-	+	?	+	+	-	1–2	1
<i>P. ivanovi</i>	-	+	-	+/-	-	-	1–2	1 (3)
(<i>P. caulifer</i>)	-	+	+	+	+	-	2–3	1
<i>P. sladeni</i>	-	-	-	+/-	+	-	2–3	1
<i>E. crassus</i>	-	+	-	+	+	+	2–3	3 (1)
<i>E. pacificus</i>	-	+	+	+	+	-	2–3	3
<i>E. vicinus</i>	-	+	-	+	+	-	2–3	3
<i>C. pedunculatus</i>	+	-	-	-	+	-	2–3	1
(<i>Caulaster</i> sp. A)	+	-	-	-	+	-	2–3	1
(<i>Caulaster</i> sp. B)	+	-	-	-	-	-	2–3	1
<i>C. semimarginalis</i>	+	+	-	-	+	-	2–3	1

Ped.—dorsal and adambulacral pedicellariae, vl.pls.—ventrolateral plates, vl.sps—ventrolateral spines, cr.o.—cribriform organ, iims ser.—complete series of inferomarginals, reaching terminal plate, ap.app.—apical appendage, seg. pap.—segmental papillae, fur. sps—furrow spines.

Most of the characters listed in Table 8 can also be observed in adults. The exceptions are *P. ivanovi* and *P. caulifer*. In the juveniles of *P. ivanovi*, an apical appendage is absent, and the inferomarginal series are continuous, while in adults, the apical appendage is present, and the inferomarginal series is interrupted. The smallest specimen of *P. caulifer* had an R of 11 mm (Table 3). The specimens with an R of 11–21 mm lack spines on the ventrolateral plates, while the specimens with an R of 20–24 mm are equipped with spines (Figure 5H). Among the features characteristic only of juveniles, the most noticeable is a ring of 3–8 large, perforated plates devoid of spines. This ring is located in the center of the dorsal disc (Figures 3A,B and 9A–C). In adult specimens, the few large plates are replaced by numerous small ones (Figures 3D,F,G,I and 8B). Only in *C. semimarginalis* the central part of the disc in both juvenile and adult specimens is covered with numerous small plates (Figure 8C). A combination of a reduced inferomarginal row with pavement of large plates on ventrolateral areas is also a unique feature of *C. semimarginalis* among the porcellanasterids. The differences from *C. pedunculatus* are significant enough to re-establish the genus *Albatrossia* with a single species: *A. semimarginalis*.

The family Porcellanasteridae is characterized by a wide range of body sizes. The maximum R for each species ranges from 146 mm in *Styracaster horridus* to 10–11 mm in *Porcellanaster sladeni*, *Caulaster semimarginalis* and *Caulaster* sp. A and B. With a decrease in size, the external morphology is greatly simplified (Figure 12). A dense cover of large paxillae changes to a predominantly bare skin space with occasional small plates with or without spines. The number of cribriform organs varies from 29 to 1 per interradius; the number of superomarginals varies from 35 to 3; the number of furrow spines varies from 10 to 1; and the number of ventrolateral plates ranges from more than 100 to their complete absence [5]. Oral, adambulacral and ventrolateral plates with a dense covering of spines are present in large species and naked in small species. The inferomarginal row is continuous, reaches the terminal plate and consists of numerous large plates in the former, and there is only one small inferomarginal plate, which does not even reach the base of the arm in the smallest species.

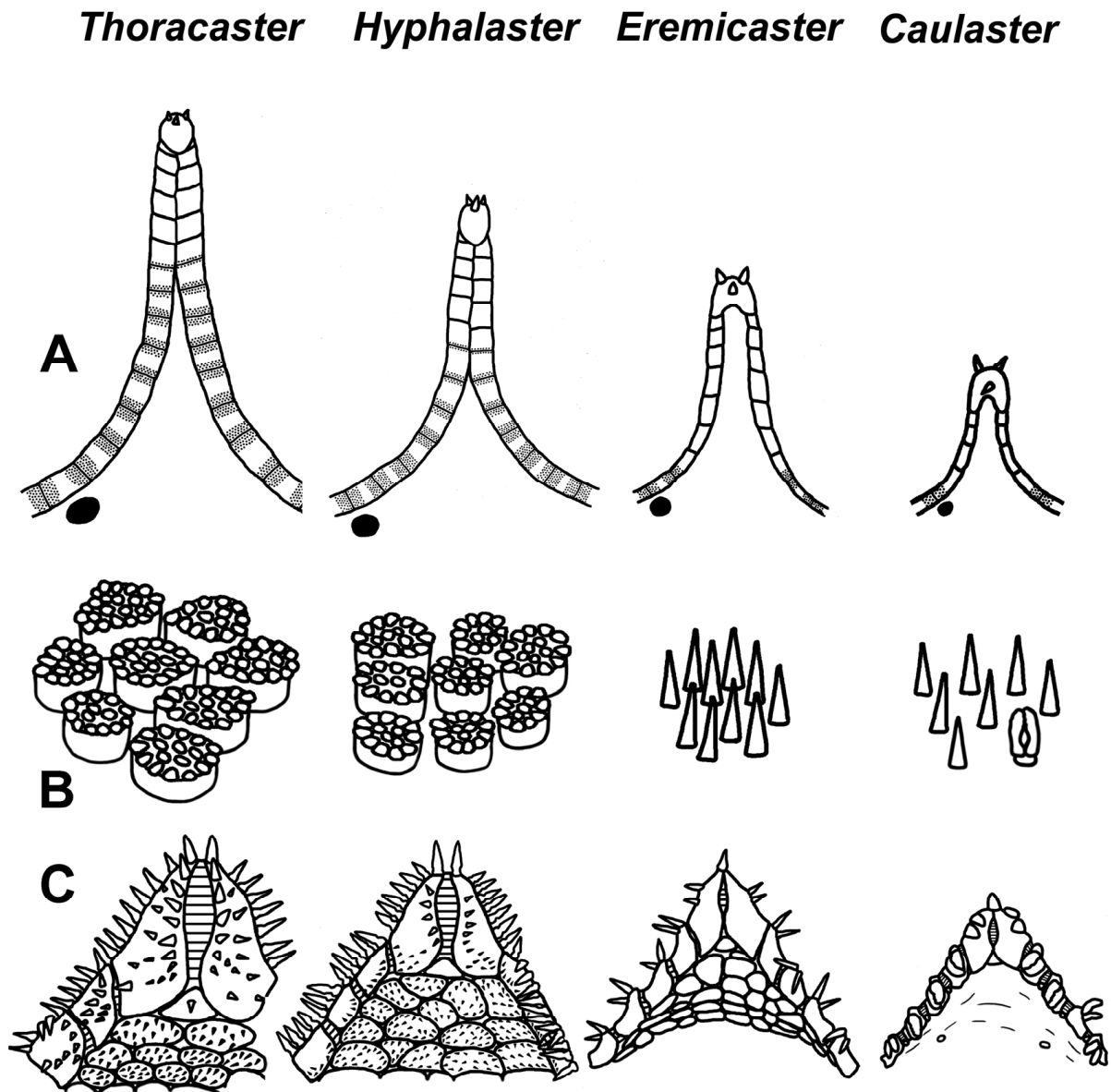


Figure 12. Comparison of the genera *Thoracaster*, *Hyphalaster*, *Eremicaster* and *Caulaster*, which are arranged in order of simplification of morphology (from left to right): (A) reducing body size and number of cribriform organs; (B) simplification of coverage of the dorsal disc; (C) decrease in the number of spines on the oral, adambulacral and ventrolateral plates.

Most likely, evolution within the family proceeded mainly from taxa with complex morphology to taxa with the simplest morphology [3–5]. The trend toward the simplification of morphology is supported by the results of a molecular analysis. In the phylogenetic trees (Figure 2A,B), the number of cribriform organs was chosen as the main measure of this simplification, since other features are correlated with this number (Figure 12). Three genera with one cribriform organ (*Caulaster*, *Porcellanaster* and *Sidonaster*) are represented on the trees and located in two different clades (Figure 2A,B), which proves the parallel evolution of these taxa leading to similar external morphology.

Data on the genetics of porcellanasterids are very limited. Only one specimen per species is included, creating a lack of information on intraspecific variation. Many of the species are not included in the genetic phylogeny. In particular, there are no genetic data on *Bentohgenia cribellosa* Fisher 1911, which has the most complex configuration of the cribriform organs, as well as on *Caulaster* sp. B, *C. semimarginalis* and *Lethmaster*

rhpidiphorus, with a single cribriform organ. The position on the phylogenetic tree of the latter two species is difficult to predict, as they differ significantly from the type species of both *Caulaster* and *Porcellanaster*. Additional data should greatly change our understanding of the evolution of porcellanasterids.

Porcellanasterids belong to the group of subsurface nonselective deposit feeders [3–5,7,87–94]. They swallow mud until the stomach is full and the disc is greatly expanded. When the organic content in the swallowed material has been utilized, the whole stomach content is ejected through the mouth, and the body of the asteroid becomes flat. Then, the asteroid moves forward and fills the stomach again to capacity. A sample of small porcellanasterids usually consists of both expanded and flat specimens. *Caulaster* sp. B is an exception: its body is always flat.

Obviously, a large amount of fecal material is permanently in the burrow. The cribriform organs, apical appendage and terminal spines are responsible for ventilating the burrow. The cribriform organs create water currents, and the apical appendage and terminal spines support the channels in the sediment that connect the burrow with the bottom water [3,5,94]. Two small porcellanasterids, *Caulaster* sp. B and *Lethmaster rhpidiphorus*, lack an apical appendage and have a poorly developed cribriform organ only in the madreporic interradius. The reduction in the structures providing ventilation probably indicates the transition of these porcellanasterids to the epibenthic lifestyle.

Mironov et al. [5] suggested that the morphological simplification of porcellanasterids was the result of two processes: a reduction in body size associated with the feeding of subsurface sediment of low nutritional value and a reduction in structures responsible for respiration due to living at greater depths. Subsurface mud is a food object of low nutritional value. The feeding strategy of porcellanasterids is probably associated with an increase in the amount of mud swallowed per unit of time and per unit of weight of the animal [5]. Such a feeding strategy could be the main reason for the decrease in the size of porcellanasterids during their evolution. First, the smaller the body size, the greater the amount of sediment swallowed per unit weight. Second, an increase in the relative amount of swallowed mud can be achieved with active forward movement, which in the sediment is easier for small animals than for large ones.

The structures responsible for respiration in the porcellanasterids are papulae. The papula cavity is connected with the coelom through a hole in the body wall [95]. In large porcellanasterids, numerous papulae are located on the dorsal disc between the paxillae, which protect the space around the papules from sediment clogging [5]. In small porcellanasterids with a single cribriform organ, papulae and paxillae usually absent. The reduction in the morphological structures responsible for respiration is characteristic of some other abyssal animals [96–102]. This reduction becomes especially noticeable when comparing the morphology of shallow- and deep-water species burrowing into the sediment. Burrowing makes the access of fresh water to the respiratory organs more difficult. For this reason, in some shallow-water-burrowing animals, the size of the respiratory organs increases. For example, the respiratory function in burrowing irregular echinoids is performed by large and flat ambulacral feet located on the upper surface of the test and arranged in so-called petaloids [103–106]. In deep-water irregular echinoids, the ambulacral feet are often reduced to tiny protrusions [100,101]. The reduction in morphological structures responsible for respiration even in burrowing deep-sea animals probably indicates a weak effect of oxygen deficiency on the respiration process under high-pressure conditions.

Below (Table 9) is a key to the porcellanasterid species with a single oral spine and without paxillae. Both juvenile and adult features are used. The R in brackets corresponds to the size at which the feature under consideration first appears.

Table 9. Key to the porcellanasterid species of the genera *Caulaster*, *Eremicaster*, *Lethmaster*, *Porcellanaster* and *Sidonaster*.

1a. Dorsal pedicellariae usually present ($R > 5$ mm). Furrow spines on proximal adambulacral. Plates are flat scale or they form pedicellariae ($R > 2.1$ – 2.5 m)	2
1b. Dorsal pedicellariae absent in both juveniles and adults. Furrow spines on adambulacral plates are spearhead-shaped (not flat scale), never form pedicellariae	5
2a. Ventrolateral areas with pavement of large plates ($R > 5$ mm *)	<i>Caulaster semimarginalis</i>
2b. Ventrolateral areas are naked or with few tiny plates ($R > 0.5$ mm)	3
3a. Cribriform organ occurs only in madreporite interradius ($R > 6$ mm *); apical appendage absent	<i>Caulaster</i> sp. B
3b. Cribriform organ occurs in all interradii ($R > 5$ mm); apical appendage usually present	4
4a. Interradial band of spine-bearing plates alternate with radial bands of spine-less plates on the dorsal disc ($R > 3$ mm); number of dorsal pedicellariae in adults usually less than 40	<i>Caulaster pedunculatus</i>
4b. The small pedicellaria-bearing and spine-bearing plates are evenly distributed over the dorsal disc; the plates are separated from each other by great skin spaces ($R > 8$ mm *); number of dorsal pedicellariae in adults more than 40	<i>Caulaster</i> sp. A.
5a. Three cribriform organs in each interradius ($R > 3.2$ – 3.5 mm)	6
5b. One cribriform organ in each interradius	8
6a. Ventrolateral plates with spines ($R > 5.4$ mm)	<i>Eremicaster pacificus</i>
6b. Ventrolateral plates without spines	7
7a. Second furrow spines on proximal adambulacral plates modified as segmental papillae ($R > 2.8$ mm)	<i>Eremicaster crassus</i>
7b. Both furrow spines are spearhead-shaped	<i>Eremicaster vicinus</i>
8a. Cribriform organ of a papilliform structure	<i>Sidonaster vaneyi</i>
8b. Cribriform organ of a lamelliform structure ($R > 3$ mm)	9
9a. On two median inferomarginal plates there is a fan-shaped coarse-scale structure ($R > 2.4$ mm); tiny hole in the center of the dorsal disc	<i>Lethmaster rhipidophorus</i>
9b. On two median inferomarginal plates there is a lower part of the cribriform organ ($R > 3$ mm) or inferomarginals with smooth surface; central hole absent	10
10a. Single furrow spines on the most adambulacral plates ($R > 2$ mm)	11
10b. Two-three furrow spines on adambulacral plates ($R > 1$ mm)	12
11a. Apical appendage and dorsal spines on superomarginal plates present ($R > 12$ mm *)	<i>Porcellanaster fragilis</i>
11b. Apical appendage and dorsal spines on superomarginal plates usually absent ($R > 1$ mm)	<i>Porcellanaster ivanovi</i>
12a. Ventrolateral areas naked or with 1–2 tiny plates ($R > 3$ mm *)	<i>Porcellanaster sladeni</i>
12b. Ventrolateral areas are provided with a pavement of large plates ($R > 1$ mm)	13
13a. Pavement of plates on ventrolateral areas is incomplete: between plates large skin spaces ($R > 11$ mm *); some ventrolateral plates with developed spine ($R > 20$ mm).	<i>Porcellanaster caulifer</i>
13b. Pavement of plates in ventrolateral areas is almost complete: between plates small skin spaces ($R > 1$ mm); plates spineless, sometimes with tiny spine or tubercle ($R > 1$ mm)	<i>Porcellanaster ceruleus</i>

* The state of the character is unknown at a smaller size of this species.

5. Conclusions

The diagnostic features of the genera *Porcellanaster* and *Caulaster* are formed in the early stages of postlarval development. In particular, the adambulacral and dorsal pedicellariae are present both in adults and juveniles of *Caulaster* at an $R > 3.5$ mm and have never been found in *Porcellanaster*. The differences between juveniles indicate that *Caulaster* representatives are not *Porcellanaster* juveniles. Based on these differences, the genus *Caulaster* with two species is re-established, and two new morphological forms are described. Three species have been restored in the genus *Porcellanaster*.

The species of *Porcellanaster* and *Caulaster* are the smallest porcellanasterids with the most simplified external morphology. They are located on the phylogenetic tree in two different clades. This indicates that the reduction in body size and a simplification of morphology occurred in two parallel branches of evolution and led to a noticeable similarity in external morphology. This similarity is most likely due to feeding and respiratory adaptations in the same habitat: the feeding of subsurface sediment of low nutritional value and respiration at a great depth.

Supplementary Materials: The following supporting information can be downloaded at: <https://www.mdpi.com/article/10.3390/d15101032/s1>, Table S1: Full list of taxa and sequences used in the present study. Accession numbers of the sequences reported for the first time are given in bold. Table S2: Estimates of evolutionary divergence between COI sequences of Porcellanasteridae.

Author Contributions: Conceptualization, A.N.M.; morphology, A.N.M.; molecular lab work and phylogenetic analysis, A.B.D., N.B.P. and I.P.V.; writing—original draft preparation, A.N.M., A.B.D. and N.B.P.; writing—review and editing, A.N.M., A.B.D. and N.B.P.; illustrations, A.N.M. and A.B.D. All authors have read and agreed to the published version of the manuscript.

Funding: This research was funded by the Ministry of Science and Higher Education, Russian Federation (grant 13.1902.21.0012, contract no. 075-15-2020-796).

Institutional Review Board Statement: Not applicable.

Data Availability Statement: The sequences obtained in this study are uploaded to GenBank (Table S1).

Acknowledgments: We thank Nadia Améziante (Muséum National d’Histoire Naturelle, Paris), Angelika Brandt (Senckenberg Research Institute, Frankfurt am Main), Marina Malyutina (Museum of the A.V. Zhirmunsky National Scientific Center of Marine Biology, Vladivostok), Bernhard Ruthensteiner (Zoologische Staatssammlung, München) and Kirill Minin, Andrey Gebruk and Antonina Kremenetskaia (Shirshov Institute of Oceanology, Moscow) for the opportunity to study porcellanasterid specimens. We are thankful to Kirill Minin for advice and help on the genetic part of the study. We are also grateful to Camille Moreau, the Academic Editor and the anonymous reviewers for constructive comments and suggestions that improved the manuscript.

Conflicts of Interest: The authors declare no conflict of interest.

References

- Belyaev, G.M. New records of ultra-abyssal starfishes of the family Porcellanasteridae. *Zool. Zhurnal* **1985**, *64*, 538–548. (In Russian)
- Clark, A.M. An index of names of recent Asteroidea. Part. 1: Paxillosida and Notomyotida. *Echinoderm Stud.* **1989**, *3*, 225–347.
- Madsen, F.J. The Porcellanasteridae. A monographic revision of an abyssal group of sea-stars. *Galathea Rep.* **1961**, *4*, 33–174.
- Madsen, F.J. On the zoogeography and origin of the abyssal fauna in view of the knowledge of the Porcellanasteridae. *Galathea Rep.* **1961**, *4*, 177–218.
- Mironov, A.N.; Dilman, A.B.; Vladychenskaya, I.P.; Petrov, N.B. Adaptive strategy of the porcellanasterid sea stars. *Biol. Bull.* **2016**, *43*, 503–516. [[CrossRef](#)]
- Belyaev, G.M.; Mironov, A.N. Starfishes *Porcellanaster* and *Caulaster* (Porcellanasteridae) from the Atlantic and the Antarctic. *Zool. Zhurnal* **1996**, *75*, 886–899. (In Russian)
- Clark, A.M.; Downey, M.E. *Starfishes of the Atlantic*; Chapman Hall: London, UK, 1992; 794p.
- Mah, C.L. World Asteroidea Database. Porcellanasteridae Sladen, 1883. World Register of Marine Species. Available online: <https://www.marinespecies.org/aphia.php?p=taxdetails&id=123130> (accessed on 30 July 2023).
- Mah, C.L.; McKnight, D.G.; Eagle, M.K.; Pawson, D.L.; Améziante, N.; Vance, D.J.; Baker, A.N.; Clark, H.E.S.; Davey, N. Phylum Echinodermata: Sea stars, brittle stars, sea urchins, sea cucumbers, sea lilies. In *New Zealand Inventory of Biodiversity: 1. Kingdom Animalia: Radiata, Lophotrochozoa, Deuterostomia*; Gordon, D.P., Ed.; Canterbury University Press: Christchurch, New Zealand, 2009; pp. 371–400. ISBN 978-1877257-72-8.
- Sladen, W.P. Asteroidea. Report on the Asteroidea collected during the voyage of H.M.S. “Challenger” during the years 1873–76. *Rep. Sci. Res. Chall. Zool.* **1889**, *30*, 1–935.
- Zhang, R.; Wang, X.; Zhou, Y.; Lu, B.; Wang, C. The first record of *Porcellanaster ceruleus* (Echinodermata: Porcellanasteridae) in the South China Sea. *Acta Oceanol. Sin.* **2018**, *37*, 185–189. [[CrossRef](#)]
- Janies, D.A.; Voight, J.R.; Daly, M. Echinoderm phylogeny including *Xyloplax*, a progenetic asteroid. *Syst. Biol.* **2011**, *60*, 420–438. [[CrossRef](#)]
- Mah, C.; Foltz, D. Molecular phylogeny of the Valvatacea (Asteroidea: Echinodermata). *Zool. J. Lin. Soc.* **2011**, *161*, 769–788. [[CrossRef](#)]
- Mah, C.; Foltz, D. Molecular phylogeny of the Forcipulatacea (Asteroidea: Echinodermata): Systematics and biogeography. *Zool. J. Linn. Soc.* **2011**, *162*, 646–660. [[CrossRef](#)]
- Feuda, R.; Smith, A.B. Phylogenetic signal dissection identifies the root of starfishes. *PLoS ONE* **2015**, *10*, e0123331. [[CrossRef](#)] [[PubMed](#)]
- Petrov, N.B.; Vladychenskaya, I.P.; Dilman, A.B.; Mironov, A.N. Taxonomic position of the family Porcellanasteridae within the class Asteroidea. *Biol. Bull.* **2016**, *43*, 483–490. [[CrossRef](#)]

17. Dilman, A.B.; Minin, K.V.; Petrov, N.B. New record of the wood-associated sea star *Caymanostella*, with notes on the phylogenetic position of the family Caymanostellidae (Asteroidea). *Zool. J. Linn. Soc.* **2021**, *20*, 1–22. [[CrossRef](#)]
18. Petrov, N.B.; Vladychenskaya, I.P.; Drozdov, A.L.; Kedrova, O.S. Molecular genetic markers of intra- and interspecific divergence within starfish and sea urchins (Echinodermata). *Biochemistry* **2016**, *81*, 972–980. [[CrossRef](#)]
19. Hoareau, T.B.; Boissin, E. Design of phylum specific hybrid primers for DNA barcoding: Addressing the need for efficient COI amplification in the Echinodermata. *Mol. Ecol. Resour.* **2010**, *10*, 960–967. [[CrossRef](#)]
20. Minin, K.V.; Petrov, N.B.; Vladychenskaya, I.P. Sea urchins of the genus *Gracilechinus* Fell & Pawson, from the Pacific Ocean: Morphology and evolutionary history. *Mar. Biol. Res.* **2015**, *11*, 253–268.
21. Folmer, O.; Black, M.; Hoeh, W.; Lutz, R.; Vrijenhoek, R. DNA Primers for amplification of mitochondrial cytochrome C oxidase subunit I from diverse metazoan invertebrates. *Mol. Mar. Biol. Biotechnol.* **1994**, *3*, 294–299. [[PubMed](#)]
22. Palumbi, S.R. Nucleic acids II: The polymerase chain reaction. In *Molecular Systematics*; Hillis, D.M., Moritz, C., Mable, B.K., Eds.; Sinauer Associates: Sunderland, MA, USA, 1996; pp. 205–247.
23. Mironov, A.N.; Minin, K.V.; Dilman, A.B. Abyssal echinoid and asteroid fauna of the North Pacific. *Deep-Sea Res. II* **2015**, *111*, 357–375. [[CrossRef](#)]
24. Glover, A.; Wiklund, H.; Rabone, M.; Amon, D.; Smith, C.; O'Hara, T.; Mah, C.; Dahlgren, T. Abyssal fauna of the UK-1 polymetallic nodule exploration claim, Clarion-Clipperton Zone, central Pacific Ocean: Echinodermata. *Biodivers. Data J.* **2016**, *4*, e7251. [[CrossRef](#)]
25. Edgar, R. Muscle: Multiple sequence alignment with high accuracy and high throughput. *Nucleic Acids Res.* **2004**, *32*, 1792–1797. [[CrossRef](#)]
26. Ronquist, F.; Teslenko, M.; Van der Mark, P.; Ayres, D.L.; Darling, A.; Ohna, S.H.; Larget, B.; Liu, L.; Suchard, M.A.; Huelsenbeck, J.P. MrBayes 3.2: Efficient Bayesian phylogenetic inference and model choice across a large model space. *Syst. Biol.* **2012**, *61*, 539–542. [[CrossRef](#)] [[PubMed](#)]
27. Nguyen, L.-T.; Schmidt, H.A.; von Haeseler, A.; Minh, B.Q. IQ-TREE: A fast and effective stochastic algorithm for estimating maximum likelihood phylogenies. *Mol. Biol. Evol.* **2015**, *32*, 268–274. [[CrossRef](#)] [[PubMed](#)]
28. Kalyaanamoorthy, S.; Minh, B.Q.; Wong, T.K.F.; von Haeseler, A.; Jermini, L.S. ModelFinder: Fast model selection for accurate phylogenetic estimates. *Nat. Methods* **2017**, *14*, 587–589. [[CrossRef](#)] [[PubMed](#)]
29. Hoang, D.T.; Chernomor, O.; von Haeseler, A.; Minh, B.Q.; Vinh, L.S. UFBoot2: Improving the ultrafast bootstrap approximation. *Mol. Biol. Evol.* **2018**, *35*, 518–522. [[CrossRef](#)]
30. Robert, E.; Kass, R.E.; Raftery, A.E. Bayes Factors. *J. Am. Stat. Assoc.* **1995**, *90*, 773–795. [[CrossRef](#)]
31. Bergsten, J.; Nilsson, A.N.; Ronquist, F. Bayesian Tests of Topology Hypotheses with an Example from Diving Beetles. *Syst. Biol.* **2013**, *62*, 660–673. [[CrossRef](#)]
32. Xie, W.; Lewis, P.O.; Fan, Y.; Kuo, L.; Chen, M.H. Improving marginal likelihood estimation for Bayesian phylogenetic model selection. *Syst. Biol.* **2011**, *60*, 150–160. [[CrossRef](#)]
33. Kumar, S.; Stecher, G.; Li, M.; Knyaz, C.; Tamura, K. MEGA X: Molecular Evolutionary Genetics Analysis across computing platforms. *Mol. Biol. Evol.* **2018**, *35*, 1547–1549. [[CrossRef](#)]
34. Kimura, M. A simple method for estimating evolutionary rate of base substitutions through comparative studies of nucleotide sequences. *J. Mol. Evol.* **1980**, *16*, 111–120. [[CrossRef](#)] [[PubMed](#)]
35. Ward, R.D.; Holmes, B.H.; O'Hara, T.D. DNA barcoding discriminates echinoderm species. *Mol. Ecol. Resour.* **2008**, *8*, 1202–1211. [[CrossRef](#)]
36. Wares, J.P. Biogeography of *Asterias*: North Atlantic climate change and speciation. *Biol. Bull.* **2001**, *201*, 95–103. [[CrossRef](#)] [[PubMed](#)]
37. Thomson, C.W. *The Voyage of the "Challenger": The Atlantic. Part 1*; Macmillan: London, UK, 1878; 396p.
38. Dilman, A.B. Asteroid fauna of the northern mid-Atlantic Ridge with description of a new species *Hymenasterides mironovi* sp. nov. *Mar. Biol. Res.* **2008**, *4*, 131–151. [[CrossRef](#)]
39. Dilman, A.B. Asteroid fauna of the northern mid-Atlantic ridge: Additional records. *Mar. Biol. Res.* **2013**, *9*, 563–586. [[CrossRef](#)]
40. Dilman, A.B. Deep-sea fauna of European seas: An annotated species check-list of benthic invertebrates living deeper than 2000 m in the seas bordering Europe; Asteroidea. *Invertebr. Zool.* **2014**, *11*, 25–42. [[CrossRef](#)]
41. Perrier, E. Première note Préliminaire des les Echinodermes, recueillis durant les campagnes de dragages sous-marines du Travailleur et du Talisman. *Ann. Sci. Nat. Zool.* **1885**, *19*, 1–72. Available online: <https://www.biodiversitylibrary.org/page/36373538> (accessed on 5 February 2023).
42. Perrier, E. Sur les Stellerides recueillis durant la mission du Talisman. *Compt. Rend. Hebd. Acad. Sci.* **1885**, *101*, 884–887.
43. Perrier, E. Echinodermes. Stellerides. *Exped. Scient. Travailleur Talisman* **1894**, *3*, 1–431.
44. Verrill, A.E. *Results of the Exploration Made by the Steamer Albatross of the Northern Coast of the United States in 1883*; US Government Printing Office: Washington, DC, USA, 1885; pp. 1–699.
45. Lieberkind, I. Asteridae der Deutschen Tiefsee-Expedition 1. Porcellanasteridae. *Wiss. Ergeb. Deutsch. Tiefsee Exp.* **1932**, *21*, 271–299.
46. Lieberkind, I. Asteroidea, pt. 1. Porcellanasteridae. *Dan. Ingolf Exp.* **1935**, *4*, 1–37.
47. Gage, J.D.; Pearson, M.; Clark, A.M.; Paterson, G.L.J.; Tyler, P.A. Echinoderms of the Rockall Trough and adjacent areas. I. Crinoidea, Asteroidea and Ophiuroidea. *Bull. Br. Mus. Nat. Hist.* **1983**, *45*, 263–308. [[CrossRef](#)]

48. Harvey, R.; Gage, J.D.; Billett, D.S.M.; Clark, A.M.; Patterson, G.L.J. Echinoderms of the Rockall Trough and adjacent areas 3. Additional records. *Bull. Br. Mus. Nat. Hist.* **1988**, *54*, 153–198.
49. Sumida, P.Y.G.; Tyler, P.A.; Billett, D.S.M. Early juvenile development of deep-sea asteroids of the NE Atlantic Ocean, with notes on juvenile bathymetric distributions. *Acta Zool.* **2001**, *82*, 11–40. [[CrossRef](#)]
50. Döderlein, L. Die Asteriden der Siboga-Expedition I. Porcellanasteridae, Astropectinidae, Benthoplectinidae. *Siboga-Exp.* **1921**, *46*, 1–47.
51. Belyaev, G.M. New sea stars from the abyssal and ultraabyssal of the Pacific Ocean. *Bull. Mosk. Ob. Isp. Prir. Ot. Biol.* **1969**, *74*, 5–25. (In Russian)
52. Belyaev, G.M.; Mironov, A.N. Bottom fauna of the West Pacific deep-sea trenches. *Trans. Shirshov Inst. Oceanol.* **1977**, *108*, 7–24. (In Russian)
53. Sladen, W.P. The Asteroidea of HMS “Challenger” Expedition. Part II. *J. Linn. Soc. Lond. Zool.* **1883**, *17*, 214–269. [[CrossRef](#)]
54. Koehler, R. Astéries recueillies par l’Investigateur dans l’océan indien. I. Les Astéries de Mer Profonde. *Echinoderma Indian Mus.* **1909**, *5*, 1–143. Available online: <https://www.biodiversitylibrary.org/page/12034817> (accessed on 5 February 2023).
55. Lambert, P.; Boutillier, J. Deep-sea echinodermata of British Columbia, Canada. *Can. Tech. Rep. Fish. Aquat. Sci.* **2011**, *2929*, 1–143.
56. Clark, H.E.S. Sea-stars (Echinodermata: Asteroidea) from “Eltain” cruise 26, with a review of the New Zealand asteroid fauna. *Zool. Publ.* **1970**, *52*, 1–34.
57. Clark, H.E.S.; McKnight, D.G. The marine fauna of New Zealand: Echinodermata: Asteroidea (sea stars) Order Paxillosida. *NIWA Biodiv. Mem.* **2000**, *11*, 5–196.
58. McKnight, D.G. Additions to the Asteroid Fauna of New Zealand: Families Benthoplectinidae, Odontasteridae, Asteroidea and Brisingidae; with notes on *Porcellanaster caeruleus* Wyville Thomson (Family Porcellanasteridae). *N. Z. Oceanogr. Inst. Rec.* **1973**, *1*, 220–239.
59. Clark, H.E.S.; McKnight, D.G. *Damnaster tasmani*, a new genus and species of Asteroidea (Echinodermata) from New Zealand. *Invert. Taxon.* **1994**, *8*, 1367–1372. Available online: <http://www.publish.csiro.au/IS/IT9941367> (accessed on 5 February 2023). [[CrossRef](#)]
60. Bernasconi, I. Algunos Asteroideos abisales del oeste de Chile. *Physis* **1967**, *26*, 443–449.
61. Bernasconi, I. Hallazgo en el oceano Antartico de *Eremicaster gracilis* (Sladen, 1883) (Asteroidea, Porcellanasteridae). *Physis* **1977**, *36*, 81–82.
62. Luke, S.R. Catalog of the benthic invertebrate collections, Echinodermata. *SIO Ref. Ser.* **1982**, *82*, 1–66.
63. Fisher, W.K. New starfishes from deep water off California and Alaska. *Bull. Bur. Fish.* **1905**, *24*, 291–320.
64. Ludwig, H. Asteroidea. Reports on an exploration of the west coast of Mexico, Central and South America and off the Galapagos Islands by the the U.S. S.S. “Albatross” during 1891. *Mem. Mus. Comp. Zool. Harv. Coll.* **1905**, *32*, 1–292. Available online: <http://biodiversitylibrary.org/page/28866803> (accessed on 5 February 2023).
65. Fisher, W.K. Asteroidea of the North Pacific and adjacent waters. *U. S. Nat. Mus. Bull.* **1911**, *76*, 1–420.
66. Clark, H.L. Echinoderms from Lower California, with descriptions of new species. *Bull. Amer. Mus. Nat. Hist.* **1913**, *32*, 187–205.
67. Clark, H.L. Asteroidea. Reports on the scientific results of the expedition to the eastern tropical Pacific, in charge of Alexander Agassiz, by the U.S. Fish comission Steamer “Albatross”, from October, 1904, to March, 1905, Lt. Cmdr., L.M. Garriett, USN commanding. Vol. 32. *Mem. Mus. Comp. Zool. Harv. Coll.* **1920**, *39*, 74–113.
68. Macan, T.T. Asteroidea. *Sci. Rep.* **1938**, *4*, 323–435.
69. Djakonov, A.M. Asteroidea of the Seas of the USSR. *Keys Fauna USSR* **1950**, *34*, 1–212. (In Russian)
70. Belyaev, G.M. Deep-sea starfishes of the genera *Eremicaster* and *Abyssaster* Porcellanasteridae: Composition and distribution. *Zool. Zhurnal* **1985**, *64*, 865–876. (In Russian)
71. Mironov, A.N.; Dilman, A.B.; Gebruk, A.V.; Kremenetskaia, A.V.; Minin, K.V.; Smirnov, I.S. Echinoderms of the Kuril-Kamchatka Trench. *Progr. Oceanogr.* **2019**, *178*, 102–217. [[CrossRef](#)]
72. Baranova, Z.I. Echinoderms of the Bering Sea. *Expl. Far-Eastern Seas. USSR* **1957**, *4*, 149–266. (In Russian)
73. Djakonov, A.M. Echinoderms (Echinodermata), except holothurians collected by the Kuril-Sakhalin Expedition in 1947–1949. *Explor. Far-East. Seas USSR* **1958**, *5*, 271–357. (In Russian)
74. Mironov, A.N.; Minin, K.V.; Dilman, A.B.; Smirnov, I.S. Deep-sea echinoderms of the Sea of Okhotsk. *Deep-Sea Res. II* **2018**, *154*, 342–357. [[CrossRef](#)]
75. Ludwig, H. Diagnose neuer Tiefsee-Seesterne aus der Familie der Porcellanasteridae. *Zool. Anz.* **1907**, *31*, 317–318.
76. Madsen, F.J. Asteroidea. *Rep. Swedish Deep-Sea Exp.* **1951**, *2*, 73–92.
77. Madsen, F.J. Echinoidea, Asteroidea and Ophiuroidea from depth exceeding 6000 m. *Galathea Rep.* **1956**, *2*, 23–32.
78. Suyehiro, Y.; Okada, Y.; Horikoshi, M.; Iwai, E. A brief note on the benthic animalson the Fourth Cruise of Japanese Expedition of Deep Seas (JEDS-4). *Oceanogr. Mag.* **1962**, *13*, 149–153.
79. Vinogradova, N.G.; Kudinova-Pasternak, R.K.; Moskalev, L.I.; Muromtseva, T.L.; Fedikov, N.F. Some regularities of quantitative distribution of bottom fauna of the Scotia Sea and the deep-sea trenches of the Atlantic sector of the Antarctic. *Trans. Inst. Oceanol. AN SSSR* **1974**, *98*, 157–182. (In Russian)
80. Amon, D.J.; Ziegler, A.F.; Kremenetskaia, A.; Mah, C.L.; Mooi, R.; O’Hara, T.; Pawson, D.L.; Roux, M.; Smith, C.R. Megafauna of the UKSRL exploration contract area and eastern Clarion-Clipperton Zone in the Pacific Ocean: Echinodermata. *Biodiv. Data J.* **2017**, *5*, e11794. [[CrossRef](#)] [[PubMed](#)]

81. Perrier, E. Sur une Asterie des grande profondeurs de l'Atlantique, pourvue d'un peduncle dorsale. *Comp. Rend. Hebdom. Séan. acad. Scie.* **1882**, *95*, 1379–1381. Available online: <https://www.biodiversitylibrary.org/page/36332511> (accessed on 5 February 2020).
82. Clark, A.M.; Mah, C. An index of names of recent Asteroidea. Part 4: Forcipulatida and Brisingida. *Echinoderm Stud.* **2001**, *6*, 229–347.
83. Dilman, A.B. Asteroid fauna of the Reykjanes Ridge. In *Biogeography of the North Atlantic Seamounts*; Mironov, A.N., Gebruk, A.V., Southward, A.J., Eds.; KMK Press: Moscow, Russia, 2006; pp. 177–192.
84. Koehler, R. Echinodermes provenant des campagnes du yacht Princesse-Alice. Asteries, Ophiures, Echinides et Crinoides. *Res. Camp. Sc. Prince Albert* **1909**, *34*, 1–317.
85. Belyaev, G.M. *Deep-Sea Ocean Trenches and Their Fauna*; Nauka Publishing House: Moscow, Russia, 1989; 256p.
86. Ahearn, C.G. Catalog of the type specimens of seastars (Echinodermata: Asteroidea) on the National Museum of Natural History, Smithsonian Institution. *Smith. Contr. Zool.* **1995**, *572*, 1–59. [[CrossRef](#)]
87. Billett, D.S.M. Echinodermata, ecology. In *Great Meteor East: A Biological Characterization*; Roe, H., Ed.; Institute of Oceanographic Science Deacon Laboratory: Southampton, 1987; pp. 163–178.
88. Carey, A.G. Food sources of sublittoral, bathyal and abyssal asteroids in the northeast Pacific Ocean. *Ophelia* **1972**, *10*, 35–47. [[CrossRef](#)]
89. Howell, K.L.; Pond, D.W.; Billett, D.S.M.; Tyler, P.A. Feeding ecology of deep-sea seastars (Echinodermata: Asteroidea): A fatty-acid biomarker approach. *Mar. Ecol. Progr. Ser.* **2003**, *255*, 193–206. [[CrossRef](#)]
90. Iken, K.; Brey, T.; Wand, U.; Voigt, J.; Junghans, P. Food web structure of the benthic community at the Porcupine Abyssal Plain (NE Atlantic): A stable isotope analysis. *Prog. Oceanogr.* **2001**, *50*, 383–405. [[CrossRef](#)]
91. Jangoux, M. Food and feeding mechanisms: Asteroidea. In *Echinoderm Nutrition*; Jangoux, M., Lawrence, J.M., Eds.; Balkema: Rotterdam, The Netherland, 1982; pp. 117–159.
92. Lampitt, R.S.; Billett, D.S.M. Perspectives on deepsea echinoderm ethology using video and time-lapse photography. In *Echinoderm Biology: Proceedings of the Sixth International Echinoderm Conference, Victoria, 23–28 August 1987*; Burke, R.D., Mladenov, P.V., Lambert, P., Parsley, R.L., Eds.; A.A. Balkema Publ.: Rotterdam, The Netherland, 1988; p. 801.
93. Sokolova, M.N. Feeding of deep-water detritophagous benthic invertebrates. *Trans. Inst. Oceanol.* **1958**, *27*, 123–153. (In Russian)
94. Shick, M.J.; Edwards, K.C.; Dearborn, J.H. Physiological ecology of the deposit-feeding sea star *Ctenodiscus crispatus*: Ciliated surfaces and animal-sediment interactions, *Mar. Ecol. Progr. Ser.* **1981**, *5*, 165–184. [[CrossRef](#)]
95. Hyman, L.H. *The Invertebrates, Vol. IV: Echinodermata*; McGraw-Hill: New York, NY, USA, 1955; 763p.
96. Allen, J.A. The adaptations and radiation of deep-sea bivalves. *Sarsia* **1979**, *64*, 19–27. [[CrossRef](#)]
97. Allen, J.A. The deep-sea species of *Dacrydium* Torell, 1859 (Dacrydiinae: Mytilidae: Bivalvia) of the Atlantic. *Malacologia* **1998**, *40*, 1–36.
98. Jirkov, I.A. Revision of Ampharetidae (Polychaeta) with modified thoracic notopodia. *Invertebrate Zool.* **2009**, *5*, 111–132. [[CrossRef](#)]
99. Kucheruk, N.V. The age and bathymetrical variation of *Nothria conchylega* (Polychaeta, Onuphidae). In *Ecological Investigations of the Shelf*; Kuznetsov, A.P., Ed.; Shirshov Institute of Oceanology: Moscow, Russia, 1980; pp. 63–72.
100. Mironov, A.N. Lifestyle of pourtalesiid sea urchins (Echinoidea: Pourtalesiidae). *Tr. Inst. Okeanol. AN SSSR* **1975**, *103*, 281–288. (In Russian)
101. Mironov, A.N. Pourtalesiid sea urchins (Echinodermata: Echinoidea) of the northern Mid-Atlantic Ridge. *Mar. Biol. Res.* **2008**, *4*, 3–24. [[CrossRef](#)]
102. Young, C.M.; Vazquez, E. *Agnezia monnioti* and *Styela gagetylei*, new deep-sea ascidians specialized for life within and below the oxygen minimum layer in the Arabian Sea. *Invertebr. Biol.* **1997**, *116*, 262–276. [[CrossRef](#)]
103. Chesher, R.H. The morphology and function of the frontal ambulacrum of the *Moira atropos* (Spatangoida). *Bull. Mar. Sci.* **1963**, *13*, 549–573.
104. Chesher, R.H. Contribution to the biology of *Meoma ventricosa* (Echinoidea: Spatangoida). *Bull. Mar. Sci.* **1969**, *19*, 72–110.
105. Kanazawa, K. Adaption of test shape for burrowing and locomotion in spatangoid echinoids. *Palaeontology* **1992**, *35*, 733–750.
106. Nichols, D. Changes in the Chalk heart-urchin *Micraster* interpreted in relation to living-forms. *Phil. Trans. Roy. Soc. Lond.* **1959**, *242*, 347–437.

Disclaimer/Publisher's Note: The statements, opinions and data contained in all publications are solely those of the individual author(s) and contributor(s) and not of MDPI and/or the editor(s). MDPI and/or the editor(s) disclaim responsibility for any injury to people or property resulting from any ideas, methods, instructions or products referred to in the content.